ISSN 1028-8546

Azərbaycan Milli Elmlər Akademiyası
Fizika-Riyaziyyat və Texnika Elmləri Bölməsi
Fizika İnstitutu

3

Fizika

Cild
VIII

2002

Bakı ✵ Elm

THE SOLUTION OF KANE'S EQUATIONS IN MAGNETIC FIELD IN JANNUSSIS FUNCTIONS REPRESENTATION

A.M. BABAYEV, O.Z. ALEKPEROV.
Institute of Physics, Azerbaijan National Academy of Sciences.
370143, Baku, H. Javid ave. 33.

The solution of Kane's equations in uniform magnetic field in the representation of Jannussis functions is found. The results can be used in calculations in different models of nanostructures with participating of Kane's semiconductors in magnetic field.

INTRODUCTION

The solution of the Kane's equations in uniform magnetic field for the first time w6.1(a)s given by Bowers and Yafet [1]. In [2] Jannussis obtained the solution of Schrodinger equation for the lattice electrons in uniform magnetic fields using the special form of functions, which he called "schrauben" (screw) functions. Later Jannussis obtained the solution of the Dirac equation in uniform magnetic field in the form represented through the screw functions. The solution of Dirac-Pauli equation which takes into account the anomalous magnetic momentum of electron in uniform magnetic field was obtained in [4] by generalization of the method of Jannussis. In this work the solutions of Kane`s equations in uniform magnetic field are given by the use of Jannussis screw functions. As it is known the Kane`s equations describe the spectra of conduction band electrons, light and spin-orbital splitting valence bands holes in A^3B^5 semiconductors such as InSb, InAs, GaAs and others.

THE SOLUTION OF THE KANE'S EQUATION IN MAGNETIC FIELD BY THE USE OF JANNUSSIUS FUNCTIONS

In eight-bands Kane's Hamiltonian the interaction of conduction band with the valence band is taken into account by single Kane's parameter *P*. The system of Kane's equations including the non dispersive heavy hole band have the form [5]:

$$(\vec{\alpha}\cdot\vec{k}\cdot P+\beta\cdot G-E)\Psi=0 \qquad (1)$$

where

$$\alpha_x=\begin{pmatrix} 0 & 0 & \frac{-1}{\sqrt{2}} & 0 & \frac{1}{\sqrt{6}} & 0 & 0 & \frac{1}{\sqrt{3}} \\ 0 & 0 & 0 & \frac{-1}{\sqrt{6}} & 0 & \frac{1}{\sqrt{2}} & \frac{1}{\sqrt{3}} & 0 \\ \frac{-1}{\sqrt{2}} & 0 & 0 & 0 & 0 & 0 & 0 & 0 \\ 0 & \frac{-1}{\sqrt{6}} & 0 & 0 & 0 & 0 & 0 & 0 \\ \frac{1}{\sqrt{6}} & 0 & 0 & 0 & 0 & 0 & 0 & 0 \\ 0 & \frac{1}{\sqrt{2}} & 0 & 0 & 0 & 0 & 0 & 0 \\ 0 & \frac{1}{\sqrt{3}} & 0 & 0 & 0 & 0 & 0 & 0 \\ \frac{1}{\sqrt{3}} & 0 & 0 & 0 & 0 & 0 & 0 & 0 \end{pmatrix} \qquad (2)$$

$$\alpha_y=\begin{pmatrix} 0 & 0 & \frac{i}{\sqrt{2}} & 0 & \frac{i}{\sqrt{6}} & 0 & 0 & \frac{i}{\sqrt{3}} \\ 0 & 0 & 0 & \frac{i}{\sqrt{6}} & 0 & \frac{i}{\sqrt{2}} & \frac{-i}{\sqrt{3}} & 0 \\ \frac{-i}{\sqrt{2}} & 0 & 0 & 0 & 0 & 0 & 0 & 0 \\ 0 & \frac{-i}{\sqrt{6}} & 0 & 0 & 0 & 0 & 0 & 0 \\ \frac{-i}{\sqrt{6}} & 0 & 0 & 0 & 0 & 0 & 0 & 0 \\ 0 & \frac{-i}{\sqrt{2}} & 0 & 0 & 0 & 0 & 0 & 0 \\ 0 & \frac{i}{\sqrt{3}} & 0 & 0 & 0 & 0 & 0 & 0 \\ \frac{-i}{\sqrt{3}} & 0 & 0 & 0 & 0 & 0 & 0 & 0 \end{pmatrix} \qquad (3)$$

$$\alpha_z=\begin{pmatrix} 0 & 0 & 0 & \sqrt{\frac{2}{3}} & 0 & 0 & \sqrt{\frac{1}{3}} & 0 \\ 0 & 0 & 0 & 0 & \sqrt{\frac{2}{3}} & 0 & 0 & -\sqrt{\frac{1}{3}} \\ 0 & 0 & 0 & 0 & 0 & 0 & 0 & 0 \\ \sqrt{\frac{2}{3}} & 0 & 0 & 0 & 0 & 0 & 0 & 0 \\ 0 & \sqrt{\frac{2}{3}} & 0 & 0 & 0 & 0 & 0 & 0 \\ 0 & 0 & 0 & 0 & 0 & 0 & 0 & 0 \\ \sqrt{\frac{1}{3}} & 0 & 0 & 0 & 0 & 0 & 0 & 0 \\ 0 & -\sqrt{\frac{1}{3}} & 0 & 0 & 0 & 0 & 0 & 0 \end{pmatrix} \qquad (4)$$

$$G=\begin{pmatrix} 0 & 0 & 0 & 0 & 0 & 0 & 0 & 0 \\ 0 & 0 & 0 & 0 & 0 & 0 & 0 & 0 \\ 0 & 0 & -E_g & 0 & 0 & 0 & 0 & 0 \\ 0 & 0 & 0 & -E_g & 0 & 0 & 0 & 0 \\ 0 & 0 & 0 & 0 & -E_g & 0 & 0 & 0 \\ 0 & 0 & 0 & 0 & 0 & -E_g & 0 & 0 \\ 0 & 0 & 0 & 0 & 0 & 0 & -E_g-\Delta & 0 \\ 0 & 0 & 0 & 0 & 0 & 0 & 0 & -E_g-\Delta \end{pmatrix} \qquad (5)$$

$$\beta = \begin{pmatrix} 1 & 0 & 0 & 0 & 0 & 0 & 0 & 0 \\ 0 & 1 & 0 & 0 & 0 & 0 & 0 & 0 \\ 0 & 0 & -1 & 0 & 0 & 0 & 0 & 0 \\ 0 & 0 & 0 & -1 & 0 & 0 & 0 & 0 \\ 0 & 0 & 0 & 0 & -1 & 0 & 0 & 0 \\ 0 & 0 & 0 & 0 & 0 & -1 & 0 & 0 \\ 0 & 0 & 0 & 0 & 0 & 0 & -1 & 0 \\ 0 & 0 & 0 & 0 & 0 & 0 & 0 & -1 \end{pmatrix}, \quad \Psi = \begin{pmatrix} \Psi_1 \\ \Psi_2 \\ \Psi_3 \\ \Psi_4 \\ \Psi_5 \\ \Psi_6 \\ \Psi_7 \\ \Psi_8 \end{pmatrix} \tag{6}$$

Here P is the Kane's parameter, E_g and Δ are values of forbidden gap and spin-orbital interaction, respectively and

$$\vec{k} = -\imath\vec{\nabla} - \frac{e}{c}\vec{A} \tag{7}$$

The vector potential is chosen in the symmetric gauge

$$\vec{A} = \frac{1}{2}[\vec{H} \times \vec{r}] \tag{8}$$

and magnetic field intensity $\vec{H} = H\vec{e}_z$ is directed along the z-axis.

As it is known the solution of equation (1) in the cylindrical coordinates with the symmetric form of vector potential $\vec{A}$ can be expressed in terms of Laguerre's functions. We will show that the solution of equation (1) with the symmetric gauge for $\vec{A}$ in rectangular coordinate system can be obtained through the Jannussis screw functions. We search for the solution of Kane's equation (1) in the form

$$\Psi = \sum_n \Psi_{k,n} \begin{pmatrix} C_{1,n}u_1 \\ C_{2,n}u_2 \\ C_{3,n}u_3 \\ C_{4,n}u_4 \\ C_{5,n}u_5 \\ C_{6,n}u_6 \\ C_{7,n}u_7 \\ C_{8,n}u_8 \end{pmatrix} \tag{9}$$

where u_1- u_8-s being the periodic part of wave functions are defined as in [1] through the combinations of spinors (s=1/2) and s,p-like band functions $|S\rangle$, $|X\rangle$, $|Y\rangle$, $|Z\rangle$. However in contrast to [1] we take $\Psi_{k,n}$ in the form of Jannussis functions (cf.[1])

$$\Psi_{k,n} = \sqrt{\frac{\lambda_H}{2\pi}\left(\frac{2}{\lambda_H}\right)^n \frac{1}{n!}} exp\left(\left(-\frac{1}{\lambda_H}\right)\left(K_x^2 + K_y^2\right) + ikr\right)\left(-K_y^2 - iK_x^2\right)^n \tag{10}$$

Here

$$K_x = k_x + \frac{1}{2}\lambda_H \cdot y\,,\; K_y = k_y - \frac{1}{2}\lambda_H \cdot x\,, \tag{11}$$

where $\lambda_H = \frac{eH}{c\hbar}$ is the square of reciprocal magnetic length. The functions $\Psi_{k,n}$ are normalized and obey the relations

$$\left(\frac{\partial}{\partial x} + i\frac{\partial}{\partial y} + \frac{1}{2}\lambda_H(x+iy)\right)\Psi_{k,n} = \sqrt{2\lambda_H n}\,\Psi_{k,n-1}, \tag{12}$$

$$\left(\frac{\partial}{\partial x} - i\frac{\partial}{\partial y} - \frac{1}{2}\lambda_H(x-iy)\right)\Psi_{k,n} = -\sqrt{2\lambda_H(n+1)}\,\Psi_{k,n+1}\,. \tag{13}$$

Substituting the wave function (9) into equation (1) and taking into account the relations (12-13) we obtain the following system of equations for the wave function coefficients C_{in}:

$$-EC_{1,n} - iP\sqrt{n\lambda_H}C_{3,n-1} + Pk_z\sqrt{\frac{2}{3}}C_{4,n} - iP\sqrt{\frac{n+1}{3}\lambda_H}_{5,n+1} + Pk_z\sqrt{\frac{1}{3}}C_{7,n} - iP\sqrt{\frac{2(n+1)}{3}\lambda_H}C_{8,n+1} = 0 \tag{14}$$

$$-EC_{2,n+1}-iP\sqrt{\frac{n+1}{3}\lambda_H}C_{4,n}+Pk_z\sqrt{\frac{2}{3}}C_{5,n+1}-iP\sqrt{(n+2)\lambda_H}C_{6,n+2}+P\sqrt{\frac{2(n+1)}{3}\lambda_H}C_{7,n}-Pk_z\sqrt{\frac{1}{3}}C_{8,n}=0 \tag{15}$$

$$P\sqrt{n\lambda_H}C_{1,n}-(E+E_g)C_{3,n-1}=0 \tag{16}$$

$$Pk_z\sqrt{\frac{2}{3}}C_{1,n}+iP\sqrt{\frac{n+1}{3}\lambda_H}C_{2,n}-(E-E_g)C_{4,n}=0 \tag{17}$$

$$Pk_z\sqrt{\frac{2}{3}}C_{2,n+1}+iP\sqrt{\frac{n+1}{3}\lambda_H}C_{1,n}-(E+E_g)C_{5,n+1}=0 \tag{18}$$

$$iP\sqrt{(n+2)\lambda_H}C_{2,n+1}-(E-E_g)C_{6,n+2}=0 \tag{19}$$

$$Pk_z\sqrt{\frac{1}{3}}C_{1,n}-iP\sqrt{\frac{2(n+1)}{3}\lambda_H}C_{2,n+1}-(E+E_g+\Delta)C_{7,n}=0 \tag{20}$$

$$iP\sqrt{\frac{2(n+1)}{3}\lambda_H}C_{1,n}-\sqrt{\frac{1}{3}}Pk_zC_{2,n+1}-(E+E_g+\Delta)C_{8,n+1}=0 \tag{21}$$

Relations for energy levels can be obtained in two ways. The first one is to demand that the determinant of matrix of coefficients of $C_{1,n}-C_{8,n+1}$ in the set of equations (14-21) to be zero. The second by substituting the coefficients $C_{3,n-1}-C_{8,n+1}$ from the equations (16-21) into the (14) and (15). So we would have the following set of equations for $C_{1,n}$ and C_{2n+1}

$$C_{1,n}\cdot\left\{-E+\frac{P^2k_z^2}{3}\left(\frac{2}{E+E_g}+\frac{1}{E+E_g+\Delta}\right)+\frac{P^2\lambda_H(2n+1)}{3}\left(\frac{2}{E+E_g}+\frac{1}{E+E_g+\Delta}\right)-\right.$$
$$\left.-\frac{P^2\lambda_H}{3}\left(\frac{1}{E+E_g}-\frac{1}{E+E_g+\Delta}\right)\right\}=0 \tag{22}$$

$$C_{2,n+1}\cdot\left\{-E+\frac{P^2k_z^2}{3}\left(\frac{2}{E+E_g}+\frac{1}{E+E_g+\Delta}\right)+\frac{P^2\lambda_H(2n+1)}{3}\left(\frac{2}{E+E_g}+\frac{1}{E+E_g+\Delta}\right)-\right.$$
$$\left.-\frac{P^2\lambda_H}{3}\left(\frac{1}{E+E_g}-\frac{1}{E+E_g+\Delta}\right)\right\}=0 \tag{23}$$

If to demand that $C_{1,n}\neq 0$ or $C_{2,n+1}\neq 0$ we will have two expressions for the light carriers spectra correspondingly:

$$-E+\frac{P^2k_z^2}{3}\left(\frac{2}{E+E_g}+\frac{1}{E+E_g+\Delta}\right)+\frac{P^2\lambda_H(2n+1)}{3}\left(\frac{2}{E+E_g}+\frac{1}{E+E_g+\Delta}\right)-$$
$$-\frac{P^2\lambda_H}{3}\left(\frac{1}{E+E_g}-\frac{1}{E+E_g+\Delta}\right)=0 \tag{24}$$

$$-E+\frac{P^2k_z^2}{3}\left(\frac{2}{E+E_g}+\frac{1}{E+E_g+\Delta}\right)+\frac{P^2\lambda_H(2n+1)}{3}\left(\frac{2}{E+E_g}+\frac{1}{E+E_g+\Delta}\right)+$$
$$+\frac{P^2\lambda_H}{3}\left(\frac{1}{E+E_g}-\frac{1}{E+E_g+\Delta}\right)=0 \qquad (25)$$

One pair of solutions of cubic equations (22) and (23) gives the dispersion relation for conduction band spin-up and spin-down states correspondingly, but the other two pairs correspond to light and spin-orbital splitting hole bands with total momentum projection *M* along (*M*=1/2) and opposite (*M*=-1/2) to the magnetic field direction.

To obtain the light carriers wave functions $\Psi_{E,J=1/2,M=+1/2}$ and $\Psi_{E,J=1/2,M=-1/2}$ we must put $C_{1,n}\neq 0, C_{2,n+1}=0$ and $C_{2,n+1}\neq 0, C_{1,n}=0$ in (9) correspondingly, expressing all other coefficients $C_{3,n}-C_{8,n}$ through them. So the wave functions for the light carriers have been obtained in the following forms

$$\Psi_{E,J=1/2,M=+1/2}=\frac{1}{\sqrt{N_1}}\cdot\begin{pmatrix}\Psi_{k,n}\\ 0\\ \frac{iP\sqrt{n\lambda_H}}{E+E_g}\Psi_{k,n-1}\\ \frac{Pk_z\sqrt{\frac{2}{3}}}{E+E_g}\Psi_{k,n}\\ \frac{iP\sqrt{\frac{n+1}{3}\lambda_H}}{E+E_g}\Psi_{k,n+1}\\ 0\\ \frac{Pk_z\sqrt{\frac{1}{3}}}{E+E_g+\Delta}\Psi_{k,n}\\ \frac{iP\sqrt{\frac{2(n+1)}{3}\lambda_H}}{E+E_g+\Delta}\Psi_{k,n+1}\end{pmatrix},\qquad \Psi_{E,J=1/2,M=-1/2}=\frac{1}{\sqrt{N_2}}\cdot\begin{pmatrix}0\\ \Psi_{k,n}\\ 0\\ \frac{iP\sqrt{\frac{n}{3}\lambda_H}}{E+E_g}\Psi_{k,n-1}\\ \frac{Pk_z\sqrt{\frac{2}{3}}}{E+E_g}\Psi_{k,n}\\ \frac{iP\sqrt{\frac{n+1}{3}\lambda_H}}{E+E_g}\Psi_{k,n+1}\\ -\frac{iP\sqrt{\frac{2n}{3}\lambda_H}}{E+E_g+\Delta}\Psi_{k,n-1}\\ -\frac{Pk_z\sqrt{\frac{1}{3}}}{E+E_g+\Delta}\Psi_{k,n}\end{pmatrix} \qquad (26)$$

In (26) E is the root of equation (24) or (25) for M=1/2 or M=-1/2, correspondingly and three roots of each of these equations correspond to conduction, light and spin-orbital splitting holes bands. The factors N_1 and N_2 are obtained from the normalization conditions of the wave functions and have the form

$$\frac{\qquad}{\qquad}\quad\frac{\qquad}{\qquad}\quad\frac{\qquad}{\qquad}\quad\frac{\qquad}{(E\quad E\qquad)},$$

$$E + E_g = 0, \tag{27}$$

i.e. the heavy hole mass is infinite in this model. To obtain the heavy hole wave functions $\Psi_{E=-E_g,J=3/2,M_j=3/2}$ and $\Psi_{E=-E_g,J=3/2,M_j=-3/2}$ is necessary to put $C_{1,n} = 0$ and $C_{2,n+1} = 0$ in (14) and (15). Then if one takes into account (27) the only nonzero coefficients in the set of equations (14-15) are $C_{3,n-1}$, $C_{4,n}$, $C_{5,n+1}$ and $C_{6,n+2}$. Taken by turns $C_{4,n}$ =0 and $C_{5,n+1}=0$ we can obtain for the heavy hole wave functions the following expressions:

$$\Psi_{E=-E_g,J=3/2,M_j=3/2} = \frac{1}{\sqrt{N_3}} \begin{pmatrix} 0 \\ 0 \\ \sqrt{\frac{(n+1)(n+2)}{3}}\Psi_{k,n-1} \\ 0 \\ -\sqrt{n(n+2)}\Psi_{k,n+1} \\ -i\sqrt{\frac{2}{3}}nk_z\Psi_{k,n+2} \\ 0 \\ 0 \end{pmatrix},$$

$$\Psi_{E=-E_g,J=3/2,M_j=-3/2} = \frac{1}{\sqrt{N_4}} \begin{pmatrix} 0 \\ 0 \\ -ik_z\sqrt{\frac{2(n+2)}{3}}\Psi_{k,n-1} \\ \sqrt{n(n+2)}\Psi_{k,n} \\ 0 \\ \sqrt{\frac{n(n+1)}{3}}\Psi_{k,n+2} \\ 0 \\ 0 \end{pmatrix}, \tag{28}$$

where the normalization factors N_3 and N_4 have the form

$$N_3 = \frac{(4n+1)(n+2)}{3} + \frac{2}{3}nk_z^2, \quad N_4 = \frac{(4n+7)n}{3} + \frac{2}{3}(n+2)k_z^2,$$

Conclusion

The solutions for the three band Kane's model in magnetic field in the representation of Jannussis function are obtained. These solutions can be useful for calculations of some physical quantities of A^3B^5 semiconductors and their different structures such as quantum wells, quantum dots and wires in magnetic field. As seen from the properties (12) and (13) these functions also facilitate the construction of coherent states for Kane's model in magnetic field.

We thank Prof. F.M.Gashimzade for helpful discussions.

[1] *R.Bowers, Y. Yafet*. Phys. Rev. B, v.115, p.1165, (1959).
[2] *A.Jannussis*. Phys. stat. sol.6, 217, (1964).
[3] *A.Jannussis*. Zeitschrift fur Physik, 190, 129-134, (1966)
[4] *A.N.Mjagkij, V.A. Bordovitsin* Izvestiya vuzov Fizika 1, 93b, 2001.
[5] *B.M.Askerov*, Kinetic effects in semiconductors, L., Nauka, 1970.

A.M. BABAYEV, O.Z. ALEKPEROV.

. . , . .

Bircins maqnit sahəsində Keyn tənliklərinin həlli Yannussis funksiyaları vasitəsi ilə tapılmışdır. Alınan nəticələr Keyn tipli yarımkeçirici nanostrukturların müxtəlif parametrlərinin maqnit sahəsində hesablanmasında istifadə oluna bilər.

А.М. Бабаев, О.З. Алекперов

РЕШЕНИЕ УРАВНЕНИЙ КЕЙНА В МАГНИТНОМ ПОЛЕ В ПРЕДСТАВЛЕНИИ ФУНКЦИИ ЯННУССИСА

Получено решение уравнений Кейна в однородном магнитном поле через функции Яннуссиса. Полученные результаты могут быть использованы при расчетах различных параметров наноструктур на основе Кейновских полупроводников в однородном магнитном поле.

Received: 30.09.02

ANTICIPATING CHAOS SYNCHRONIZATION IN TIME-DELAYED SYSTEMS

E. M. SHAHVERDIEV, R.A. NURIEV, G.N. GASIMOVA
Institute of Physics, Azerbaijan National Academy of Sciences
370143, Baku, H. Javid ave. 33.

R.H. HASHIMOV,
Azerbaijan Technical University, 370073 Baku, Azerbaijan

Using the Ikeda model we demonstrate analytically that anticipating synchronization can be obtained in chaotic time-delayed systems governed by two characteristic delay times. We derive existence and stability conditions for the dual-time anticipating synchronization manifold.

The theory is in full agreement with numerical simulations.

PACS number(s):05.45.Xt, 05.45.Vx, 42.55.Px, 42.65.Sf

1. Introduction

There are different types of sychronization in interacting chaotic systems. Complete, generalized, phase, lag and anticipating synchronizations of chaotic oscillators have been described theoretically and observed experimentally. Complete synchronization implies coincidence of states of interacting systems, $y(t)=x(t)$ [1,2]. A generalized synchronization, introduced for drive-response systems, is defined as the presence of some functional relation between the states of response and drive, i.e. $y(t)=F(x(t))$, [3]. Phase synchronization means entrainment of phases of chaotic oscillators, $n\Phi_x-m\Phi_y=const$(n and m are integers) whereas their amplitudes remain chaotic and uncorrelated [4]. Lag synchronization appears as a coincidence of shifted-in-time states of two systems, $y(t)= x_\tau(t)\equiv x_\tau(t-\tau)$ with positive τ and for the first time has been studied in between symmetrically coupled non-identical oscillators [5]. Lag synchronization in time-delayed systems is investigated in [6-9]. Anticipating synchronization [10] also appears as a coincidence of shifted-in-time states of two coupled systems, but in this case the driven system anticipates the driver, $y(t)=x(t+\tau)$ or $x=y_\tau$, $\tau>0$. An experimental observation of anticipating synchronization has been reported recently [11]. Possible explanation of this phenomenon is considered in [12]. The concept of inverse anticipating synchronization is introduced in [13].

Chaos synchronization is of fundamental importance in a variety of complex physical, chemical and biological systems [14-16]. Application of chaos synchronization has been advanced in secure communications, optimization of non-linear systems' performance, modeling brain activity and pattern recognition [14-16]. Time-delayed systems are ubiquitous in nature, technology and society because of finite signal transmission times, switching speeds and memory effects [17,18]. Therefore the study of chaos synchronization in these systems is of considerable practical significance. Because of their ability to generate high-dimensional chaos, time-delayed systems are good candidates for secure communications based on chaos synchronization.

In [10] anticipating chaos synchronization was studied in the case of a single delay time. In [19] it was demonstrated that by augmenting the phase space of the driven system (by considering a chain of driven systems), one can accomplish anticipation times that are multiples of the coupling delay time. Anticipating chaos synchronization for systems with two delay times: a delay in the coupled systems themselves and a coupling delay was investigated (it numerically) in [20].

In this paper, using the Ikeda model, we *analytically* generalize the concept of anticipating synchronization to the cases, when there are two delay times in the coupled systems: where the delay time in the coupling is different from the delay time in the coupled systems themselves. We derive existence and stability conditions for the corresponding anticipating synchronization manifold. We support our theoretical results by numerical simulations.

2. Anticipating chaos synchronization in time-delayed systems with two characteristic delay times

For clarity of presentation we reproduce here the definition of anticipating chaos synchronization in [10]:

The driver system

$$\frac{dx}{dt} = -\alpha y + f(x_{\tau'}) \tag{1}$$

synchronizes with a driven system of the form

$$\frac{dy}{dt} = -\alpha x + f(x\ ) \tag{2}$$

on the anticipating synchronization manifold

$$x = y_\tau \tag{3}$$

From Eqs. (1-2) it follows that

$$\frac{dx}{dt} - \frac{dy_\tau}{dt} = -\alpha(x - y_\tau) + f(x_\tau) - f(x_\tau) = -\alpha(x - y_\tau)\ .$$

We define the error signal by symbol Δ: $\Delta\equiv x-y_\tau$. Then $\frac{d\Delta}{dt} \equiv -\alpha\Delta$. In many representative cases chaos synchronization can be understood from the existence of a global Lyapunov function of the error signals [21,22]. Thus

by introducing the Lyapunov function $L = \frac{1}{2}\Delta^2$ we obtain that for $\alpha>0$ the anticipating synchronization manifold $x=y_\tau$ is globally attracting and asymptotically stable.

Now we shall consider the case of anticipating chaos synchronization in time-delayed with two characteristic delay times; we confine ourselves to the demonstration of principles using specific example: the Ikeda model [10,20].

Consider the following unidirectionally coupled Ikeda model.

$$\frac{dx}{dt} = -\alpha x + m_1 \sin x_{\tau_1}$$

$$\frac{dy}{dt} = -\alpha y + m_2 \sin y_{\tau_2} + m_3 \sin x_{\tau_2} \qquad (4)$$

where α is a positive constant; m_1,m_2 and m_3 are constants; τ_1 is the feedback delay in the coupled systems; τ_2 is the coupling delay.

Now we shall analytically demonstrate that $x = y_{\tau_1-\tau_2}$ with $\tau_1 > \tau_2$ can be the anticipating synchronization manifold; find the existence and stability conditions for anticipating synchronization, and then compare the analytical results with numerical simulations.

From Eqs. (4) it follows that under the condition

$$m_1 = m_2 + m_3 \qquad (5)$$

the dynamics of the error $\Delta = x - y_{\tau_1-\tau_2}$ obeys the following equation:

$$\frac{d\Delta}{dt} = -r\Delta + s\Delta_{\tau_1} \qquad (6)$$

with $r = \alpha$ and $s = (m_1 - m_3)\cos x_{\tau_1}$. It is obvious that $\Delta=0$ is the solution of Eq.(6). The stability condition for the trivial solution $\Delta=0$ of Eq.(6) can be found by investigating the positively defined Krasovskii-Lyapunov fuctional

$$V(t) = \frac{1}{2}\Delta^2 + \mu\int_{-\tau}^{0} \Delta^2(t+t_1)dt_1$$

(where $\mu > 0$ is an arbitrary positive parameter). According to [10,18,23] the sufficient stability condition for the trivial solution of Eq.(6) is: $r>|s|$. Then the sufficient stability condition for the anticipating synchronization manifold $x = y_{\tau_1-\tau_2}$ reads:

$$\alpha > |m_2| \qquad (7)$$

The condition $m_1 = m_1 + m_2$ is the existence (necessary) condition for anticipating synchronization for the unidirectionally coupled modified Ikeda model.

We also have numerically studied Eqs.(4). The driver system x in Eqs.(4) behaves chaotically for, e.g. $\tau_1=3$, $\alpha=5$, $m_1=20$. The other parameters' values used in numerical simulations are $\tau_2=1$, $m_2=3$,$m_3=17$. We perform simulations of (4) by employing an Runge-Kutta-Fehlberg algorithm with automatic step size control. Figure 1 shows:(a) time series of the driver x(t) (solid line) and driven system $y(t)$ (dotted line). After transients, the driven system's trajectory is shifted $\bar{\tau}_1 - \bar{\tau}_2 = 2$ time units to the left, thus anticipating the driver. Thus numerical simulations fully support the analytical approach.

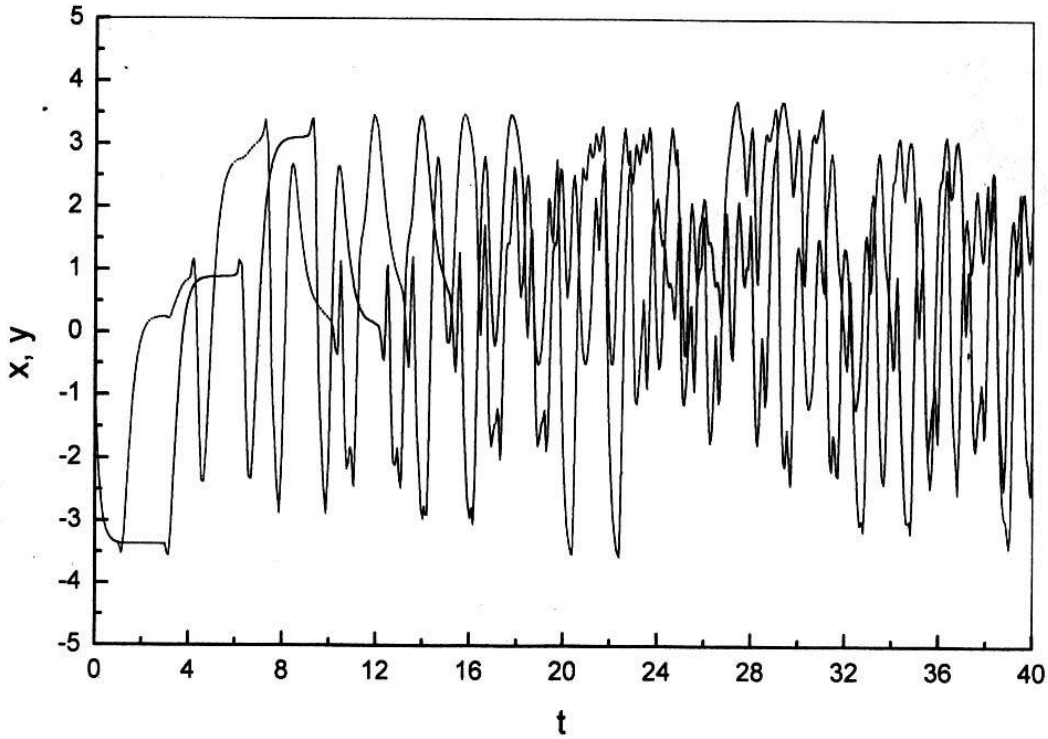

Fig. 1. Numerical simulation of two coupled modified Ikeda equations (4):(a) time series of the driver $x(t)$ (solid line) and driven system

y(t) (dotted line). After transients, the driven system's trajectory is shifted 2 time unit to the left, thus anticipating the driver.

In conclusion, in this paper using the Ikeda model we have for the first time demonstrated analytically that anticipating synchronization can be obtained in chaotic time-delayed systems governed by two characteristic delay times. We have shown that the anticipation time is the difference between the delay time in the coupled systems and the coupling delay time and derived both existence and stability conditions for the anticipating synchronization manifold.

Synchronization of coupled chaotic systems restricts the evolution of synchronized systems to the synchronization manifold and therefore eliminates some degrees of freedom of the joint system, thus leading to significant reduction of complexity. In this context from a fundamental point of view, new types of chaos synchronization, including anticipating synchronization can be considered as a novel ways of reducing unpredictability of chaotic dynamics.

Possible practical applications of anticipating chaos synchronization may exploit the fact that driven system {anticipates} the driver. For example this phenomenon can be used for rapid prediction-because no computation is involved- by simply coupling the identical response system to the master system; in secure communications anticipation of the future states of the transmitter (master laser) at the receiver (slave laser) allows more time to decode the message; another opportunity is in the control of delay-induced instabilities in a wide range of non-linear systems. Also anticipating synchronization may be of interest for the understanding of natural information processing systems.

[1] *L. M. Pecora and T. L. Carroll*. Phys. Rev. Lett. 1990, 64, 821.
[2] *E.Ott, C.Grebogi and J.A.York,* Phys. Rev. Lett. 1990, 64, 1196.
[3] *N.F. Rulkov, M.M. Sushchik, L.S. Tsimring and H.D.I.Abarbanel*. Phys.Rev.E 1995, 51, 980.
[4] *M.G. Rosenblum, A.S. Pikovsky and J. Kurths.* Phys. Rev. Lett. 1996, 76, 1804.
[5] *M.G. Rosenblum, A.S. Pikovsky and J. Kurths.* Phys. Rev. Lett. 1997,78, 4193.
[6] *S. Sivaprakasam, E.M. Shahverdiev, K.A. Shore*. Phys. Rev. E 2000,62,7505.
[7] *E.M. Shahverdiev, S. Sivaprakasam and K.A. Shore.* Phys.Lett. A 2002, 292, 320.
[8] *E.M. Shahverdiev and K.A. Shore.* Phys. Lett. A 2002, 295, 217.
[9] *E.M. Shahverdiev, S. Sivaprakasam and K.A .Shore.* Phys. Rev. E 2002, 66, 0472xx
[10] *H.U.Voss.* Phys.Rev.E 2000, 61, 5115
[11] *S. Sivaprakasam, E.M. Shahverdiev, P.S. Spencer and K.A. Shore.* Phys.Rev. Lett.2001, 87, 154101
[12] *E.M. Shahverdiev, S. Sivaprakasam and K.A. Shore*, Phys. Rev. E 2002,66,017206
[13] *E.M. Shahverdiev, S. Sivaprakasam and K.A. Shore*, Phys. Rev. E 2002, 66, 017204
[14] CHAOS, Special issue on chaos synchronization, 1997, No 4
[15] *G. Chen and X. Dong*, From Chaos to Order. Methodologies, Perspectives and Applications (World Scientific, Singapore, 1998)
[16] Handbook of Chaos Control, Ed. H.G.Schuster (Wiley-VCH, Weinheim, 1999).
[17] *J.K. Hale and S.M.V .Lunel*, Introduction to Functional Differential Equations (Springer, New York, 1993)
[18] *L.E. El'sgol'ts and S.B. Norkin*, Introduction to the theory and applications of differential equations with deviating arguments (Acadamic Press, New York, 1973).
[19] *H.U. Voss,* Phys. Rev. Lett. 2001,87, 014102
[20] *C. Masoller*, Phys. Rev. Lett. 2001,86,2782
[21] *R. He and P.G. Vaida*, Phys. Rev. A 1992,46,7387
[22] *E.M. Shahverdiev*. Phys. Rev. E 1999,60,3905
[23] *K. Pyragas*. Phys. Rev. E 1998,58,3067

E.M. Şahverdiyev, P.H. Həşimov, R.A. Nuriyev, G.N. Qasımova

ANTİSİPATSİON SİNXRONLAŞMA REJİMİNİN GECİKƏN VƏ DUAL-ZAMAN SİSTEMLƏRİNDƏ ARAŞDIRILMASI

İkeda modeli araşdırılıb, belə gecikən və dual-zaman sistemlərində antisipatsion sinxronlaşma rejimi tapılıb. Öyrənilən halda siqnalın aparan sistemdən (ötürücü) aparılan sistemə (qəbuledici) yayılma vaxtı ötürücüdə əks-əlaqə xarakterik zamanından fərqlidir. Antisipatsion sinxronlaşma rejimində qəbuledicinin indiki halı ötürücünün gələcək halına sinxronlaşıb. Varlıq və stabillik şərtləri tapılıb. Analitik və ədədi üsulla araşdırma nəticələri üst-üstə düşür.

Э.М. Шахвердиев, Р.Г. Гашимов, Р.А. Нуриев, Г.Н. Касимова

АНТИСИПАЦИОННАЯ СИНХРОНИЗАЦИЯ ХАОТИЧЕСКИХ КОЛЕБАНИЙ В СИСТЕМАХ С ЗАПАЗДЫВАНИЕМ С ДВУМЯ ХАРАКТЕРНЫМИ ВРЕМЕНАМИ

На основе исследования модели Икеды найден режим антисипационной синхронизации хаотических колебаний в системах с запаздыванием с двумя характерными временами, когда время распространения сигнала от ведущий системы (передатчик) к ведомой системе (приемник) отличается от характерного времени обратной связи в передатчике. (В режиме антисипационной синхронизации настоящее состояние приемника синхронизируется к будущему состоянию передатчика). Получены условия существования и стабильности антисипационного режима синхронизации.Аналитические выводы подтверждаются численным моделированием.

Received: 24.09.02

THE REFLECTION OF THE PARALLEL-POLARIZED ELECTROMAGNETIC WAVE AT ITS INCIDENCE ON THE TWO-LAYER DIELECTIC-METAL SYSTEM UNDER THE ANGLE

E.R. KASIMOV
Institute of Physics, Azerbaijan National Academy of Sciences
370143, Baku, H. Javid ave. 33.

Conditions of the full reflectionless absorption origin of the parallel-polarized electromagnetic wave at its incidence under the angle on the absorbing dielectric layer, applied on the metal substrate, were found. Their dependencies on the wave cover thickness, the incidence angle and dielectric properties of the cover material have been investigated.

The problem of the cross-polarized radiation reflection, falling under the angle on the plane two layer dielectric-metal system was solved in paper [1] and conditions of full radiation absorption origin in such system at strictly fixed selective values of the radiation frequency, the layer thickness and dielectric properties of the cover material were found. Taking into consideration the interest to the reflectionless wave absorption origin in layered media, we will observe the problem of the parallel-polarized radiation absorption from the plane two-layer dielectric-metal system as the next step in this direction.

For the given type of the incident wave polarization the complex expression of the coefficient ρ of the wave reflection from the examined plane two-layer system is equal to:

$$\dot{\rho} = \frac{Z_0 \cos\alpha_0 - Z_{вх}\cos\alpha}{Z_0 \cos\alpha_0 + Z_{вх}\cos\alpha} \quad ; \qquad (1)$$

where $Z_{вх} = Zth\gamma l$ is the input resistance of the two-layer system, Z_0, Z are wave resistances of the vacuum and the cover substance, respectively, $\cos\alpha = \sqrt{1 - \sin^2\alpha_0 / \varepsilon}$; α_0 is the wave incidence angle on the two-layer system, α is the angle of the wave refraction in the cover layer and is at the same time the angle of the wave incidence on the dielectric-metal interface, l is the thickness of the cover layer [2-4].

The wave spreading constant γ in the cover substance included in the expression for the input resistance Z_{in} is equal to:

$$\gamma = \gamma_0 \frac{\cos\alpha}{\cos\alpha_0} \quad ; \qquad (2)$$

where : $\gamma_0 = i2\pi/\lambda$, λ is the constant of the wave spreading and the wave length in the vacuum, respectively.

The reflectionless wave absorption in the examined two-layer system may occur in the point of one of minima of the dependence of the modulus of the wave reflection coefficient ρ on the thickness of the cover layer l and if the condition ρ=0 is fulfilled in this point. Let us add notations $p = \sin^2\alpha_0$ and $\lambda_b = \lambda / \sqrt{1-p}$, ., where λ_b is the wave length in the free space in the direction of the wave spreading relatively to the normal of the layer surface. As $Z = Z_0/\sqrt{\varepsilon}$ then taking into account expression (1)-(2) we get:

$$th\frac{2\pi l}{\lambda_b}\sqrt{\varepsilon^{\bullet}} = \frac{Z_0\cos\alpha_0}{Z\cos\alpha} = \frac{\varepsilon}{\varepsilon^{\bullet}} \quad ; \qquad (3)$$

where $\varepsilon^{\bullet} = \varepsilon' - i\varepsilon''$; $\varepsilon_1 = \dfrac{\varepsilon' - p}{1-p}$;

$$\varepsilon_2 = \frac{\varepsilon''}{1-p} \ .$$

The dielectric constant ε' and dielectric losses ε'' of the cover substance are connected with the refraction coefficient n and the factor of dielectric losses γ of this resistance by the known equations:

$$\varepsilon' = n^2\left(1 - y^2\right); \qquad \varepsilon'' = 2n^2 y \quad ; \qquad (4)$$

where $n = \lambda/\lambda_g$; $y = \mathrm{tg}\delta/2$; $\delta = \mathrm{arctg}\ \varepsilon''/\varepsilon'$; λ_g is the wave length in the cover material.

For the convenience of the further examination we take by the analogy, that:

$$\varepsilon_1 = n^2(1 - y^2) \quad ; \quad \varepsilon_2 = 2n^2 y \quad ; \qquad (5)$$

where $n = \lambda_b / \lambda_g^{\bullet}$; $y = tg\delta / 2$; $\delta = arctg\,\varepsilon_2/\varepsilon_1$; $\lambda_g^{\bullet}$ is the wave length in the cover substance at the wave spreading under the given angle to the limiting plane surfaces.

Using these notations in equations (3), we will obtain after the transformations:

$$th(2\pi x y + i2\pi x) = N(1 - iY) \quad ; \qquad (6)$$

where $x = l/\lambda_g^{\bullet}$; $N = \dfrac{n^2(1-p)\left[\left(1-y^2\right) + 2y\right]}{n\left(1+y^2\right)}$;

$$Y = \frac{2y - y\left(1 - y^2\right)}{\left(1 - y^2\right) + 2y}$$

Let us divide the equation (6) on the imaginary and real parts. After respective transformations we will get two equations, which describe conditions of the reflectionless wave absorption in the examined system:

$$Ysh4\pi xy + \sin 4\pi x = 0 \quad ; \qquad (7)$$

$$N\left(1+Y^2\right)=th2\pi\chi\gamma-Ytg2\pi x\ . \qquad (8)$$

From their joint solution we obtain:

$$th4\pi\chi\gamma=\frac{2N}{N^2\left(1+Y^2\right)+1}; \qquad (9)$$

$$tg4\pi x=\frac{2NY}{N^2\left(1+Y^2\right)-1}. \qquad (10)$$

Since the conditions of the reflectionless wave absorption in the system are fulfilled in minimum points of the dependence ρ on l and at cover thickness close to values multiple to Δ, we get:

$$x=\frac{2N_0-1}{4}+\Delta; \qquad (11)$$

where N_0 is the number of the zero of the minimum dependence ρ on l, Δ is in general case small, but not the zero value, determined from the solution of equations (10) and (11)

$$\Delta=\frac{1}{4\pi}arctg\frac{2NY}{N^2\left(1+Y^2\right)-1}\ . \qquad (12)$$

Substituting the expression (11) in equations (9) and (10) and excluding from them the value Δ as the intermediate parameter, we obtain:

$$\pi\left(2N_0-1\right)+arctg\frac{2NY}{N^2\left(1+Y^2\right)-1}=\frac{1}{2\gamma}ln\frac{\left(1+N\right)^2+\left(NY\right)^2}{\left(1-N\right)^2+\left(NY\right)^2} \qquad (13)$$

The equation (13) determines the connection between values N and Y, and consequently, between n, y, ε' and ε'' of the cover substance of the two-layer system, at which the full absorption of the incident radiation occurs in the system.

Then as it follows from equations (11) and (12), the required thickness of the cover layer is determined from the expression:

$$\frac{l_0}{\lambda}=\frac{1}{n\sqrt{1-p}}\left[\frac{\left(2N_0-1\right)}{4}+arctg\frac{2NY}{N^2\left(1+Y^2\right)-1}\right] \qquad (14)$$

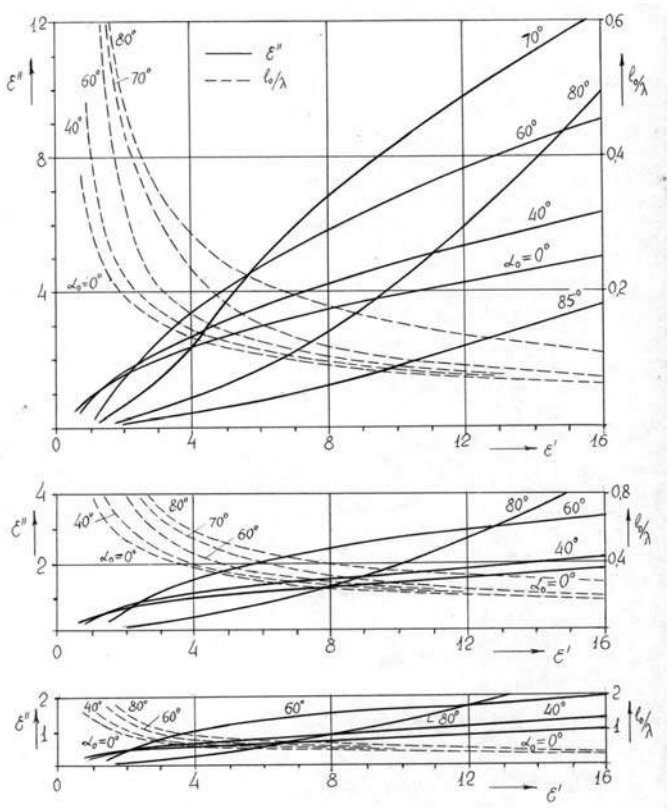

Fig.1. The dependence between the dielectric constant ε' and dielectric losses ε'' at the reflectionless absorption of the cross-polarized wave, incident under the angle α_0 on the two-layer dielectric metal system at N_0=1,2,3. N_0 is the number of the zero minimum of the dependence of the modulus of the wave reflection coefficient on the thickness of the cover layer.

Obtained equations were used for the determination of the dependence between selective values ε',ε'', l_0 of the cover substance, the length of the radiation wave λ and the angle of the wave incidence α_0, at which conditions of the full absorption of the electromagnetic radiation in the examined two-layer system is fulfilled. These dependence are given at N_0=1,2 and 3 on fig.1. At low angles of the wave incidence α_0 and in the region of high values ε' all curves of the family are placed upper of their limiting dependence for α_0=0, which corresponds to the case of reflectionless wave absorption at its normal incidence. At higher values α_0 curves have S-shaped form and with growth α_0 the curves bend point shifts to the part of larger values ε' with the visual growth of the value ε''. Then in the region of low values ε' the part of family curves places below the limiting dependence for α_0=0. The similar type of family curves $\varepsilon''(\varepsilon')$ exits and with N_0 growth, but with closer its position to the X axis (see fig,1b,c)

Selective values of the cover layer thickness l_0 reduce with α_0, ε' growth and increase with N_0 rise, but numerically, they are always higher than the value multiple to λ These deflections value from the multiplicity Δ considerably increases with α_0 and N growth (see fig.2).

Selective values of the wave incidence angle and respective cover layer thickness, at which the wave reflection is absent, may be determined by equations (13)-(14) or graphically by means of fig.1,2; if values ε'_0 and ε''_0 of the cover substance are known for the given frequency of the incident radiation. As it follows from fig.1, at incidence angles, lesser than 60° and at any N_0 dependencies $\varepsilon''(\varepsilon')$, except the region ε'=1,5; are placed upper of the limiting curve, corresponding to the case of the normal wave incidence (α_0=0). If the working point with such values ε'_0 ,

ε''_0 is placed in the coordinate plane [ε', ε''] between 2 limiting curves with values N_0=1 and N_0=K, then it should be expected in such cover substance no smaller, than k-1 of strictly fixed angles of the wave incidence and respective cover layer thicknesses, at which the cover fully absorbs the wave. The greater selected thickness of the cover layer corresponds to the greater angle of the reflectionless wave incidence. At α_0>60° the appearance of additional reflectionless angles of the wave incidence are possible, even in limits of one and the same values N_0.

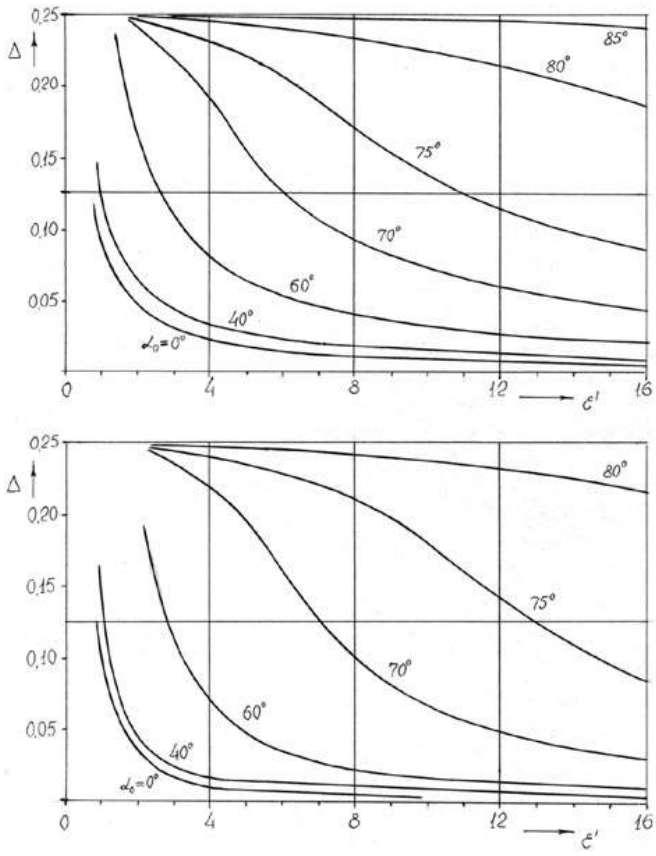

Fig.2. The deflection value Δ of the cover layer thickness on multiple values of wave length quarter in the cover substance versus its dielectric constant and the incidence angle α_0 at N_0=1,2.

For illustration fig.3 presents dependencies of the modulus of the microwave radiation reflection coefficient with the wave length 3.2 cm on the incidence angle on the dielectric-metal system, in which the ethyl spirit and acetone, having according to references at the indicated wave length values ε'=3.85, ε''=10.5 and ε'=20.5, ε''=3.55, are chosen as cover substances. As it follows from the figure, the full microwave radiation absorption is possible in the ethyl spirit layer at wave incidence angles 38.5°(N=2) and 59.2°(N=k) and corresponding to these angles relative thickness of the cover substance layer, equal to l/λ =0.41 and 0.74. For the cover on the base of acetone, the reflectionless incident radiation absorption occurs at wave incidence angles 57.6°(N=2), 69.6° (N=3), 73.2° (N=4) and corresponding (to these angles) relative thickness of the cover substance layer, equal to l/λ=0.17,0.28 and 0.49.

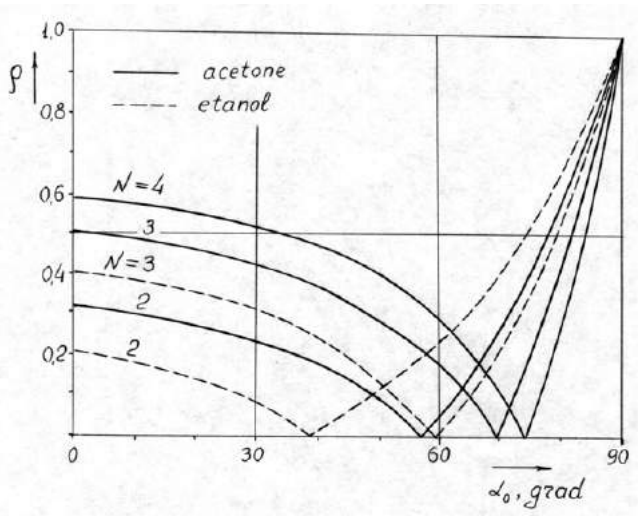

Fig.3. The dependence of the modulus of the cross-polarized wave reflection coefficient ρ on its incidence angle α_0 on the two-layer electric-metal system.

Conducted theoretical investigations confirm the possibility of the experimental phenomena observation of the reflectionless absorption of the electromagnetic radiation of the given frequency in the two-layer dielectric-metal system at strictly fixed of layer thicknesses for the applied cover materials and for incidence angles of a wave with the fixed polarization.

[1] *R.M. Kasimov*. Fizika, 2002, v. 8, №1.
[2] *A.F. Kharvei*. Tekhnika sverkhvisokikh chastot M: Sov. Radio, 1965, chast' 1, p.724 (in Russian).
L.M. Brekhovskikh. Volni v sloistikh sredakh M: Izd.AN SSSR, 1967, p.502 (in Russian).
[3] J. *Preißner.* NTZ Arch.1989, v.11. № 4. p..175-182
Y.Y. Akhadov. Dielektricheskiye parametri chistikh zhidkostey M: Izd. MAI, 1999, p.856 (in Russian).

E.R. Qasımov

DİELEKTRİK-METAL İKİLAYLI SİSTEMƏ BUCAQ ALTINDA DÜŞƏN PARALEL-POLYARİZASİYALI ELEKTROMAQNİT DALĞASININ ƏKS OLUNMASI

Metal təbəqəyə çəkilmiş udan dielektrik layına bucaq altında düşən paralel polyarizasiyalı elektromaqnit dalğasının tam əks olunmayan udmasının əmələgəlmə şərtləri tapılmışdır. Həmin şərtlərin örtüyün qalığından, dalğanın düşmə bucağından və örtüyün dielektrik xassələrindən asılılığı tədqiq edilmişdir.

Э.Р. Касимов

ОТРАЖЕНИЕ ПАРАЛЛЕЛЬНО-ПОЛЯРИЗОВАННОЙ ЭЛЕКТРОМАГНИТНОЙ ВОЛНЫ ПРИ ЕЕ ПАДЕНИИ ПОД УГЛОМ НА ДВУХСЛОЙНУЮ СИСТЕМУ ДИЭЛЕКТРИК-МЕТАЛЛ

Найдены условия возникновения полного безотражательного поглощения параллельно-поляризованного электромагнитного излучения при его падении под углом на слой поглощающего диэлектрика, нанесенного на металлическую подложку. Исследуется их зависимость от толщины покрытия, угла падения и диэлектрических свойств материала покрытия.

Received: 14.05.02

THE INFLUENCE OF THE TEMPERATURE MODE ON THE RELAXATION PROCESS VELOCITY IN POLYMERS

N.F. AHMEDOV, S.K. ABUTALIBOVA, T.I. ISMAILOVA, F.A. AHMEDOV
Baku State University
Acad. Z. Khalilov str., 23, Baku

The relaxation process in polymers has been investigated at quasi-linear temperature variation. Taking into consideration the fact, that the relaxation time obeys the Alexandrov-Lazurkin-Gurevich formula, the rheology equation of visco-elastic body has been solved. The analysis of the obtained solution has show that if the polymer has high elasticity then the temperature, at which the process rate is equal to zero, should not be more, than half of the two characteristic temperatures sum. It has been revealed, that the process rate at some temperature range passes through minimum. This fact is explained by the change of the macromolecules conformational state.

The main peculiarity of mechanical properties of polymers is a relaxation processes proceeding in them. The processes nature sharply depends on the temperature regime. The thermo- mechanical method is convenient for determination of specific characteristics of mechanic polymers properties [1]. The essence of this method consists of the determination of the temperature dependence of the deformation on the temperature at the constant interaction on the polymer of the external voltage. In the present paper the high-elastic state of the amorphous linear polymer is reproduced by a model of the visco-elastic Kelvin body, and the delay time is described by the Alexandrov-Lazurkin-Gurevich formula [2].

$$\tau = \tau_0 e^{\frac{u-\gamma\sigma}{RT}} . \qquad (1)$$

In thermomechanical investigation the temperature varies in time. Then in the previous formula τ and T will be $\tau(t)$ and $T(t)$, respectively. Let the temperature varies according to the following dependence on time,

$$T = T_c + T_T(1 - e^{-\alpha t}), \qquad (2)$$

where T_c, T_T are glassing and yielding temperatures, respectively and α is the scale factor. At thermomechanical tests the linear heating regime is usually applied. The choice of the indicated regime of the temperature variation on time allows to avoid mathematical difficulties. At not large times the selected dependence slightly differs from the linear one.

The rheology equation of the visco-elastic body, applied to the Kelvin model, may be put down in the following simple form [2].

$$\frac{d\varepsilon}{dt} = (\frac{\sigma}{E} - \varepsilon)\frac{1}{\tau(t)}$$

Dividing on variables and integrating, we obtain

$$\varepsilon = \frac{\sigma}{E}\left[1 - exp(-\int_0^t \frac{dt'}{\tau(t')})\right] \qquad (3)$$

With regard (1) and (2) in (3) we receive the deformation dependence on the time in the following form:

$$\varepsilon = \frac{\sigma}{E}\left\{1 - exp\left(-\frac{1}{\tau_0}\int_0^t exp\left[-\frac{u-\gamma\sigma}{R(T_c + T_T(1-e^{-\alpha t'}))}\right]dt'\right)\right\},$$

or

$$\varepsilon = \frac{\sigma}{E}\left\{1 - exp\left(-\frac{A}{\alpha\tau_0}\left(\frac{1}{T_c + T_T - T}\left(1 + \frac{A}{4T}\right) - \frac{1}{T_c + T_T - T_c}\left(1 + \frac{A}{4T_0}\right)\times\right.\right.\right.$$
$$\left.\left.\left.\times\frac{1}{T_c + T_T}\left(1 + \frac{A}{T_c + T_T}\right)\left(\frac{T}{T_c + T_T - T} - \frac{T_o}{T_c + T_T - T_c}\right) + \frac{A}{4(T_c + T_T)}\left(\frac{1}{T} - \frac{1}{T_o}\right)\right)\right)\right\} \qquad (4)$$

where $A = \frac{u - \gamma\sigma}{R}$.

Simplifying the integration result we have confined by first two sum terms in the range of the integral exponentional function and neglected logarithmic terms because of its small value in comparison with other terms.

As it is seen from the obtained expression at $T=T_c$ the exponent is equal to zero, and respectively, the deformation is equal to zero, but at $T=T_c+T_T$ the deformation approaches to $\frac{\sigma}{E}$. The same result is obtained for the deformation of the examined model by the time at the constant voltage.

According to the problem condition T_c corresponds to the polymer transition from glassy to high elastic state. At $T \leq T_c$ the deformation of the examined model is equal to zero. It means, that neither segments nor macromolecules can change their mutual position (order) under the influence of the applied voltage. As a rule, at thermomechanical tests the applied voltage is smaller than that of the forced deformation. The deformation equality to zero at $T=T_0$ shows, that in the present problem the above-mentioned condition is fulfilled, the heat motion and activation under the influence of the external voltage are not yet enough for the potential barrier passage, the interaction energy between kinetic units, including segments, exceeds that of the heat motion and the work, conducted by the external force, all together.

The separate segments transition occurs at the temperature growth and twisted macromolecules acquire the opportunity to rectify under the influence of heat and external force.

The typical peculiarity of polymers in the glassy state with hard chains is the structure porosity and the possibility of the free links motion. It is explained by the low fragility of polymers in comparison with low-molecular glasses, where small molecules may transfer as a one whole, and where any visible growth of the intermolecular distance, being higher than the equlibrium distance, means the start of the material division on component parts.

Though the transition velocity of separate links of the glassy polymer may be negligibly low, it increases at the effect of the external voltage, making easier the internal potential barriers passage. Therefore the quick variations of the macromolecule conformation at rather great loads are possible. The voltage growth leads to the A coefficient reduction, as it is seen from the formula (4). The forced elasticity occurs at $\gamma\sigma$. From that moment according to formulas (5) and (7) the deformation velocity and relaxation time in the narrow temperature range quickly grows and then the process velocity is set by the polymer transition in high-elastic state.

The obtained dependence of the deformation on the temperature shows, that the deformation develops non-monotonous. Its variation velocity has the following form.

$$\frac{d\varepsilon}{dT} = \frac{\sigma a}{E\alpha\tau_0} \frac{4T^2 + 2AT - A(T_c + T_T)}{2T^2(T_c + T_T - T)^2} \cdot e^{f(T)} \qquad (5)$$

where *f(T)* is the exponent of the exponential function of the expression (4).

As it is seen from the latter equation the deformation development velocity depends on the relationship between the coefficient A and the temperature. It may be both positive and negative, and at

$$T_n = \frac{A}{4}\left(\sqrt{1 + 4\frac{T_c + T_T}{A}} - 1\right) \qquad (6)$$

it is equal to zero, and this condition is fulfilled for any $A>0$, i.e. $U > \gamma\sigma$.

The calculations show, that when the coefficient A varies from $4x10^{-4}$ (T_c+T_T) up to $2x10^3$ (T_c+T_T) the temperature, at which the relaxation rate is equal to zero, varies from *0,02* (T_c+T_T) up to *0,5* (T_c+T_T), and the straight line, determined by the expression $T=0,5(T_c+T_T)$, is asymptote of the given dependence .

The *A* coefficient value characterizes the hardness of the deformed polymer system. The obtained results mean, that whatever hard is the macromolecule, if it reveals the high-elasticity, then the temperature, at which the thermomechanical curve is going out on the straight line, should not exceed the half of the sum of two characteristic temperatures.

At high values of the coefficient *A* in the temperature interval from T_c up to T_n the deformation velocity is negative, i.e. the compression of the polymer block occurs. It is described by the fact, that the frozen structures are defrosted, kinetic units acquire some mobility and under the force effect, caused by the system hardness, are much tighter packed. At further temperature increase the modulus of the negative velocity reduces up to zero ($T= T_n$), and then the deformation grows. The wider is the temperature range of negative values of the deformation velocity, the higher is the hardness of the polymer system. The upper limit of this region approaches to the half of the sum of two typical temperatures. It should be noted, that the "collapse" velocity of the polymer block is very small, it is much smaller, than the velocity of the temperature variation is [3,4].

The smaller the molecule flexibility is, the larger is the segment sizes, the higher is T_c, the higher is the transition temperature of the polymer chain from one conformational state into another. Since the segment value is directly connected with the T_c value, then the latter also depends on the test mode. At the reduction of the temperature action duration, i.e. the flexibility variation might not be revealed at its velocity growth, so as the macromolecule deformation, demanding the passage of the intermolecular and innermolecular interaction forces, occurs within the final time interval.

By comparing the obtained formula with the formula of the deformation relaxation at the constant temperature we obtain for the time delay the following expression:

$$\tau = \tau_0 e^{\frac{AT_T\left[2T_T(T_c+T_T)-T(2T_c+T_T)\right]}{8TT_c(T_c+T_T-T)(T_c+T_T)}} \qquad (7)$$

As it is to be expected, the time delay depends on the *A* coefficient, expressing the activation energy of the process and temperature. It is monotonously growing function of the activation energy. But versus the temperature the time delay has high values at temperatures, close to T_c, but it sharply increases at the negligible growth. This reduction is not monotonous. Not only the variation of the time delay value occurs, but also that of the velocity. At the achievement of the temperature, determined by the formula, the velocity of the time delay fall passes through minimum.

$$T_m = \frac{2T_T(T_c + T_T)\left(1 - \sqrt{1 - \frac{2T_c + T_T}{2T_T}}\right)}{2T_c + T_T} \qquad (8)$$

Taking into consideration the fact, that the activation energy is higher, than that of the heat motion and $(2T_c+T_T)<2T_T$, we get the equality of temperatures T_n and T_m by determined formulas (6) and (8), respectively. It follows, that temperatures T_n and T_m for the examined model are structurization temperatures or neck-formation. The structurization temperature (neck-formation) depends on the loading mode (deformation) and the velocity of the temperature variation. This dependence is not seen from the formula (8). If we take into consideration, that T_c and T_T are functions of the load and temperature variation mode, then the dependence of the structurization temperatures on these modes becomes obvious [5].

The process velocity is determined by the coefficient α in the formula (2). At the fulfillment of the given formula linearity, i.e. at $\alpha<<1$, the velocity of the temperature variation may be accepted.

$$\frac{dT}{dt} = \alpha T_T$$

The velocity of the temperature variation increases with the α growth, and respectively, T_m grows, the system hardness becomes higher.

Such circumstance corresponds to the temperature time superposition in polymers. The temperature growth, intensifying the heat motion, accelerates the rectification and segment transition under the voltage effect, the temperature reduction, delay these processes, decelerates deformation. But with the growth of temperature variation velocity, the deformation is not in time. At the change of the latter, the process is delayed, and the velocity is reduced. As it was noted, at the linear amorphous polymers, the sample extension is made of 2 components, one of which is caused by the chain smoothing, and the second one is caused by the transition of segments one with respect to another. In some time of the mechanical and temperature fields application the equilibrium between these fields effect is established and almost stationary mode begins.

[1] *V.A. Kargin.* "Izbranniye trudi " Problemi nauki o polimerakh." M:Nauka, 1986, p. 96-106.
[2] *A.A. Malkin*, *A.A. Askadskii*, *V.V. Kavriga*. "Metodi izmeneniya mekhanicheskikh svoystv polimerov." M: Khimiya, 1978, p. 43-45.
[3] *A.E. Teishev*, *A.Y. Malkin*. "Visokomol. Soyedin." A, 1990, v.8, p. 1746.
[4] *G.M. Golovachev*, *Y.Y. Gotlib*. "Visokomol.Soyedin" A, 1996,v.38, №6, p. 993.
[5] *Y.Y. Gotlib*, *A.A. Gurtovenko.* "Visokomol.Soyedin" A, 2001, v. 43, № 3, p. 496.

N.F.Əhmədov, S.K. Abutalıbova, T.İ. İsmayılova, F.A. Əhmədov

POLİMERLƏRDƏ RELAKSASİYA PROSESİNİN SÜRƏTİNƏ TEMPERATURUN DƏYİŞMƏ TƏRZİNİN TƏSİRİ

İşdə temperaturun kvazixətti dəyişməsi halında polimerlərdə relaksasiya prosesi öyrənilmişdir. Tədqiqatda relaksasiya müddətinin Aleksandrov – Lazurkin – Qureviç düsturuna tabe olduğu qəbul edilərək özlü elastik jismin reoloci tənliyi həll olunmuşdur. Həllin təhlili göstərir ki, polimer yüksək elastikliyə malikdirsə, prosesin sürətinin sıfra bərabər qiymətinə uyğun gələn temperatur iki xarakteristik temperaturun cəminin yarısından böyük olmamalıdır. Məlum olmuşdur ki, relaksasiya prosesinin sürəti müəyyən temperatur intervalında minimumdan keçir. Bu fakt polimerin konformasiya halının dəyişməsi ilə izah edilmişdir.

Н.Ф. Ахмедов, С.К. Абуталыбова, Т.И. Исмаилова, Ф.А. Ахмедов

ВЛИЯНИЕ ТЕМПЕРАТУРНОГО РЕЖИМА НА СКОРОСТЬ РЕЛАКСАЦИОННОГО ПРОЦЕССА В ПОЛИМЕРАХ

Был изучен релаксационный процесс в полимерах при квазилинейном измерении температуры. Принимая, что время релаксации подчиняется формуле Александра-Лазуркина-Гуревича, было решено реологическое уравнение вязкоупругого тела. Анализ полученного решения показал, что если полимер обладает высокой эластичностью, то температура, при которой скорость процесса становится равной нулю, не должна превышать половины суммы двух характеристических температур. Было выявлено, что скорость процесса при некотором температурном интервале переходит через минимум. Этот факт объясняется изменением конформационного состояния макромолекул.

Received: 14.10.02

THE LOW-FREQUENCY DIGITAL SHAPER OF REFERENCE PULSES

Ch.O. QAJAR, S.A. MUSAYEV, M.R. MENZELEYEV
Institute of Physics, Azerbaijan National Academy of Sciences
370143, Baku, H. Javid ave. 33.

The digital device for reference pulses formation with the high accuracy (<0.3 %) which allows to adjust the phase of a reference signal of recording systems with low-frequency modulation was developed and constructed.

In microwave spectra of polyatomic molecules displacements or enlargements of spectral lines related with the frequency of square-wave stark modulation are often observed [1].

In particular, this effect may be observed in spectra of asymmetric top type molecules with double RF-MW resonances, when magnitudes of its radiofrequencies are near or coincide with frequency of molecular modulation [2].

To exclude such interactions it was decided to construct microwave spectrometer with low frequency stark modulation. For this purpose the square-wave stark modulator (SWSM), a generator of unipolar rectangular impulses was constructed earlier [3].

In this paper the description of low-frequency digital shaper of reference pulses (SRP) is presented (fig.1). It functionally replaces the available analog phase shifters, which use at low frequencies is limited by them phase shift dependence from frequency of modulating pulses, temperature, magnitude of supply voltage, instability of a zero line and other factors, in a recording part of standard microwave spectrometer and enables to adjust phase of a reference signal of the phase-sensitive detector with the high accuracy (not worse than 0.3 %).

The digital circuit of SRP (fig.2) consistently divides frequency of the driving generator and provides a capability of adjustment of an angle of phase shift between pulses of SWSM and reference signal of phase-sensitive detector in a range 0-360° with the step 1°.

The schematic circuit of SRP is presented on fig.3. The basis of the circuit is decimal counters - dividers D1, D2 and D3, as which the microchips CD4017 are used. The pulse former 2, on a signal of coincidence of pulse sequences of counters D1, D2, D3, forms reference pulses of the modulating generator on its output. Either fronts or falls of these pulses (depending on position of the «+ 180» switch) synchronize the pulse former 1, the similar coincidence circuit of which receives those pulse sequences of counters D1-D3, which given by «1», «10», «100» switches positions and been in congruence with the given angle of shift of a phase. In result on the pulse former 1 output there are reference pulses of the phase-sensitive detector moved on a phase on an angle, unequivocally determined by a position of «1», «10», «100» and «+ 180» switches. The coincidence circuits of both pulse formers compose by elements of a logic microchip 3NO-AND D4 (CD4023). Directly forming units are the D-triggers of microchip D5 (CD4013).

The angle of a phase shift is a digital function of a position of the appropriate switches and is independent of the entrance frequency of the specifying generator and other factors capable to influence on the analog phase shifter and, finally, reduce the occurrence of tool mistakes in measurements.

Presented SRP steadily works in a range of output frequencies from 0 up to 10kHz. Thus frequency of following of pulses of the driving generator $F=360f$, where f is a frequency of reference (output) pulses. At a level of a supply voltage of the circuit + 9V the reference pulses in all range of operating frequencies have the following parameters: on-off time ratio 2, front duration 250ns, fall duration 200ns.

Thus the increase of a frequency range is possible not only by usage of more high-speed microchips, but also, if there is no necessity for the so high accuracy of adjustment of a phase, by an increase of a step of quantization of a phase.

SRP can find a use as phase rotating intermediate in any systems of synchronous detecting. In case of use SRP in structure of microwave spectrometer with molecular modulation it can be built in structure of the modulating generator or (and) of the synchronous detector as an electronic card, or, being supplemented by a power unit to be made out as the separate device.

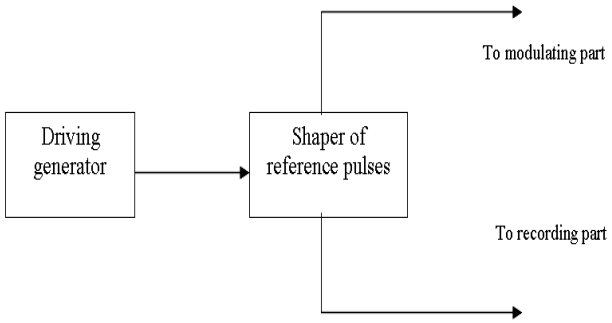

Fig.1 SRP connection block-diagram

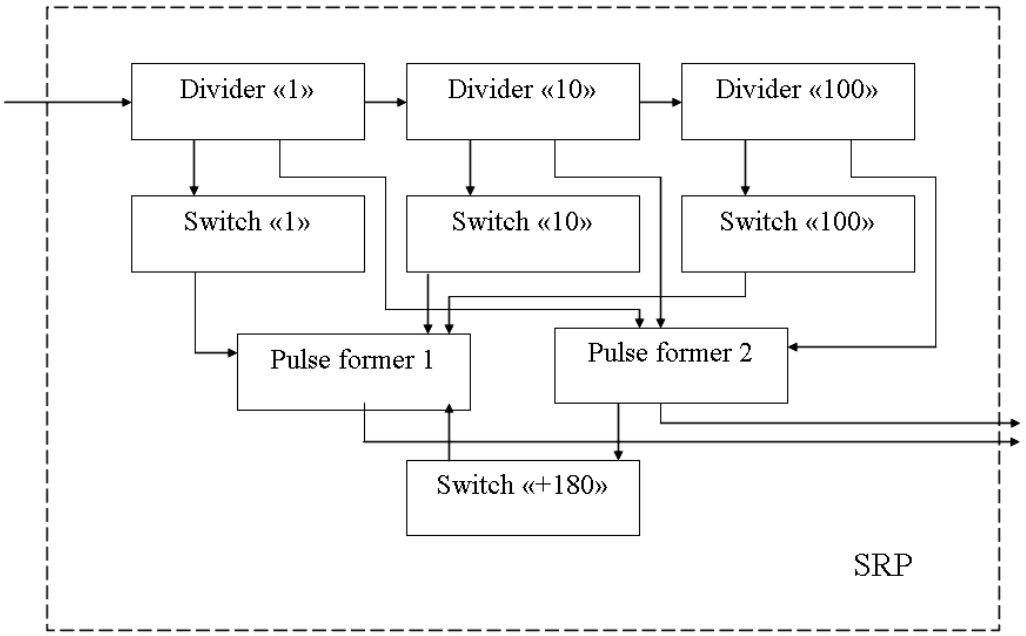

Fig.2 Block-diagram of shaper of reference pulses

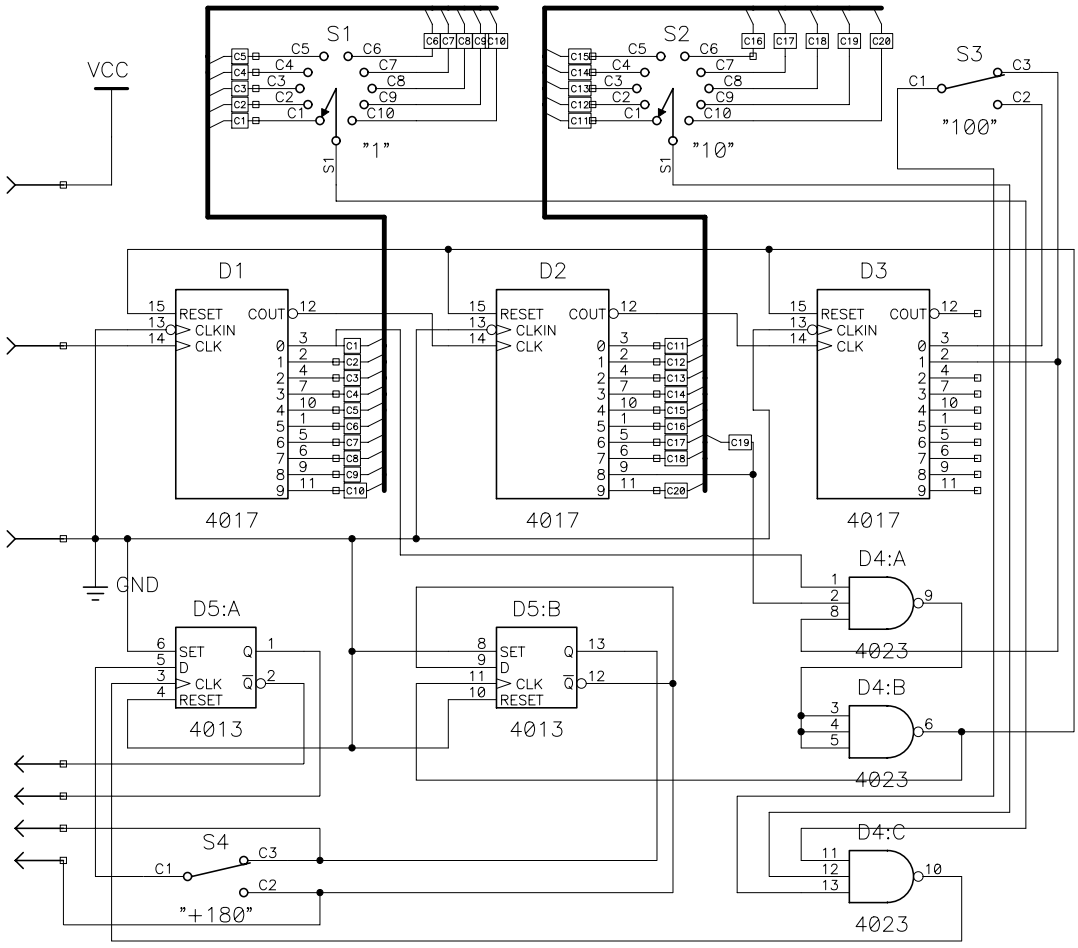

Fig.3 Schematic diagram of shaper of reference pulses

[1] *E. Hirota.* Microwave spectrum of isopropanol, J. Chem. Phys. 2001, v.1, №2, p.240-248.
[2] *S.A. Musayev.* Reports of AS of Azerbaijan 2001, vol. LVII, №1-3, p. 38-43.
[3] *Ch.O. Qajar, S.A. Musayev, M.R. Menzeleyev.* «Generator of unipolar rectangular impulses» Proc. of Az.TU, Baku 2001, p. 141-144.

Ç.O. Qacar, S.A. Musayev, M.R. Menzeleyev

AŞAĞI TEZLİKLİ ÖZÜL İMPULSLARIN RƏQƏMLİ FORMALAŞDIRICISI

Aşağı tezlikli qeydetmə sistemlərinin özül tezlik siqnalının fazasını yüksək dəqiqlik ilə (<0.3%) qoymağa imkan verən özül tezlik impulsları formalaşdırılan rəqəmli qurğu işlənib hazırlanmış və düzəldilmişdir.

Ч.О. Каджар, С.А. Мусаев, М.Р. Мензелеев

НИЗКОЧАСТОТНЫЙ ЦИФРОВОЙ ФОРМИРОВАТЕЛЬ ОПОРНЫХ ИМПУЛЬСОВ

Разработано и изготовлено цифровое устройство для формирования опорных импульсов, позволяющее с большой точностью (<0.3%) устанавливать фазу опорного сигнала регистрирующих систем с низкочастотной модуляцией.

Received: 14.10.02

ON THE COMMUTATOR CONSTRUCTION WITH THE APPLICATION OF DIODES ON THE BASE OF COMPOUND SEMICONDUCTORS

G.A. ABBASOV, M.N. IBRAGIMOV, M.J. RADGABOV
Azerbaijan Architectural-Building University,
h.5, A.Sultanova, Baku, Azerbaijan

Peculiarities of the switching diode on the base of compound semiconductors are considered. The switching diode has such indices as memory property, two stable states, it does not consume the energy from the feed supply. These properties allow applying the switching diode as a switching element. The construction of the rectangular commutator with the application of the switching diode on the base of compound semiconductors as the switching element is described. The process of connection installation between input and output tappings of rectangular commutator is stated.

The development of the electron technique leads to the wide use of quick-acting, small-sized, non-contact elements in various spheres. Each sphere raises to electron elements its specific claims.

One of the main spheres, where electron elements are widely used, is the sphere of switching technique [1]. The sphere of the switching technology raises to electron elements such claims: they should have the memory property, two stable states and should not consume the energy in stable states [2]. Among electron elements, used in the switching technology, the switching diode on the base of compound semiconductors has the great interest [3, 4, 5].

The scheme of the switching diode on the base of the semiconductors Cu_2Se, which is worked out by researchers of Institute of Physics of Azerbaijan AS, is represented on fig.1.

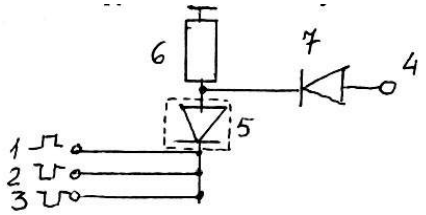

Fig 1. The scheme of the switching diode on the base of the semiconductor Cu_2Se.

The scheme of the switching diode contains: tappings (1, 2, 3) are input, the tapping (4) is output, element (5) is the switching diode, element (6) is the resistive resistance, element (7) is the rectifying diode. The switching diode operates on the following principle.

The diode (5) switches in one of two stable states, corresponding to the open state, at the positive signal receipt on the input tapping (1).

The signal, corresponding to the informational signal, is received on the output tapping (4) under the influence of the small negative signal, received on the input tapping (2). In the open state of the switching diode, the informational signal on the exit may be received infinite number of times. The negative signal is given on the end of information transmission with the sufficiently high amplitude and the switching diode (5) is locked. After this the switching diode is ready for the opening and the new information transmission.

Thus, it is good to use the switching diode on the base of the semiconductor Cu_2Se as the switching element. Let us observe the construction of the rectangular commutator with the use of switching diodes. The commutator scheme is given on fig.2.

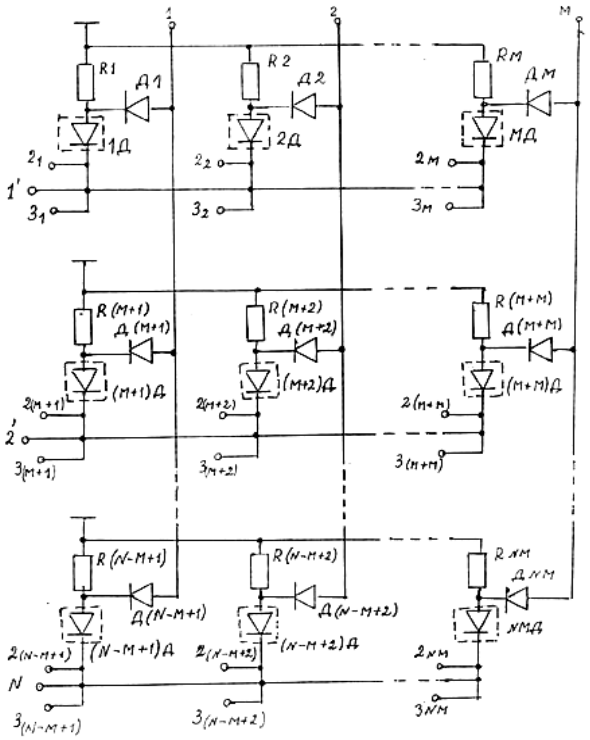

Fig.2. The commutator scheme with the application of switching diodes.

The commutator has the rectangular shape and contains: input tappings (1,2…,N), output tappings (1,2…M), switching diodes {1D,2D,…..MD, (M+1)D,(M+2)D,….; (M+M)D,….(N-M+1)D,(N-M+2)D,….NMD}; tappings for diodes switch in the open state (2_1,2_2,…2_m,$2_{(m+1)}$,$2_{(m+2)}$,…, $2_{(m+m)}$,$2_{(N-m+1)}$,$2_{(N-M+2)}$,….,$2_{(NM)}$), tappings for diodes switch to the closed state (3_1,3_2,…,3_M,3_{M+1},3_{M+2},…,3_{M+M},…,3_{N-M+1},…, 3_{N-M+2}…,3_{NM}), rectifying diodes [D1,D2,….DM,D(M+1), D(M+2),..,D(M+M),D(N-M+1),D(N-M+2),…,DNM]; limiting resistive resistance [R1,R2,…,RM,R(M+1),R(M+2),…,R(N+M),R(N-M+1), R(N-M+2),…,RNM].

The commutator operates on the following principle. One of 1D,2D,…,MD,(M+1)D,(M+2)D,…(M+M)D,…,(N-M+ 1) D, (N-M+2)D,NMD switching diodes are led to the open state for the connection installation between one of 1,2,..M

entries and one of 1,…N exits. The positive signal on one of $2_1,2_2,\ldots 2_m,2_{(m+1)},2_{(m+2)},\ldots\ldots,2_{(m+m)},2_{(N-m+1)},2_{(N-m+2)},\ldots,2_{(NM)}$ tappings is given to set the respective switching diode to the open state. Information transmission between given entry and required exit is provided after the opening of the respective switching diode. The closed state of the respective switching diode is provided on the end of information transmission between the given entry and required exit of the negative signal with the sufficiently high amplitude, given on one of $3_1,3_2,\ldots,3_M,3_{M+1},3_{M+2},\ldots,3_{M+M},\ldots,3_{N-M+1}\ldots,3_{N-M+2}\ldots,3_{NM}$ tappings. The closed switching diode is again led to the open state by the positive signal for next information transmission.

Then signals, received on the exit of the switching diode through rectifying diodes, do not pass to the exit. The pulses transmission from the given entry to the required exit only with such polarity, which corresponds to the polarity of informational signals, is provided by means of rectifying diodes D1,D2,…,DM,D(M+1),D(M+2),..,D(M+M),D(N-M+1),D(N-M+2),…,DNM.

It is necessary to note, that in the commutator switching diodes in two stable states (that is in open and closed states) do not consume the energy from the feed source. This peculiarity of the switching diode makes the commutator scheme profitable from the economical point of view.

Let us consider the example of the connection installation between one of input and one output tappings.

If, for example, it is required to connect the output (input) tapping (2) with the input (output) tapping (1), then the switching diode 2D is led to the open state. The positive signal is given on the tapping (2_2) for this purpose. The informational signal from the input tapping ($1^{'}$) through the switching diode 2D and through the rectifying diode D2 transfers to the closed state on the signal, received from the taping (3_2), on the end of the informational signal transmission. After this the switching diode 2D is ready for the opening and the next informational signal transmission.

[1] *O.N. Ivanova.* Electron switching-Issue "Communication", M.1971.

[2] *V.E. Benesh.* Mathematical basis of the phone theory-Translation from English; M."Communication" issue, 1968.

[3] *G.A. Abbasov.* The construction of logic and memory schemes with the application of new switching diodes on the base of compound semiconductors-Reports of republic conference of young physicists, 30 May, 1972.

[4] *G.B. Abdullayev, Z.A. Aliyarova, G.A. Abbasov etc.* "The author certificate № 82581-Priority from 23 January, 1972.

[5] *G.B. Abdullayev, E.N. Zamanova, G.A. Abbasov, Z.A. Aliyarova.* The semiconductive switch-The author certificate № 664419-Priority from 7 December, 1979.

H.A. Abbasov, M.N. İbrahimov, M.Y. Rəcəbov

MÜRƏKKƏB YARIMKEÇİRİCİ DİODLARIN KOMMUTATORLARDA TƏTBİQİ

Məqalədə mürəkkəb yarımkeçirici diodlar üzərində kommutator qurğularının yığılmasının mümkünlüyü göstərilmişdir. Çevirici diodlar iki tarazlıq vəziyyətdə olmaqla yaddaşa malikdirlər. Özü də bu vəziyyətdə mənbədən enerji tələb etmirlər. Bu xüsusiyyət həmin diodlardan yaddaş elementi kimi istifadə etməyə imkan verir. Məqalədə düzbucaqlı kommutator təsvir edilmişdir. Eyni zamanda kommutatorun giriş və çıxış sıxacları arasında birləşmənin yaradılma prinsipi izah edilmişdir.

Г.А. Аббасов, М.Н. Ибрагимов, М.Я. Раджабов

О ПОСТРОЕНИИ КОММУТАТОРА С ИСПОЛЬЗОВАНИЕМ ДИОДОВ НА ОСНОВЕ СЛОЖНЫХ ПОЛУПРОВОДНИКОВ

Рассматриваются особенности переключающего диода на основе сложных полупроводников. Переключающий диод обладает такими показателями, как свойство памяти, два устойчивых состояния, непотребление энергии от источника питания и др. Эти свойства позволяют использовать переключающий диод в качестве коммутационного элемента. Описывается построение прямоугольного коммутатора с использованием переключающего диода на основе сложных полупроводников в качестве коммутационного элемента.

Излагается процесс установления соединений между входными и выходными выводами прямоугольного коммутатора.

Received: 08.07.2002

ELECTRIC PROPERTIES OF $AgFeS_2$ IN THE AREA OF THE PHASE TRANSITION

S.A. ALIYEV, Z.S. GASANOV, S.M. ABDULLAYEV
Institute of Physics, Azerbaijan National Academy of Sciences.
370143, Baku, H. Javid ave. 33.

The research of temperature dependences of the Hall coefficient *R(T)* and the electroconductivity $\sigma(T)$ of $AgFeS_2$ in the area of the phase transition (PT) was carried out. Parameters of the phase transition, determining the spreading degree, were found. It was shown, that in $AgFeS_2$ PT is of considerably eroded character.

INTRODUCTION

Solids, with a polymorphism property, have always been under investigation. It is caused both by practical and scientific interests, following from the polymorphism property. It is known, that physical properties, such as: band structure, electric, segneto-electric, heat, magnetic properties also change at the polymorphous transformation.

Jump-shaped variations of physical properties of the substance at PT are the base for the creation of different transformers.

Reliable data about the value and the rule of the investigated effect change in the area of PT, the temperature range of the transition, the impurities influence on these properties, the deflection from the steochiometry, electric and magnetic fields, ionizing radiation and other effects are necessary for the stable work of such devices.

The collection of such data allows to reveal ways of the sensitivity increase, stabilization and phenomena control at PT, to investigate rules of separate phases distribution and gives the information for the interpretation of physical properties, proceeding at PT. The interest to the PT research has grown after the high-temperature super-conductors discovery. One of actual tasks of the given tendency is the matter of the separate phases coexistence in the transition region, and the determination of PT parameters, determining the spreading degree. Theoretical aspects of eroded phases transition (EPT) are considered in [1, 2].

Experimental data are presented in [3-7]. In paper [7] Ag_2Te electric and heat properties in PT area are interpreted in framework of the EPT theory. Parameters, determining the spreading degree, were calculated, it was established, that in Ag_2Te structural PT's have the eroded nature. Electric and magnetic fields, impurities, the excess of Te (up to 0,75 %) and Ag (up to 0,25 %) have not the essential influence on the spreading degree. It was shown, that PT parameters, calculated by data of heat and electric properties of the phase transition are in agreement with data, obtained from temperature dependences of the *X*-rays reflections intensities [3,4] and may be applied for the determination of PT parameters of first and second rows.

Triple compounds $AgFeTe_2$, $AgFeSe_2$, $AgFeS_2$ are analogues to Ag_2Te, Ag_2Se and Ag_2S. They have the polymorphism property and at PT electric and heat properties are changed by the jump. A number of works are devoted to the research of kinetic phenomena and the electron dispersion law in $AgFeTe_2$, $AgFeSe_2$, and $AgFeS_2$ [8-10]. However the above-mentioned problems, connected with PT, are not discussed in them. Therefore in the present paper the task is to investigate the temperature dependence of the Hall coefficient *R(T)* and the electroconductivity $\sigma(T)$ in $AgFeS_2$ in the PT area, to determine PT parameters and to reveal the spreading degree.

EXPERIMENTAL RESULTS AND THEIR DISCUSSION

It should be noted, that the experimental device, allowing to conduct measurements to a high precision and great time lag in the PT area in adiabatic and isothermal conditions, is needed for the successful fulfillment of the above-mentioned research. In paper [11] the cryostat construction, allowing to conduct simultaneously complex research of electric, galvanic and thermomagnetic, and also heat properties of the solid body in the wide temperature range [2-400 K] is given. Some changes in cryostat construction are made for such research realization in the PT area. Particularly, the working part of the cryostat (where the sample of the metal casing is installed) is considerably removed from its soldered part. The sample installation is conducted by more high-heat solder than the casing is. The sample and the standard are soldered on the additional support with the bad heat conduction (testalite, covered by the copper) at the realization of the differential thermal analysis (DTA). Hot and cold junctions of differential thermocouples are soldered on the face edge of the sample and the standard on the identical level. It allows to remove the background signal of the thermocouple and to record $\Delta T_y(T)$ without noises and it provides the high precision of the measurement of the released and absorbed heat in the PT area.

DTA may be measured in isothermal and adiabatic conditions. The heat source provides the constancy of the heat velocity *T(t)* (beginning from 0,1; 0,2 … K/min.)

Temperature dependences of the Hall coefficient *R(T)* and electroconductivity $\sigma(T)$ of $AgFeS_2$ are presented on fig.1.

As it is seen the electroconductivity at PT by the jump increases more than an order. It is much more, than it is in $AgFeTe_2$ and $AgFeSe_2$. Because of the strong electron gas degeneration in $AgFeS_2$, the Hall coefficient has a low value, therefore it is difficult to fix its change in the PT area.

Such strong change of $\sigma(T)$ at PT gives perspectives to create switching devices on its base. The problems of α and β phases coexistence are observed in theoretical papers [1,2]. Formulae, allowing to calculate PT parameters, determining the PT spreading degree in the condensed system, according to which the switching function *L* of another phase is introduced, are presented in them. Without going into details of the theory and application methods, we refer to paper [7], where methods of the experimental data proceeding and formulae, applied for this purpose, are described in details [3-6]. The function *L* may be determined by the formula (3),

where the constant α, characterizing the PT spreading degree, which depends on the volume of possible phase functions, energy and temperature, is included.

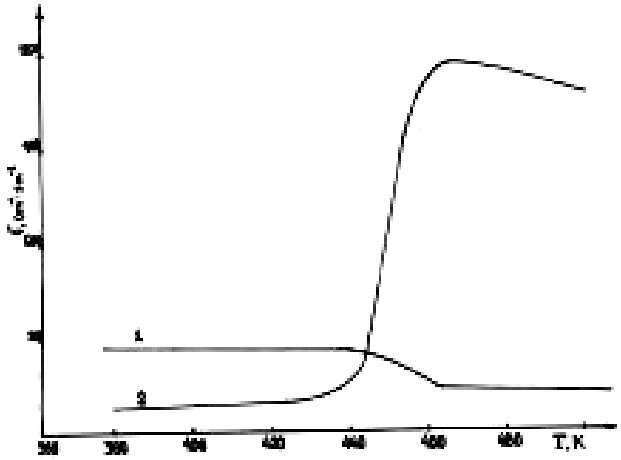

Fig. 1. Temperature dependences of Hall coefficient $R(1)$ and electroconductivity $\sigma(2)$ in $AgFeS_2$.

Taking into consideration, that the switching function characterizes the relative phase share in their coexistence area, it may be introduced as a formula (4). The mass distribution of each phase m_α and m_β is determined by the experimental data of any temperature dependence in the PT area.

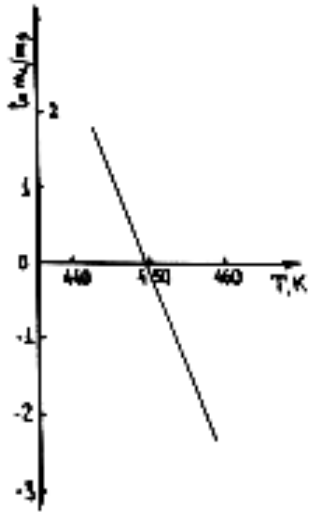

Fig. 2. Temperature dependence of the phases distribution *ln*, m_α, m_β in $AgFeS_2$.

Then T_0, at which both phases masses are equal quantitatively and constant α, are determined by the dependence of *ln*, m_α, m_β on T. Such dependence for $AgFeS_2$, obtained by $\alpha(T)$ data, is presented on fig.2.

The point of the straight line crossing (interaction) with the T axis gives the value T_0. The formula (5), from which it follows, that the straight line slope (ln, m_α, m_β) gives the constant α value, follows from the comparison of formulae (3) and (4). The temperature dependence $L(T)$ is determined by calculated values of T_0 and by the formula (3) and is presented on fig.3. The temperature dependence of the derivative L on T-$dL/dT(T)$, calculated by formula (6), is presented on this figure. The dependence $dL/DT(T)$ expresses the temperature variation of the temperature velocity of the phase transformation $\alpha \leftrightarrow \beta$. Thus, it is obtained for $AgFeS_2$, T_0=443 K, α=0,28, at the temperature (T=T_0) dL/dT=0,07.It follows from these data, that in $AgFeS_2$ and as well as in its analogue, the structural phase transformation has strongly spread nature, Identical data for $AgFeTe_2$ and $AgFeSe_2$ are equal, respectively, T_0=420 K, α=0,18, dL/dT=0,022.

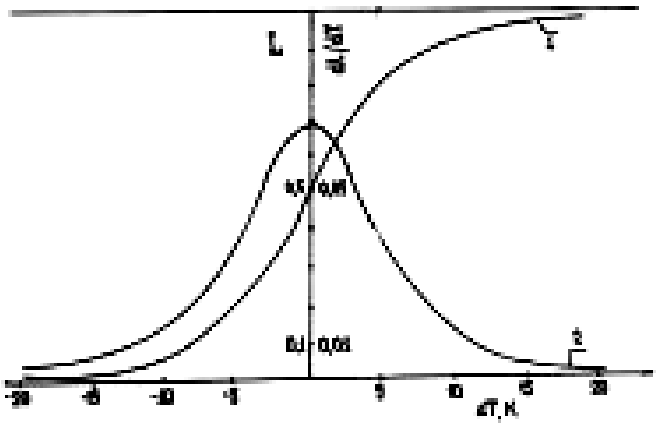

Fig. 3. Temperature dependences of the switching function L(1) and temperature velocity of PT dL/DT (2) in $AgFeS_2$.

Comparing obtained data of Pt parameters we may conclude, that electric properties vary more sharply in $AgFeS_2$ at PT and the PT spreading is somewhat lesser, than it is in $AgFeTe_2$ and $AgFeSe_2$.

[1] *B.N. Rolov.* "Razmitiye fazoviye perekhodi", Riga, 1972, p. 311.

[2] *B.N. Rolov.* Izv. AN, Latvia SSR, seriya fizik. tekhn. Nauk 4, 33, 1983.

[3] *K.P. Mamedov, M.F. Gajiyev, Z.D. Nuriyev.* DAN SSSR, 231, 1, 94, 1976.

[4] *K.P. Mamedov, M.F. Gajiyev, Z.D. Nuriyev.* FTT 19, 7, 2190. 1977.

[5] *E.S. Krupnikov, F.Y. Aliyev, A. Aliyev.* FTT 33, 11, 3408. 1991.

[6] *S.A. Aliyev, F.F. Aliyev, G.P. Pashayev.* "Neorganic. materiali", 29, 8,1073. 1993.

[7] *S.A. Aliyev, F.F. Aliyev, Z.S. Gasanov.* FTT 40, 9. 1998.

[8] *M.I. Aliyev, Z.S. Gasanov, F.Z. Huseynov.* "Neorganic. materiali", v.X, № 10, 1897,1974.

[9] *M.I. Aliyev, R.M. Mirzababayev, Z.S. Gasanov, G.D.Sultanov, F.Z. Huseynov.* Dokladi AN Az. SSR, v. XXXII, № 8, 16, 1976.

[10] *M.I. Aliyev, Z.S. Gasanov.* Dokladi AN Az. SSR, v. XXXIII, № 11, 35, 1977.

[11] *S.A. Aliyev, D.G. Arasli, Z.F. Agayev, Sh.S. Ismayilov, E.I. Zulfigarov.* Izv. AN SSR, seriya f.t.m.n. 6, 67, 1982.

S.A. Əliyev, Z.S. Həsənov, S.M. Abdullayev

$AgFeS_2$ KRİSTALININ FAZA KEÇİDİ OBLASTINDA ELEKTRİK XASSƏLƏRİ

$AgFeS_2$ kristalının faza keçidi (FK) oblastında Holl əmsalı $R(T)$ və elektrik keçiriciliyinin $\sigma(T)$ temperatur asılılığı tədqiq edilmişdir. FK-nın yayılma dərəcəsini müəyyən edən parametrlər təyin edilmiş və göstərilmişdir ki, kristalında FK yüksək yayılma dərəcəsinə malikdir.

С.А. Алиев, З.С. Гасанов, С.М. Абдуллаев

ЭЛЕКТРИЧЕСКИЕ СВОЙСТВА $AgFeS_2$ В ОБЛАСТИ ФАЗОВОГО ПЕРЕХОДА (ФП)

Проведено исследование температурной зависимости коэффициента Холла $R(T)$ и электропроводности $\sigma(T)$ $AgFeS_2$ в области фазового перехода (ФП). Определены параметры ФП, определяющие степень размытия. Показано, что в $AgFeS_2$ ФП носит сильно размытый характер.

Received: 13.07.02

THE CALCULATION OF ADIABATIC COMPRESSIBILITY AND HEAT CAPACITY OF PERFLUOROCARBONS FROM ACOUSTIC DATA

A.U. MAHMUDOV, S.H. SADIKHOVA, E.Z. ALIYEV
Baku State University
Acad. Z. Khalilov str., 23, Baku

Using experimental data on the velocity of the ultrasound wave spreading, density, isothermal compressibility and heat expansion coefficient we have calculated the adiabatic compressibility and the heat capacities C_p and C_v of some perfluorocarbons. The values of adiabatic compressibility for various perfluorocarbons are qualitatively connected with their molecular structure. Values of heat capacities difference C_p -C_v for investigated perfluorocarbons mainly depend on the heat expansion coefficient, since molecular interaction in them is weak.

In our previous paper [1] the data on the bulk properties of some perfluorocarbons were presented. Heat expansion coefficient, isothermal compression and thermal coefficient of the pressure versus the temperature were calculated on the base of semiempiric state equation for perfluorocarbons. The investigation of these dependencies research showed, that above indicated coefficient depend both on the molar mass, and on the perfluorocarbons structure.

In the present paper the adiabatic compressibility and heat capacities C_p and C_v of perfluorocarbons are calculated on the base of experimental data on the velocity of the ultrasound wave spreading and on the density. Besides practical value the actuality of the research of the heat physical and heat properties of perfluorocarbons in the wide state parameters range have exceptionally important scientific mean, allowing to extend the modern imagination of the liquid state theory. The velocity of the ultrasound wave spreading in investigated perfluorocarbons was determined by the impulse method. The method is based on the measurement of time interval, during which the ultrasound wave, obtained by the short rectangular electric impulse as a result of radiant piezoelement excitation, passes twice the fixed distance between strictly parallel placed radiant and receptor piezoelements. The rectangular pulse recurrence frequency is measured providing that the pulse, passing the investigated substance once and the pulse, twice reflected from receptive and radiant piezoelements coincidence. The sound velocity subject the condition $\alpha\lambda << \pi$ is determined by the formula:

$$v = 2Lf,$$

where α is a coefficient of the ultrasound wave absorption, λ is an ultrasound wave length, L is a distance between piezoelements, f is a rectangular pulse recurrence frequency.

Measurements showed, that in investigated perfluorocarbons the velocity of the ultrasound wave spreading is approximately two times smaller, than in hydrocarbons. Obviously, it may be explained by the low intermolecular interaction, promoting the increase of the adiabatic compressibility and by the high density of perfluorocarbons due to hard fluorine atoms presence in their molecules.

The values of the relative temperature coefficient of the sound velocity $1/v(\partial v/\partial T)_p$ are approximately 1,2 times larger in the investigated perfluorocarbons, than they are in hydrocarbons. It is possibly explained by the fact, that the critical temperature is low for perfluorocarbons, than for hydrocarbons.

Measurements of the ultrasound wave spreading velocity may be observed as a method of the adiabatic compressibility $\beta_{\alpha\partial}$ determination:

$$\beta_{\epsilon Л} = 1/\rho v^2,$$

where ρ is a density and v is a velocity of the ultrasound wave spreading. There are no other direct methods of the $\beta_{\alpha\partial}$ value measurement, and the method precision is high, as it is possible to measure the sound velocity and density to a high precision degree. The structural formulae of investigated perfluorocarbons are presented below:

1. Perfluorobutylamine

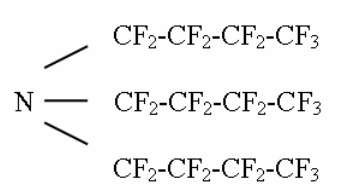

Molar mass
M[$(C_4F_9)_3N$]=671 gr/mole

2. Perfluororizononane

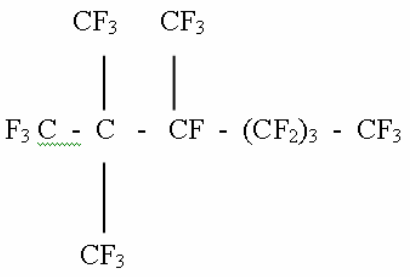

M (C_9F_{20})=488 gr/mole.

3. Perflfluoromethyldibutylamine

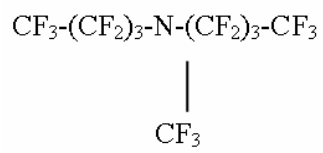

M $[CF_3(C_4F_9)_2N]$=521 gr/mole

4. Perfluorotripropylamine

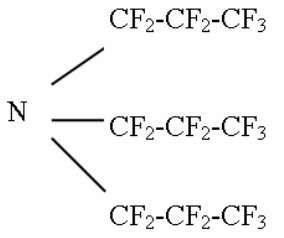

M$[(C_3F_7)_3N]$=521 gr/mole.

5.Perfluorodecaline

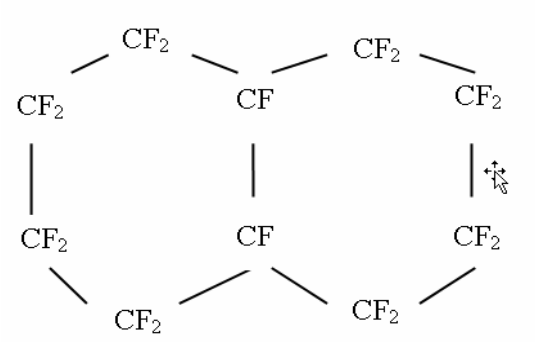

M $(C_{10}F_{18})$= 462 gr/mole

6.1.3 - perfluorodimethylcyclohexan

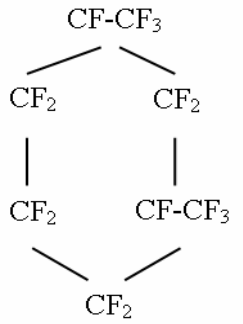

M(C_8F_{16})=400 gr/mole.

7.1 Perfluoroethyldecalizole

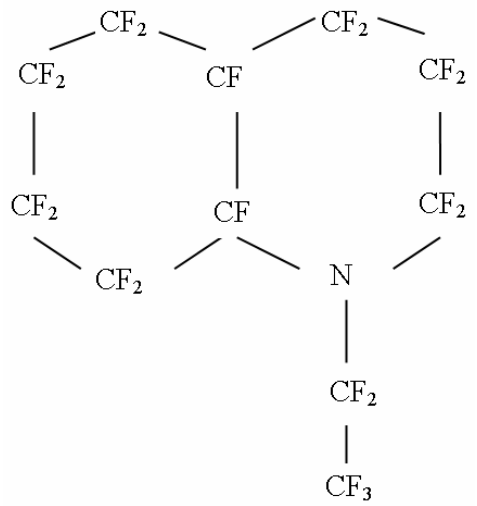

M$(C_{11}F_{21}N)$=545 gr/mole.

8. Perfluoro-2-methyl-pentane-3

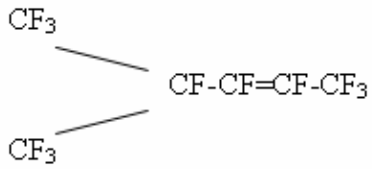

M(C_6F_{12})= 300 gr/mole.

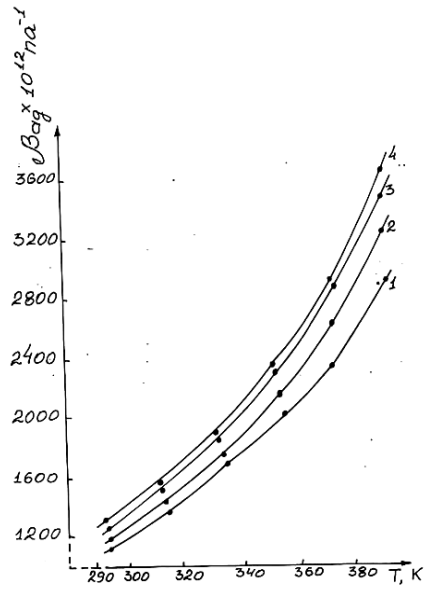

Fig.1

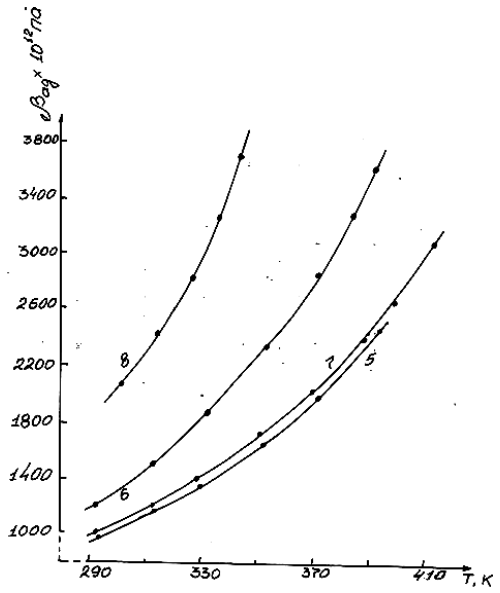

Fig. 2

Curves of adiabatic compressibility versus the temperature of investigated perfluorocarbons at the pressure 0,1 MPa are presented on fig.1 and 2. As it is seen from fig.1 and 2, the adiabatic compressibility of perfluorocarbons increases with the temperature increase, it is explained by the fact, that at the heating as a result of the heat expansion, the liquid volume increases, the distance between molecules grows, the repulsion force between molecules reduces and the compression is facilitated.

The adiabatic compressibility of perfluoropropylamine (curve 4) is lesser, than the adiabatic compressibility of perfluorobutylamine (curve 1), it is explained by the fact, that structure groups CF_2, replacing the intermolecular interaction to inner-molecular, reduce the compressibility, and consequently, increase the sound velocity. These data confirm the known empiric rules of Partkhasaratkhi and Parshada [2], which indicate the qualitative connection of the sound velocity, and consequently, the liquid compressibility with details of the molecules structure.

Data on the adiabatic compressibility of perfluorodecaline 1.3-perfluoromethylcyclohexan and 1-perfluoroethidecalozine (curves 5, 6, 7) may be analogously explained. The high value of the adiabatic compressibility of 1-perfluoroethidecalozine in comparison with perfluorodecaline is connected with the fact, that the latter molecules have the compact structure (the spherical symmetry of the atom groups location), side atom groups of 1- perfluoroethidecalozine molecules create more space between molecules, and consequently its structure becomes more porous in comparison with the perfluorodecaline structure, it reflects on the value of the sound velocity, and soon the adiabatic compressibility.

For perfluoroizononane and perfluoromethyldibutylamine (curves 2 and 4), molecules structures, which are close, values of the adiabatic compressibility differs negligibly.

The adiabatic compressibility of perfluoro2-methyl-pentane-3 (curve 8) exceeds the value of adiabatic compressibility of perfluoroisononane and perfluorodibutylamine (curves 2 and 3), it may be explained by the fact, that obviously, the number of CF_2 groups is more at the latter molecule, it leads to the compressibility reduction according to Partkhasaratkhi and Parshada rules. By using data on the adiabatic compressibility and the heat expansion coefficient of the investigated perfluorocarbons, presented in papers [1, 2, 3], heat capacities C_p and C_v and their differences were calculated. Calculation results, carried out at the temperature T-293,15 K and the pressure P=0,1 MPa, are presented in the following table:

Table

Perfluorocarbons $\frac{Дж}{кг \cdot ж}$	1	2	3	4	5	6	7	8
C_p	669	874	868	1166	526	855	452	805
C_V	563	750	749	1028	403	674	399	663
C_p-C_v	106	119	119	138	123	181	53	142

Perfluorocarbons names, presented in the same sequence, as their structural formulae, are indicated by numbers 1,2,3,4,5,6,7,8.

The value C_v is determined by the formula:

$$C_v = \frac{\alpha^2 T}{\rho \beta_{u3}(\beta_{u3}/\beta_{ag} - 1)} \qquad (1)$$

As the calculation error does not exceed 3%. The values of C_p, C_p - C_v are determined from formulae $\frac{C_p}{C_v} = \frac{\beta_{u3}}{\beta_{ag}} = \beta_{u3}\rho C^2$, whose calculation errors do not exceed 3%.

The modern experimental methods of C_v determination are cumbersome and are give errors not lesser 5-10%.

Therefore, the C_v calculation, following from the sound velocity and other experimental data on the formula (1), is considered as more convenient and profitable.

As it is seen from the table data, the difference C_p - C_v for all investigated perfluorocarbons is higher, than it is for the universal gas constant R. It is known, that C_p- C_v heat capacities difference depends on the heat expansion coefficient and on the value of intermolecular interaction forces, the value of C_p - C_v heat capacities difference for investigated perfluorocarbons mainly depends on the heat expansion coefficient, since the intermolecular interaction in them is the weak by its nature.

[1] *A.U. Mahmudov, S. Kh. Sadikhova, E.Z. Aliyev.* Fizika, rizyaziyyat yer elmleri.
[2] *L. Bergman.* "Ultrazvuk i ego primineniye v nauke i tekhnike" IA, 1965 (in Russian).
[3] *M.P. Mustafayev, Y.M. Naziyev, M.K. Gakhramanov*. "Teplofizika visokikh temperatur" v.33, №3, 1995, p.359-365 (in Russian).
[4] *Y.M. Naziyev, M.P. Mustafayev, S.A. Javadova*. "Teplofizika visokikh temperatur", v.32, № 3, 1993, p.378-382 (in Russian).

A.U. Mahmudov, S.X. Sadıxova, E.Z. Əliyev

PERFTORKARBONATLARDA AKUSTİK METODLA ADİABATİK SIXILMA ƏMSALININ VƏ İSTİLİK TUTUMLARININ HESABLANMASI

Perftorkarbonatlarda sıxlığın, izotermik sıxılma əmsalının, istidən genişlənmə əmsalının və ultrasəs dalğalarının yayılma sürətlərinin təcrübi qiymətlərinə görə onların adiabatik sıxılma əmsalları və C_p, C_v istilik tutumları hesablanmışdır.

Adiabatik sıxılma əmsallarının müxtəlif perftorkarbonatlar üçün hesablanmış qiymətləri onların molekulyarı quruluşu ilə keyfiyyət cəhətdən əlaqələndirilmişdir. İstilik tutumları arasındakı fərq C_p - C_v əsasən perftorkarbonatların istidən genişlənmə əmsalından asılı olduğu göstərilmişdir, çünki bu maddələrdə molekullar arası qarşılıqlı təsir çox azdır.

А.У. Махмудов, С.Х. Садыхова, Э.З. Алиев

ВЫЧИСЛЕНИЕ АДИАБАТНОЙ СЖИМАЕМОСТИ И ТЕПЛОЕМКОСТИ ПЕРФТОРУГЛЕРОДОВ ИЗ АКУСТИЧЕСКИХ ДАННЫХ

Используя экспериментальные данные по скорости распространения ультразвуковых волн, плотности, изотермической сжимаемости и коэффициенту теплового расширения, рассчитаны адиабатная сжимаемость и теплоемкости C_p и C_v некоторых перфторуглеродов. Значения адиабатической сжимаемости для различных перфторуглеродов качественно связываются с их молекулярным строением. Значения разности теплоемкостей C_p - C_v для исследованных перфторуглеродов в основном зависят от коэффициента теплового расширения, поскольку межмолекулярное взаимодействие в них весьма мало.

Received: 14.10.02

SOME PECULIARITIES OF THE CHARACTERISTICS OF CHAOTIC OSCILLATIONS OF THE SOLAR CENTIMETER RADIO EMISSION

Sh. Sh. GUSEINOV

Shemakha Astrophysical Observatory of the Azerbaijan National Academy of Sciences
SHAO, Yu. Mammadaliyev settlement, Pirqulu, Shamaky, 373243, Azerbaijan Republic

Some peculiarities of the numerical analysis of chaotic fluctuations and their application to the analysis of the fluctuations of centimeter wavelengths radio emission of the Sun are considered. On the basis of Takens algorithm on the one-dimensional realization of dynamic system its phase portrait is constructed. Using the Grassberger-Procacci formula the correlation integral which allows determining the fractal dimension of the attractor and the entropy of the dynamic system is calculated. For determination of the character of the system the results of statistical processing of fluctuations of the solar radio emission are analyzed. From the results of fractal analysis it is shown that in the temporary series of fluctuations of centimeter radio emission of the Sun the low dimensional determined chaos is present. Thus, the specified calculations of the correlation dimension and *K*- entropy in the solar temporary series are possible at optimum - minimum length of the sample ≥700.

Introduction

The problem of turbulence in hydrodynamics is common for the plasma physics, the weather forecast, the theory of planets and stars, radiophysics and many other sciences.

The new methods, which have been developed in last two decades, allowed to reach a notable progress in the consideration of laws of dissipative systems [1,5].

The theory of determined chaos has not been used yet in analyses of nonlinear processes in atmosphere of the Sun. In this paper we give brief description of the main points of the applied methods of the determined chaos and the problems of applications to the fluctuations of the centimeter radio emission of the Sun.

1.The main characteristics of dynamic regimes

The dynamic regime can be analyzed by the method of Fourier analysis. But this method does not allow to discriminate between the determined chaos and the "white noise". Suppose that the dynamic regime is determined by the set of functions $x_i(t), i = 1,2,...,N$ (for example, for the Sun it is temporary sequence of the intensities of the radio emission $I_0(t)$).

The instant ($t=t_0$) state of the system in the *N*-dimensional phase space is defined by the point *P* with coordinates $x_1(t_0), x_2(t_0),...,x_N(t_0)$ and the evolution of the system is expressed by the phase trajectory. If there is stable regime in the system the phase trajectories converge to some subset of the phase space. This space is called an attractor. In this respect an investigation of space trajectories allow us to get only qualitative information about the system.

For the quantitative description of the attractor some parameters are used. The most informative parameters are the spectral power, the dimension, and the entropy.

The dimension and entropy are very useful parameters when the system is in the strange attractor regime. Strange attractor is the mathematical picture of the determined chaotic oscillations. The strange attractors is the attracting trajectories of the determined chaotic system in the phase space.

The dimension *D* and Kolmogorov *K*– entropy are important characteristics of the non-linear systems [3-6]. Fractal dimension is the quantitative characteristic of the set of points in the *n*-dimensional space, which shows the density of points filling the subspace when their number becomes very large.

2. The Takens's lag method and the Ruelle-Takens model

For the complete and direct study of the motion, which forms the foundation of dynamic systems, it is necessary to construct its phase portrait. Takens [7] suggested an effective method for the evaluation of geometrical characteristics of the attractor and for restoring the trajectory in phase space by time lags on the basis of measurements of one variable of the dynamic system.

Thus, the one-dimensional temporary series of $x_i(t)$ allow constructing the multi-dimensional phase space of dynamic system.

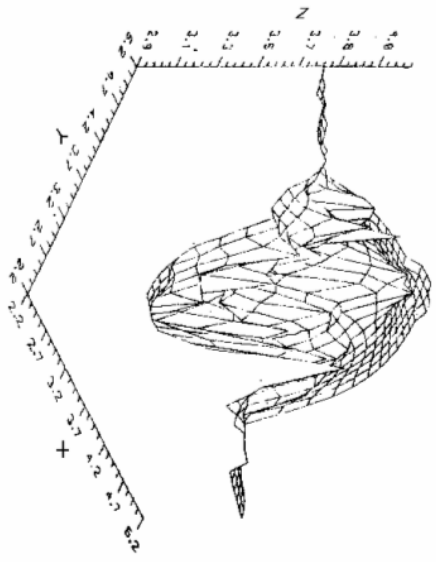

Fig.1. 3-D phase portrait of fluctuations in solar atmosphere within 10 hours.

In fig.1 three-dimensional 10-hour phase portrait of solar atmosphere is shown. These temporary series consist of Δt=0,5 min intervals. Observations of $I_к(t)$ were carried out on 26 August, 1984 at λ=3,6 cm at 22 m radio telescope of RAS FJ RAN (Pushino). The complex nature of the phase trajectory behaviour is seen which indicates its unstable

nature of time evolution of the inhomogeneous structure of the solar atmosphere.

So, it is very difficult to make some kind of derivations on the behaviour of solar atmosphere on the basis of three-dimensional graphs of the phase trajectory.

To date several methods for the description of transition from the laminar regime of flow to the turbulent regime are offered.

One of them is the model suggested by Ruelle and Takens (1971) [8]. This model has for the first time cast doubt on the Landau's theory [9] of turbulence according to which for an occurrence of turbulence infinite number of Hopfs' bifurcations are required.

The approach of Ruelle and Takens is as follow. The spectrum of power of the dynamic system will be developed as function of regulating parameter as follows. The spectrum of power will in the beginning contain one frequency (f_1), then two frequencies (f_1, f_2), sometimes three, arise. With the arising in the spectrum of the third frequency the broadband noise component, which is characteristic for chaos, will appear.

As an example in fig. 2 (a,b,c) series of average spectra of power density (averaged on 10 spectra) is shown. The data on fluctuations are from the observations at the radio telescope RT-64 of special design office of Moscow Energetic Institute (OKB MEI) at wavelength λ=5.2 and 8.1cm carried out in 1983 and at RT- 22 in Pushino at λ=3.6 cm carried out in 1984. The technique of spectral processing of these observational data is given in author's work [10].

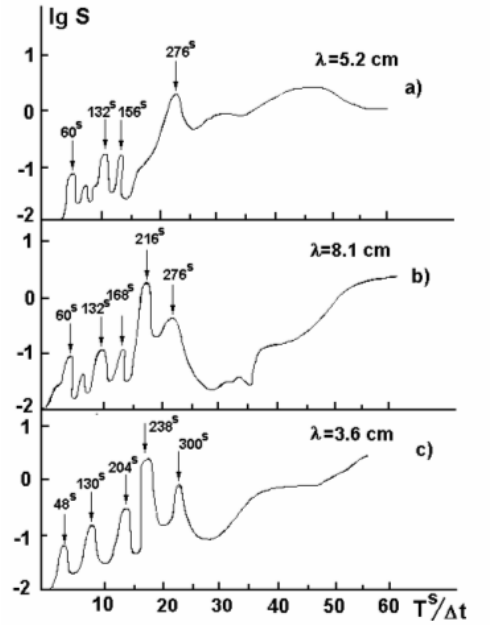

Fig.2 (a,b,c) The average spectra of power dencity of fluctuations of radio emission of the quiet Sun at various radio telescopes.

From fig. 2 (a,b,c) it can be seen that in the fluctuations of the centimeter radio emission of the Sun there is broad spectrum of frequencies. This feature of chaos is especially important when the system has small dimension.

From the above it follows, that in such cases the calculation of the dimension of the attractor and the entropy of dynamic system allows to obtain valuable information

3. Determination of dimensionality and entropy from the observational data

Last years for the determination of the dimension of the attractor more effective methods have been developed. Grassberger and Procaccia [11, 12] have in detail studied and derived certain relation between the point-to-point dimensionality and the correlation dimensionality [13].

In determination of the point-to-point dimensionality the continuous trajectory is considered as the discrete one. Then the distance between pairs of points are calculated as $S_{ij} = \left|\vec{x}_i - \vec{x}_j\right|$. The correlation function is determined as

$$C(r) = \lim_{N\to 0} \frac{1}{N^2} \text{ (number of pairs } (i,j), \text{ for which } S_{ij}<r)$$

For many attractors this function depend on r at $r \to 0$ as

$$\lim_{r\to 0} C(r) = a\, r^d ,$$

therefore the fractional dimensionality may be determined by a slope of the line in the (ln$C$, ln r) diagram

$$d = \lim_{r\to 0} \frac{\log C(r)}{\log r}$$

It is found that if the distance between any of two points is less than the given value of r, then $C(r)$ may be calculated by a more effective way, i.e.

$$C(r) = \frac{1}{N^2} \sum_{i=1}^{N} \sum_{j=1}^{N} H\left(r - \left|\vec{x}_i - \vec{x}_j\right|\right) = \frac{1}{N} \sum_{i=1}^{N} \frac{N_i(r)}{N}$$

where H is the Heviside function: $H(x)$=1 if x>0, and (x)=0 when x<0.

The value of the correlation integral (3) may be calculated in terms of d, beginning from d=2. Calculations come to an end, if the estimations of the value C(r) display the tendency to saturation and the change of correlation dimensionality stops.

In the case of pure "white noise" for any value of d the saturation of the correlation integral does not occur. This property of the correlation integral is used to distinguish the chaotic processes of dynamic origin from the white noise.

The Kolmogorov entropy is very important characteristic of chaotic processes in a phase space of random dimensionality. In practice the correlation entropy K_2, which is the low-value estimation of the K – entropy, $K_2 \leq K$, is used. The correlation entropy and the correlation integral are related by equation [11]

$$C(r) = r^{v} \exp(-d\tau\, K_2) ,$$

which makes it possible to determine K_2 with the help of the calculated values of $C(r)$ from:

$$K_2 = \frac{1}{\tau_m} ln \frac{C_d(r)}{C_{d+m}(r)}$$

The condition $K_2 > 0$ is the sufficient condition for an existence of chaos. The entropy of K is the measure of chaos: $K = 0$ - for the regular motion, $K = \infty$ - for the random systems with determined chaos.

4. The analysis of factors which affect on precise value of C(r)

It should be noted that the adequacy of conformity of the correlation integral, calculated on the basis of experimental data, with the real one depends on many factors.The most important among them are the length of realization T, i.e. the number of data N time delay τ, the intervals of readings Δt, and the presence of noise and trend in the temporary series. The choice of these parameters is as in the work [14].

5. Determination of N_{min} by the data on fluctuations of centimeter radio emission of the Sun.

It is known that the solar atmosphere at centimeter wavelength radio range is continuously observed only in the limited time intervals. Therefore, the problem of determination of N_{min} for solar atmosphere, which is necessary for correct calculation of correlation integral, is extremely important. Measurements of fluctuations of centimeter radio emission of the Sun with Δt=0,5 min are used to calculate the correlation integral (3). The most long-term series which are consist of 800 – 1000 readings is used. Each temporary series was broken on a few consecutive enclosed each into other series for which the amount of data gradually grew. The most short of them consists of 200 points.

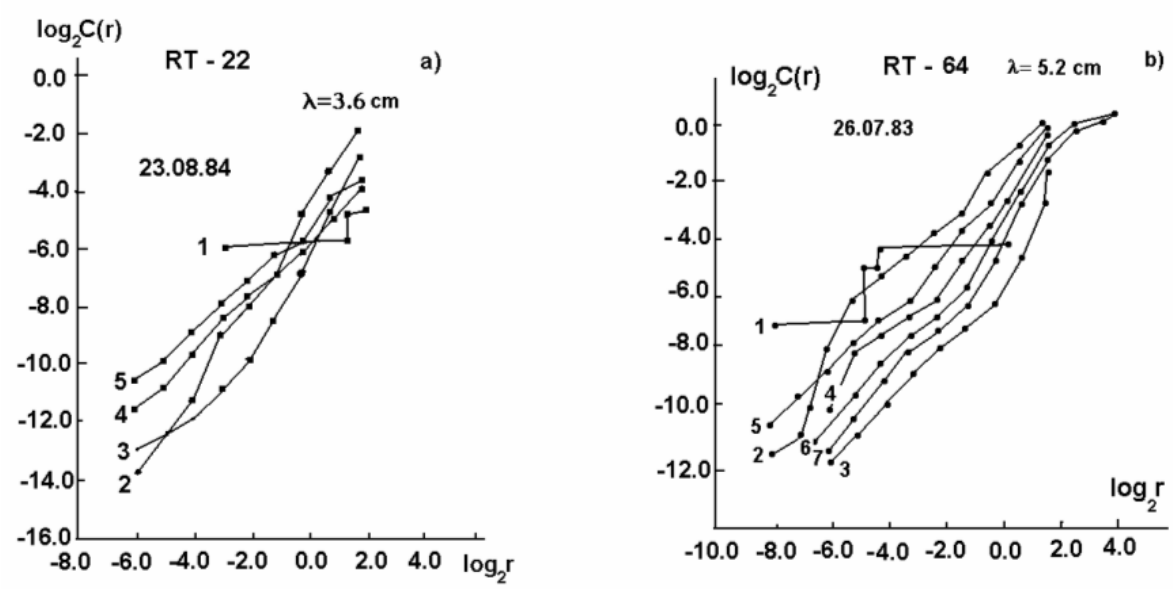

Fig.3 (a,b) The diagrams of correlation integrals of temporary series of filtered data on the fluctuations of the centimeter radio emission of the quiet Sun.

In fig. 3, as an example, graphs of correlation integrals in which numbers of points are increased from 200 to 1000 are presented. In calculations d=4. At 200 and 300 on the graphs evident breaks which do not permit to determine the dimension of the attractor are seen. Although at N=400; 500; 600 extended domains of scaling appeared. At N=700; 800; 900 the values and slopes of curves do not actually differ, i.e. the saturation of correlation integrals begins.

Thus, it is safe to say, that for the calculation of the real value of the correlation integrals as a minimum about 700 measurements of the fluctuations of the centimeter radio emission of the Sun are required.

Conclusions

Results derived in this work allow to make the following conclusions

1. With the aid of Takens's algorithm by one-dimensional realization of dynamic system their multidimensional phase portrait may be constructed.
2. The calculations of the Grossberger-Procaccia's correlation integral by using the observational data allow to determine the fractal dimension of the attractor and the entropy of the dynamic system.
3. The spectrum of power density constructed by using long-term observational material on the fluctuations of the centimeter radio emission of the Sun shows a wide band of frequencies, and the auto correlation function fades with time.
4. In most cases fluctuations are non-stationary and their amplitudes, phases and periods are varied with time.
5. The nonstationarity raises an internal chaos and increases the entropy of the dynamic system. Therefore, the spectrum

at the same time is determined and stochastic due to nonlinearity of the system and the parameters.

1. The optimum minimum sample of the temporary series of measurements of fluctuations of the solar radio emission at which the value of the correlation integral become stable should be N≈700 points.
2. The fractal dimensionality does not characterize a chaotic nature of dynamic system. In dynamic experiments it is better not to rely on any the only one criterion of chaos. For the larger reliability it is necessary to use two, three and etc. characteristics, for example, the Fourer spectrum, the indices of Lyauponov, or the fractal dimensionality. In this case it is save to say that the system is the chaotic or strange one.

Acknowledgements

I am very grateful to Dr Ju.S. Karadganov from Physical and Technical Institute of the Turkmenistan Academy of Sciences for numerous discussions and valuable advice.

[1] *A.S. Monin*. O prirode turbulentnosti. Usp.Fis.Nauk , 1978, v.125, n 1, p.97-122 (in Russian)
[2] *M.I. Rabinovich*. Stokhasticheskie avtokolebaniya i turbulentnost'. Usp.Fis.Nauk, 1978, v. 125, n.1, p.123-169(in Russian)
[3] *G. Shuster*. Determinirovanniy khaos. M.: Mir Pub.Co, 1988, 240 p. (in Russian)
[4] *F. Mun*. Khaoticheskie kolebaniya. M.: Mir Pub.Co, 1990, 312 p. (in Russian)
[5] *P. Berje, I. Pomo, L.K. Vidal*. Porjadok v khaose. O deterministicheskom podkhode k turbulentnosti., M.: Mir Pub.Co, 1991, 364 p. (in Russian).
[6] *V.C. Afraimovich, A.M. Reiman*. Razmernost' i entropia v mnogomernikh sistemakh. Nelineinie volny. Dinamika i evolutia. M.: Nauka Pub.Co, 1989, p.238-282.(in Russian)
[7] *F. Takens*. Detecting strange attractor in turbulence. Lect.Notes Math., 1981, v.898, p.336-382.
[8] *D. Ruelle, F. Takens.* On the nature of turbulence. Com. Math. Phys. 1971, v.20, n.1, p. 167-192.
[9] *L.D. Landau*. O probleme turbulentnosti. Dokl. Acad. Nauk, 1944, v.44, n.3, p.339-342 (in Russian).
[10] *Sh.Sh. Guseinov*. O solnechnoi i atmosfernoi prirode fluktuatciy santimetrovogo radioizluchenya Solntca. Dissertation, Phisiko-Tekhnicheskii Inst., Ashgabat, Turkmenistan, 1993, 135 p.
[11] *F. Grassberger, Procaccia.* Estimation of the Kolmogorov entropy from a chaotic signal. Phys. Rev. A. 1983, v.28, n. 4, p. 2591-2593
[12] *F. Grassberger, Procaccia*. Measuring the attrangeness of strange attractore. Physica D. 1983, v.9, n.1/2, p. 189-208.
[13] *F. Grassberger, Procaccia.* Characterization of strange attractore. Phys. Rev. Lett. 1983, v.50, n. 5, p. 346-349.
[14] *Ju.Sh. Karadgev, B.B. Pirnijazov.* Nekotorie voprosi chislennogo analiza khaoticheskikh kolebaniy. Preprint Acad.of Sci Turkmenistan, Phisiko-Tekhnicheskii Inst., Ashgabat 1993, 26 p. (in Russian)

Ş.Ş. Hüseynov

XAOTİK RƏQSLƏRİN XARAKTERİSKALARININ BƏ'Zİ XÜSUSİYYƏTLƏRİ

Baxılır xaotik rəqslərin ədədi təhlilinin bə'zi xüsusiyyətlərinə və onların santimetrlik dalğa uzunluğunda Günəş radioşüalanması fluktuasiyalarının təhlilinə tətbiqinə. Takensin alqoritmi əsasında dinamik sistemlərin birölgülü qiymətlərinə görə, onun fəza portreti qurulmuşdur. Qrassberqer – Prokaççia düsturu ilə dinamik sistemlərin entropiyasını və fraktal ölçü dərəcəsini tə'yin etməyə imkan vərən korelyasiya inteqralı hesablanmışdır. Sistemin növünü tə'yin etmək üçün bir neçə qöstəricidən, məsələn Furye spektrindən və fraktal ölçü dərəcəsindən istifadə edilmişdir. Korelyasiya və spektr təhlil üsullarının – maksimum entropiya üsulu (MEÜ) və spektr-zaman təhlil üsulunun (SZTÜ) köməyi ilə Günəş radioşüalanması fluktuasiyalarının statistik işlənməsinin nəticələri təhlil olunmuşdur. Beləliklə, Günəşin zaman sıralarına görə dəqiqləşdirilmiş korelyasiya ölçü dərəcəsi və K- entropiyanın hesablanması, sıranın minimum optimal uzunluğu N>700 olduqda mümkündür.

Ш. Ш. Гусейнов

НЕКОТОРЫЕ ОСОБЕННОСТИ ХАРАКТЕРИСТИК ХАОТИЧЕСКИХ КОЛЕБАНИЙ

Рассматриваются некоторые особенности численного анализа хаотических колебаний и применение их для анализа флуктуаций радиоизлучения Солнца в сантиметровом диапазоне волн. На основе алгоритма Такенса по одномерной реализации динамической системы построен ее фазовый портрет. Рассчитан корреляционный интеграл по формуле Грассберга-Прокаччиа, который позволяет определить фрактальную размерность аттрактора и энтропию динамической системы. Проанализированы результаты статистической обработки флуктуаций радиоизлучения Солнца для определения вида системы. По результатам фрактального анализа показано, что во временных рядах флуктуации сантиметрового радиоизлучения Солнца присутствуют низко-размерный детерминированный хаос. Таким образом, уточненные вычисления корреляционной размерности и К – энтропии по солнечным временным рядам возможны при оптимально минимальной длине выборки ≥700.

Received: 01.07.02

THE ENERGY SPECTRUM OF CHARGE CARRIERS IN n-Ag_2Te

F.F. ALIEV
Institute of Physics of the Azerbaijan National Academy of Sciences
H. Javid av. 33, Baku, 370143

It is shown, that Ag atoms create small donors levels in Ag_2Te, which are placed on the distance ($7\cdot10^{-5}T\cdot K^{-1}$-0.002) eV from the conduction band bottom. It is established that the stoichiometric composition Ag_2Te has the *n*-type conductivity beginning from the deficiency of Ag > 0.01at %.

A number of works [1-5] were devoted to the establishment of the energy spectrum of charge carriers in Ag_2Te. The authors [1] valued the width of the prohibited band $E_g<6meV$ and supposed, that the slitless state takes place in Ag_2Te at low temperature. The behavior of Hall coefficient R in the temperature interval 250-300 K is caused by the increase of the efficient density of the valence band state that is by the presence of the additional valence band with the high density of states, placed below along the energy axis. Conclusions made by authors [2] suggest, that silver may be the two-electron donor in $A_2^{I}B^{IV}$, which gives two electrons to the conduction band ($Ag^{+}\rightarrow Ag^{3+}+2e^{-}$); under this condition the formed two-electron state is localized either because of the strong interaction with the lattice or because of the interaction with vacancies and other imperfections. Moreover, according to their opinion, silver compounds, unlike copper compounds, have always the electron type of conductivity even at $T\rightarrow 0$ also at the definite deficiency of silver in comparison with the stoichiometry.

It has been noted in paper [5] that the excess of Te in Ag_2Te leads to *r*-type in the homogeneity region; and Ag to the *p*-type conductivity. Authors [4] have valued the activation energy (0.04±0.01)eV and have supposed that local energy levels arise in the prohibited band. It is shown in work [5], that peculiarities in temperature dependences of electric and thermoelectric parameters of *p*-Ag_2Te are connected with acceptor levels, placed on the distance ($0.03–7\cdot10^{-5}T\cdot K^{-1}$)eV from the conduction band bottom.

In spite of numerous works [1-5], devoted to the establishment of the energy spectrum of charge carriers in *n*-Ag_2Te this issue is still open. In this work the attempt has been made to solve given issue, taking into account conclusions [5].

Determination of some impurity state parameters

The temperature and concentration dependences of coefficients: Hall *R*, electroconductivity σ and thermoemf α_0 in *n*-Ag_2Te (fig.1) are connected with the state of donor impurities [2]. As it is known from [5], at the high value of concentration of donors N_d and at low value of E_g [6] the experimental determination of activation energy of the donor E_d for Ag_2Te is very difficult. We may act in the following way to determine E_d.

Authors [7] have showed that the law of electron dispersion in *n*- Ag_2Te submits to the Kain model and interaction of electrons has non-elastic character. Then the thermoemf coefficient at any degree of electron gas degeneration with the non-standard band is determined as [8]:

$$\alpha_0 = \frac{K_0}{e}\left[\frac{I^1_{r+1,2}(\mu^*,\beta)}{I^0_{r+1,2}(\mu^*,\beta)} - \mu^*\right] \qquad (1)$$

where $\mu^*=\mu/K_0T$ is the reduced chemical potential ; μ and I_n^m (μ^*, β) are the level and two-parametric Fermi integral. Here $\beta=K_0T/E_g$ is the parameter, characterizing a band non-standard.

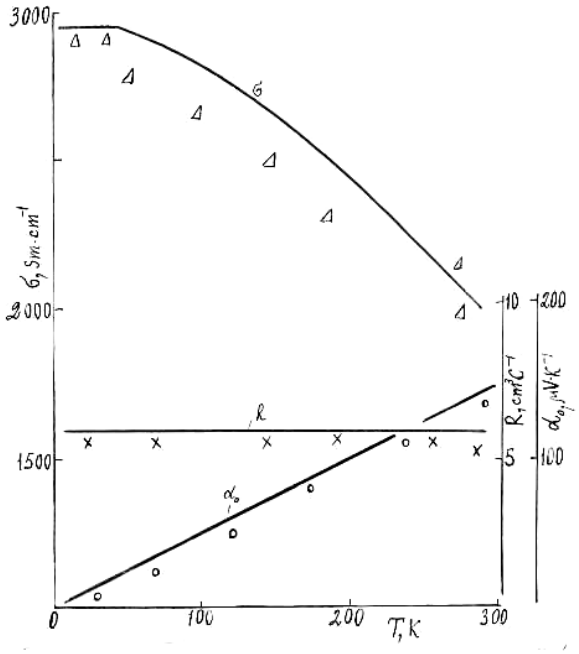

Fig.1. Temperature dependences of the Hall coefficient *R* (at *H*=12 kЭ), electroconductivity σ and thermoemf α_o (solid lines are calculated).

The value μ was determined from the formula (1) at the temperature 15 K. If values N_d and m_n (m_n is the effective mass of electrons on the Fermi level) are known, then E_d may be found by means of inequality:

$$\exp\left(\frac{E_d}{K_oT}\right) >> \frac{(2m_nK_oT)^{3/2}}{32\pi^{3/2}\hbar^3 N_d}.$$

According to [8]:

$$E_d = K_0 T \ln\left[\frac{2\pi^{3/2}\hbar^3 N_d}{(2m_n K_0 T)^{3/2}}\right] - 2\mu . \qquad (2)$$

Using values N_d=1.1·10^{18}cm^{-3}, m^*_o=0.022m_o [5] at 15 K, the value ~-0.1 meV (at the count from the conduction band bottom) has been received for E_d. If it is taken into account that $E_g(T)$ [6] and $E_d(T)$=(7·10^{-5} T ·K^{-1}-0.002) eV, then the value E_{do} equals ~2 meV at T=0K.

In the case of a simple monovalence donor impurity, for which only the spin-degeneration β=1/2 is appropriated, the electron concentration on donor levels with the energy E_i=-E_d is determined according to [9]:

$$n_d = N_d\left\{1 + \frac{1}{2}exp\left[-(E_d + \mu)/K_0 T\right]\right\}^{-1} . \qquad (3)$$

There is some information in literature [10,11], that the telluride of silver refers to compensated semiconductors. At very low temperature ($T\to 0$), when the concentration may be neglected of conductivity electrons n and holes p in the valence band, the neutrality equation has the form [9]:

$$N_a\left[1+2\,exp(-E_a^*-\mu^*)\right]^{-1} = N_d\left[1+exp(E_d^*-\mu^*)\right]^{-1}, \qquad (4)$$

where μ^*= -(E_a^*+E_d^*)/2, E_a^*=E_a/K_oT, E_d^*=E_d /K_oT, N_a is the concentration of acceptors. Taking into account values E_a [5] and E_d at $T\to 0$, it has been received, that $N_a/N_d \approx 0.47$, that is the boundary type conductivity Ag_2Te has been determined. Then the main part plays the position of $\mu(K')$(K'=N_a/N_d is the degree of compensation). Calculations have been made at $K'\to 0$, μ=0.99E'_d and at $K'\to 1$ $\mu = -\frac{E_d''}{2^{1/3}(1-K')^{1/3}}$ [12], where $E_d' = e^2/\chi r_d$, $E_d'' = \left(\frac{4\pi}{3}N_d\right)^{1/3}\frac{e^2}{\chi}$, is the energy of Coulomb interaction, χ is the dielectric constant, $r_d = \left(\frac{4\pi}{3}N_d\right)^{1/3}$ is the average distance between donors (fig. 2). The count has been made from the level of the isolated impurities.

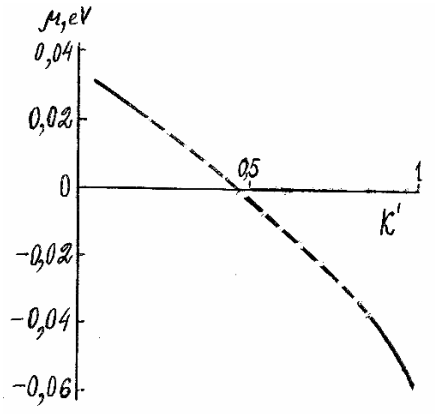

Fig.2. Positions of the Fermi level with respect to the level of the isolated impurities as the function of the compensation degree K^1.

Another the most important characteristic is the bond energy $U(r_o)$, that is the energy necessary for an electron transition from a donor level to the conduction band bottom.

Let us assume for calculation of $U(r_o)$, that electron is moving in the potential field:

$$U(r_o) = -e^2/\chi r_o , \qquad (5)$$

where r_o is the distance from the electron till the impurity center. The formula (5) justifies itself if the radius of the impurity state is large in comparison with the lattice constant a_o.

Taking into account the little difference between values r_o and r_d the value ~0.3 meV has been received for $U(r_o)$ at $N_d \cong 1.1\cdot 10^{18}$cm^{-3}.

Using formulas (1) and (3), temperature dependences $\alpha_o(T)$, $R=1/n\alpha e$ and $\sigma=en_d U_n(T)$ (fig. 1) have been calculated; $U_n(T)$ has been taken from (5).

The discussion of received data

Low values of E_{do} and $U(r_o)$ show, that atoms Ag in Ag_2Te create small donor levels. Even at $T<<E_d/K_o$ ions Ag^+ of the main lattice give electrons to the conduction band. The ratio $N_a/N_d \approx 0.47$ corresponds to the situation, when the deficiency of 0.01 at % Ag creates donor concentration $N_d \approx$ 6,2·10^{16} cm^{-3} in the stoichiometric composition; the crystal has the n-type conductivity. In this case the hole concentration is more in several times than the electron concentration and therefore the material should be considered as holy. Then R would be negative. It is necessary to note that Ag_2Te σ and R are determined almost completely by electrons [13, 14] in its own conductivity field. These and some other consequences follow from large ratio of electron and hole mobility [5].

The received boundary values of N_a/N_d are in agreement with data of authors [4]. They considered, that beginning with $n\approx$1.2:1.8·10^{18} cm^{-3}, the crystal has the n-type of conductivity, that is caused by redundant (with respect to the stoichiometry) Ag atoms in interstice, and N_d could be decreased till N_d< 4.2 ·10^{16} cm^{-3} at sample annealing in the vacuum at $T_o<T$ (T_o is the temperature of the phase transition) at expense of the creation of Ag vacancies at simultaneous reduction of an Ag content in interstices.

Let us consider now the question on the position of the Fermi level in the impurity band at T=0K (fig. 2). As it is known [12], the compensation degree K^1 gives the notion about the value μ_2. In the case of Ag_2Te at K^1<0.47 almost all donors have electrons and therefore, are found in the upper part of the impurity band and they are slightly ionized. That is why μ is positive, that is the greater part of donors are filled by electrons and only small their part is free and has the positive charge. At $K^1\geq$0,47 the value $\mu<0$ that leads to the start of the electron compensation with an excess of Te caused by the deviation from the stoichiometry [11].

Special interest has following facts. Firstly the degeneracy region shifts to more high temperatures (fig.1), secondly the divergences takes place from p-Ag_2Te [5], the resonant scattering of electrons on donor impurities in n-Ag_2Te is not observed. According to the first fact, the degeneracy region shifts to the conduction band with the rate

$dE_d/dT=7\cdot10^{-5}$ eV·K^{-1} and enters to this band at the temperature ~10 K. In this case the hybridization of donor and band states occurs, which is the main reason of the broadening (γ) of the donor band in n-Ag_2Te. Then in the whole interval of temperatures all non-compensated donor impurities $N=N_d-N_a$ are ionized giving their electrons to the conduction band. Therefore all kinetic effects have the appearance characteristic for strongly doped narrow-slit semiconductors (fig. 1).

For explanation of the second fact, it is necessary to determine the full width Γ_d and the broadening of the band of the donor level. The width Γ_d is determined as [16]:

$$\rho_i(\varepsilon)=\frac{N_i}{\pi}\frac{\Gamma_d}{(\varepsilon-E_d')+(\Gamma_d/2)^2}, \qquad (6)$$

where ρ_i is the density of impurity states. At $K^1<<1$ this value is determined as [12].

$$\rho_i(\varepsilon)=\frac{N_i}{\gamma_0\sqrt{\pi}}exp\left(-\frac{\varepsilon^2}{\gamma_0^2}\right), \qquad (7)$$

Where $\varepsilon=e^2/\chi\, r_d$, $\gamma_o=0.26\, E_d^*\,(K^l)^{1/2}$, N_i is the impurity concentration, creating the band, whose middle corresponds to the energy E_d.

Taking into account the value $\rho_i(\varepsilon)$ at $N_d=1{,}1\cdot10^{18}$ cm^{-3}, it has been received from (7) and (6), that $\Gamma_d\approx0.25$ meV. The given calculation has been made also for the width of the band of the acceptor level Γ_a in p-Ag_2Te and $\Gamma_d\approx0{,}003$ meV has been received.

The broadening of the band impurity level at the expense of impurity –band transitions equals [17]:

$$\Upsilon=h/t, \qquad (8)$$

where h is the Plank constant, t is the average time of a carrier in the impurity state with respect to the transition in the band.

Proceeding from the principle of the detailed balance and comparing frequencies of direct (band-impurity) and indirect (impurity-band) transitions, it is possible to receive the expression [17].

$$\rho_z/\tau=\rho_{i/t}, \qquad (9)$$

where ρ_z is the density of band states and τ is the average time of a carrier in the band state with respect to the transition in the impurity, where they are determined in [5]. If ρ_z, τ and ρ_i are known, then $t\approx8.1\cdot10^{-12}$s follows from (9) and from (8) we have $\gamma\approx1.3$ meV.

On the second fact, we can note, that the condition $\Gamma_d^*>>\mu^*$ (where $\Gamma_d^*=\Gamma_d/K_oT$) or $\gamma/\Gamma_d\approx1$ [16] should be satisfied for realization of a resonant scattering. In the case of n-Ag_2Te calculations show reverse, i.e $\mu^*>>\Gamma^*$ and $\gamma/\Gamma_d\approx5.2$.

Therefore the resonant scattering of electrons on donor impurities in n-Ag_2Te is not observed. So we may conclude from above-mentioned interpretations and conclusions [5] that Ag atoms in Ag_2Te create small donor levels and Te atoms create acceptor levels, placed on distances (0.002–$7\cdot10^{-5}$ T,K^{-1}) and (0.030–$7\cdot10^{-5}$ T,K^{-1}) eV from the conduction band bottom, accordingly, which completely control electric and thermoelectric properties of Ag_2Te in the given model.

[1] *A.S. Koroleva, V.Y. Martinov, P.P. Petrov*. Second International Sumposium on materials of chalcogenic oxygen containing semiconductors. Thesis of reports. T.P- 1986, p. 47.

[2] *I.A. Drabkin, B.Y. Moijes.* FTP-1987, v.21. Issue 9, p.1715-1717.

[3] *S.A. Aliev, F.F. Aliev*. Izv. AN SSSR series "Non-organic materials"-1989. v. 25. № 2,p. 241-246.

[4] *V.V. Gorbachev, I.M. Putilin.* Izv. AN SSSR series "Non-organic materials"-1975, v. 11, № 9, p. 1556-1560.

[5] *F. F. Aliev, E.M. Kerimova and S.A. Aliev*. FTP – 2002, v.36, №8, p. 932-936.

[6] *F.F. Aliev*. Second International Symposium on Mathematical and Computational applications. Baku. September 1-3, 1999, p.80

[7] *S.A. Aliev, U.H. Suyutov, M.I. Aliev*. FTP-1973, v.7, Issue 10, p. 2024-2027.

[8] *B.M. Askerov*. "Kinetic effects in semiconductors". L. "Science"-1970, p. 303.

[9] *B.M. Askerov.* "Electron phenomenon of transfer in semiconductor ". M. "Science"-1985, p. 318.

[10] *V.L. Vinetskii, G.A. Holodar.* "Statistic interaction of electrons and defects in semiconductors" - Kiev "Naukova Dumka", 1969, p. 186

[11] *S.A. Aliev, F.F. Aliev. F.F.* Izv. AN SSSR series "Non-organic materials"-1988. v. 24. № 2.p. 341-343.

[12] *B.I. Schlovskii, A.L. Efros.* "Electron properties of alloy semiconductors" M: "Science"-1979. p.416.

[13] *V.M. Berezin, G.P. Vyatkin, V.N. Copev, P.I. Carikh.* FTP-1984, v.18, Issue 2, p. 312-315.

[14] *L.S. Koroleva, I.E. Lopatinskii, P.P. Petrov.* Second International Symposium on materials of chalcogenic oxygen containing semiconductors. Thesis of reports. T. P.-1986, p.46.

[15] *V.F. Masterov, L.F. Zakharenkov.* FTP-1990, v. 24, Issue 2, p. 610-630.

[16] *V.I. Kaydanov, S.A. Nemov, Y.I. Ravich.* FTP-1992, v. 26, Issue 2, p. 201-222.

[17] *V.I. Kaydanov, S.A. Nemov*. FTP-1981, v. 15, Issue 3, p. 542-550.

F.F. Əliyev

n-Ag_2Te KRİSTALINDA YÜKDAŞIYICILARIN ENERJİ SPEKTRİ

Müəyyən olunmuşdur ki, Ag atomları Ag_2Te kristalında, keçirici zonanın dibindən ($7\cdot10^{-5}$T·K^{-1}-0.002) eV məsafədə kiçik donor səviyyələri yaradırlar. Təmiz nümunələrdən Ag>0.01 at% başlayaraq bütün nümunələr özünü n-tip kimi aparırlar. Əsas və aşqar

səviyyələrin hibridləşməsi və eləcə də aşqar səviyyəsinin onun əsas eninə olan nisbəti, yəni $\gamma/\Gamma_d \approx 5.2$ olduğu üçün, n-Ag_2Te kristalında cırlaşma oblastının yuxarı temperatura sürüşməsi və elektronların donor aşqarlarından rezonans səpilməsi müşahidə olunmamışdır.

Ф.Ф. Алиев

ЭНЕРГЕТИЧЕСКИЙ СПЕКТР НОСИТЕЛЕЙ ЗАРЯДА В n-Ag_2Te

Установлено, что атомы Ag в Ag_2Te создают мелкие донорные уровни, расположенные от дна зоны проводимости на расстоянии ($7\cdot10^{-5}T\cdot K^{-1}$-0.002) эВ. Выявлено, что начиная с недостатка Ag>0.01at% в стехиометрическом составе теллурид серебра имеет n-тип проводимости. Показано, что отношениеуширения уровня за счет гибридизации примесных и зонных состояний γ к полной ширине полосы Γ_d очень большая, т.е. $\gamma/\Gamma_d \approx 5.2$. Благодаря последнему в n-Ag_2Te область вырождения смещается к более высоким температурам, а также не наблюдается резонансное рассеяние электронов на донорных примесях.

Received: 12.02.02

Abelian Lagrangian Algebraic Geometry and *ALAG*-quantization

BY A. L. GORODENTSEV
(Institute of Theoretical and Experimental Physics)

ABSTRACT

This is an algebraic geometrical feeling of how to quantize a classical mechanical system (symplectic manifold (M,ω)) prequantized by $U(1)$-bundle ('quantum phase' $L \to M$). Mathematically, it can be considered as an attempt to explain the interaction between symplectic geometry of Lagrangian cycles *inside* M and algebraic geometry of Abelian connections *over* M.

CONTENT

§1. What we mean as 'the quantization'.

1.1. Classical mechanical system is presented by a smooth (maybe non compact) $2n$-dimensional C^∞-manifold M called *a phase space* and equipped with a closed 2-form ω that has to induce a skew symmetric isomorphism $\omega : TM \xrightarrow{\sim} T^*M$. Then, each function $f \in C^\infty(M)$ produces the Hamiltonian vector field $H_f \stackrel{\text{def}}{=} \omega^{-1}(df)$ and there is a Lie algebra structure on $C^\infty(M)$ given by the Poisson bracket $\{f,g\} \stackrel{\text{def}}{=} \omega(H_f, H_g)$.

1.2. Dirac's quantization concept supposes to construct an *irreducible* representation of complex smooth functions on M by linear endomorphisms of some complex Hilbert space $\mathcal{H}$:

$$C^\infty(M,\mathbb{C}) \xrightarrow{Q} End_{\mathbb{C}}(\mathcal{H})$$

such that $Q(1) = \mathrm{Id}$, real functions go to the self adjoint operators, and *the Dirac commutator relations* $Q(\{f,g\}) = [Q(f), Q(g)]/ih$ hold. Unfortunately (or fortunately, maybe), this is impossible by the Van Hove theorem. Mathematical attempts to budge this problem are concentrated in enlarging a classical area and, simultaneously, relaxing some of the previous 'quantization rules'. The 'quantum mathematics' looks today like a radioactive decay via *algebraic*, *analytic*, and *geometric* emanations shown on fig. A.

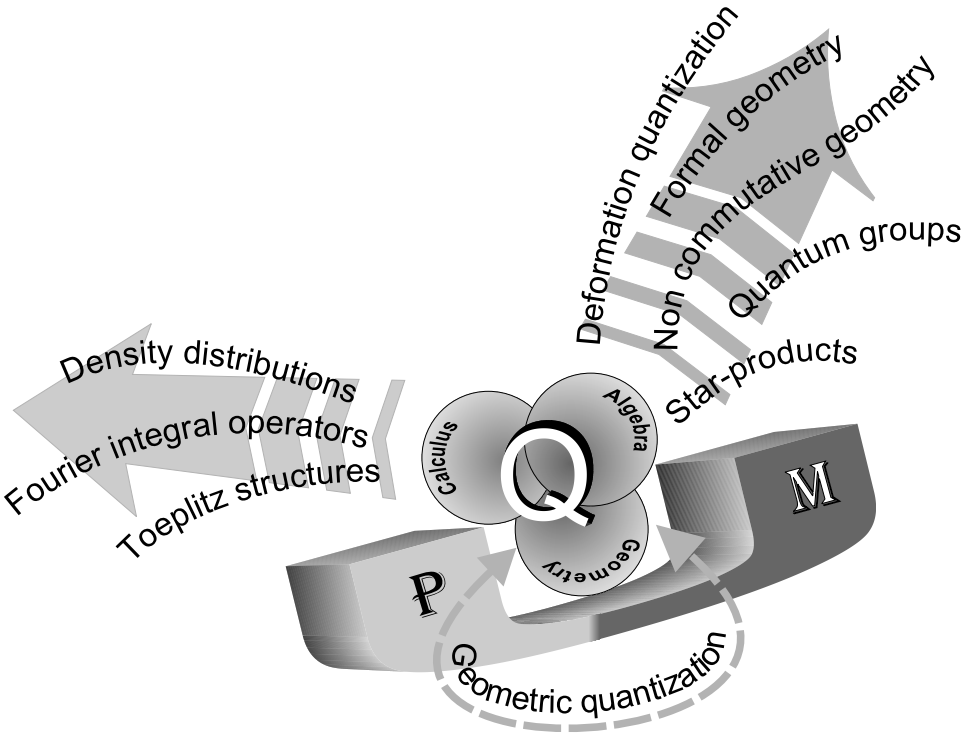

Fig. A. 'Quantum decay of mathematics'.

Geometrically, most of the modified quantization rules aim at a choice of a suitable function class that can be quantized in a consistent fashion. This choice is nothing but a choice of some auxiliary structure on the manifold.

1.3. Geometrical prequantization equipment of a classical mechanical system (M, ω) consists of a complex Hermitian line bundle[1] $L \longrightarrow M$ and a Hermitian connection a on L such that the curvature form $F_a \stackrel{\text{def}}{=} da$ satisfies the following *compatibility condition*

$$F_a = p^*\omega \tag{1-1}$$

where $P \xrightarrow{p} M$ is the principal $U(1)$-bundle tautologically associated with L (i. e. the bundle of unit circles in the fibers of L).

1.3.1. Remark. We always consider the connection a as a real $U(1)$-invariant 1-form on P. In terms of this form, 'the vertical projection' $TP \longrightarrow \mathfrak{u}(1) = i\mathbb{R}$ is given by $v \mapsto 2\pi i\, a_k(v)$ and 'the horizontal hyperplanes' in TP_k are the kernels of a.

1.3.2. Remark. Prequantization equipment exists iff the cohomology class of ω is integer:

$$[\omega] \in H^2(M, \mathbb{Z}) \subset H^2(M, \mathbb{R})\,.$$

In this case the compatibility condition (1-1) implies that $[\omega] = c_1(L)$ and a presents a contact structure on P, that is the top form

$$a \wedge (da)^{\wedge n} = a \wedge (p^*\omega)^{\wedge n} \tag{1-2}$$

nowhere vanishes and produces a volume element on P.

1.3.3. Remark. Usually, L, P are included in a series of bundles $L^{\otimes k}$, P_k, where $P_k \xrightarrow{p_k} M$ is the principal $U(1)$-bundle tautologically associated with the line bundle $L^{\otimes k}$. The number $1/k$ plays here the 'Planck constant' role: we go to the 'quasiclassical limit' as $k \to \infty$. The Hermitean connection a on L induces the Hermitian connections a_k on $L^{\otimes k}$ with curvature $kp^*\omega$.

1.4. Geometric quantization takes the Hilbert space $\mathcal{H}$ being the space of smooth sections $C^\infty(M, L)$ and lets $f \in C^\infty(M)$ act on $\Gamma^\infty(M, L)$ as:

$$Q(f) \stackrel{\text{def}}{=} \nabla_{H_f} + f \ : s \mapsto \nabla_{H_f}(s) + fs \tag{1-3}$$

where ∇_{H_f} is a covariant derivative along the Hamiltonian vector field H_f induced by the connection a.

1.4.1. LEMMA. *The operators $Q(f)$ satisfy all the Dirac conditions except for irreducibility.*
□

Unfortunately, the space $\mathcal{H}$ is 'two times larger' than it should be. Geometrically speaking, to take just 'a half of $\Gamma^\infty(M, L)$' we have to fix some *polarization* on M.

1.5. Polarization of M is a choice of complex n-dimensional tangent planes distribution $T' \subset TM \otimes \mathbb{C}$ closed w.r.t. the Lie brackets of vector fields. It allows to reduce $\mathcal{H}$ to a subspace of *polarized* sections $\mathcal{H}' \subset \Gamma^\infty(M, L)$, which a covariantly constant along all the vector fields from T'.

[1] its sections are the 'quantum states' and the Hermitian structure allows to define their probabilities

Typically, this gives the irreducibility of the geometric quantization procedure but leads to an other problem: only a function $f \in C^\infty(M)$ whose Hamiltonian field H_f preserves T' may be represented as an operator on $\mathcal{H}'$ via (1-3). This kills a lot of interesting Hamiltonians.

1.6. Basic example: Kähler polarization. Let M be equipped with an integrable complex structure I compatible with ω in the sense that M_I is a complex Kähler manifold with the Kähler form ω. Then, the antiholomorphic tangent subbundle $T'' \subset TM \otimes \mathbb{C}$ gives *a polarization* on M called *the Kähler polarization*. In this case, L turns to a holomorphic positive line bundle on M_I (with the $\overline{\partial}$-operator induced by the Hermitian connection a) and the space of polarized sections turns to the space of global *holomorphic* sections $H^0(M_I, L)$. Certainly, only the holomorphic Hamiltonians may be quantized via this approach.

1.6.1. Wave functions and states. The space

$$\mathcal{H}_k \stackrel{\text{def}}{=} H^0(M_I, L^{\otimes k})$$

is called *a wave function* space of level k. Its projectivization $\mathbb{P}\mathcal{H}_k$ is called a space of *states*.

$\mathcal{H}_k$ is a Hilbert space w.r.t. scalar product

$$\langle\, s_1\,,\ s_2\,\rangle_k \stackrel{\text{def}}{=} \int_M (s_1, s_2)_{L^{\otimes k}}\, \omega^{\wedge n}$$

where $(\,*\,,\,*\,)_{L^{\otimes k}}$ is the Hermitian form on $L^{\otimes k}$.

For $k \gg 0$ there is the canonical holomorphic projective embedding

$$\varphi_k : M_I \xrightarrow{x \mapsto Ann(x)} \mathbb{P}H^0(M_I, L^{\otimes k})^* \tag{1-4}$$

The Hermitian structure on $L^{\otimes k}$ gives an antiholomorphic isomorphism

$$H^0(M_I, L^{\otimes k})^* \xrightarrow{\ \sim\ } H^0(M_I, L^{\otimes k})$$

whose composition with the above projective map gives an antiholomorphic embedding of M_I into the space of states. The states sitting in its image are called *coherent*.

1.6.2. The Hardy space. A subbundle of unit balls $D \subset L^*$ is a strictly pseudoconvex domain with the boundary P^*. Hence, the space of holomorphic functions on D is a closed subspace in the Hilbert space $L^2(P)$ (w.r.t. the volume element induced by the contact form a^*). This subspace is called *the Hardy space*. It comes with the natural $U(1)$-action, i. e. admits the orthogonal weight decomposition.

1.6.3. LEMMA. *The Hardy space component of weight k coincides with the space $\mathcal{H}_k = H^0(M_I, L^{\otimes k})$, of level k wave functions, and Hermitian structure induced on $\mathcal{H}_k$ from $L^2(P^*)$ coincides with the initial Hermitian structure on $\mathcal{H}_k$.* □

So, the Hardy space is nothing but $\bigoplus_k \mathcal{H}_k$.

1.7. Toeplitz operators. Write $L^2(P^*) \xrightarrow{\Pi_k} \mathcal{H}_k$ for the canonical orthogonal projector (called *the k-th Szegö projector*) and let $f \in C^\infty(M)$. Each $\psi \in H^0(M_I, L^{\otimes k}) \subset L^2(P^*)$ can be multiplied by $p_{-1}^* f$ in $L^2(P^*)$ and then sent back to $H^0(M_I, L^{\otimes k})$ by Π_k. The resulting map

$$T_f^{(k)} : H^0(M_I, L^{\otimes k}) \xrightarrow{\psi \mapsto \Pi_k(p_{-1}^* f \cdot \psi)} H^0(M_I, L^{\otimes k})$$

is called *k-th Toeplitz operator* of f.

1.8. Berezin – Toeplitz approach takes $f \in C^\infty(M)$ to the operator $T_f^{(k)} \in End_{\mathbb{C}}(\mathcal{H}_k)$ instead of the differential operator (1-3) used in the standard geometric quantization method. This representation

$$C^\infty(M) \xrightarrow{T^{(k)}} End_{\mathbb{C}}(\mathcal{H}_k)$$

satisfies all the Dirac quantization principles except for the commutator relation:

$$ih\, T^{(k)}_{\{f,g\}} \neq \left[T_f^{(k)}, T_g^{(k)}\right] .$$

1.8.1. LEMMA. *Although for each level k it does preserve neither Lie nor associative algebra structures the discrepancy has 'good quasi-classical behavior':*

$$\left\| ihT^{(k)}_{\{f,g\}} - \left[T_f^{(k)}, T_g^{(k)}\right] \right\| \sim O(1/k)$$

as $k \to \infty$. □

1.8.2. Observation. Although an output of the Berezin quantization (wave function spaces, e.t.c.) *a priori* depends on the choice of a polarized complex structure I on M, in several examples (elliptic curves, say) the moduli space of the polarized complex structures on M admits a *flat* projective bundle with fibers $\mathbb{P}\left(H^0(M_I, L^{\otimes k})\right)$.

1.9. Projective geometrical version of the Dirac's quantization concept[1] deals with the Kähler manifold $\mathbb{CP}_\infty = \mathbb{P}(\mathcal{H})$ instead of the vector space $\mathcal{H}$. It comes with complex structure, Riemannian metric G, and compatible symplectic structure Ω (last two are real and imaginary parts of the canonical Fubini - Studi metric on $\mathbb{P}(\mathcal{H})$). Each self adjoint linear operator $\mathcal{H} \xrightarrow{A} \mathcal{H}$ induces the expected value function $\widehat{A} \in C^\infty(\mathbb{P}(\mathcal{H}))$ by the rule

$$\widehat{A}(v) = \langle\, v\,,\, Av\,\rangle$$

where $v \in \mathcal{H}$ is normalized by $\langle\, v\,,\, v\,\rangle = 1$. A function $\widehat{A} \in C^\infty(\mathbb{P}(\mathcal{H}))$ comes by this way iff its Hamiltonian flow w. r. t. the symplectic structure Ω preserves the Riemannian metric G. Moreover, the correspondence $A \longmapsto \widehat{A}$ is the Lie algebra homomorphism, i. e. sends the commutator of linear operators to the Poisson bracket of smooth functions w. r. t. to Ω. So, the Dirac postulates for the quantization of some classical mechanical model (M, ω) mean nothing but the existence of an irreducible Poisson algebra representation

$$C^\infty(M) \longrightarrow C^\infty(\mathbb{P}(\mathcal{H}))$$

1.10. The main idea of ALAG is to replace the 'linear' space $\mathbb{P}(\mathcal{H})$, which is the simplest possible algebraic variety, by more general 'non linear' algebraic variety $\mathcal{B}$ whose geometry encodes 'the quantization' of M. Namely, we show that any real analytic variety M equipped with smooth symplectic form and compatible smooth prequantization data (L, a) (note that all these data lives in 'smooth real geometry') leads canonically to some (infinite dimensional) complex Kähler manifold $\mathcal{B} = \mathcal{B}(M, \omega, L, a)$ equipped an integrable complex structure, Riemannian metric G, compatible symplectic structure Ω, and holomorphic prequantization data

[1] for detailed review see: *A. Ashtekar, T. A. Schilling. Geometrical Formulation of Quantum Mechanics.* Prep. `arXiv: gr-qc/9706069`

$\mathcal{L} \longrightarrow \mathcal{B}$, $\mathcal{A}$ (which also can be quantized in its turn) together with the natural Poisson algebra homomorphism (*dynamical correspondence*) $C^\infty(M) \longrightarrow C^\infty(\mathcal{B})$ which allows to translate classical Hamiltonian dynamics on M to its quantized version[2] on $\mathcal{B}$.

Practically, we will construct some *universal* Kähler structure on the space of appropriate Lagrangian cycles on M. Its projective geometrical properties encode the geometry of any particular quantization construction, for example, the Berezin - Toeplitz one. So, this is the first step to develop the true 'geometry of quantization', the whole of which is waited looking like

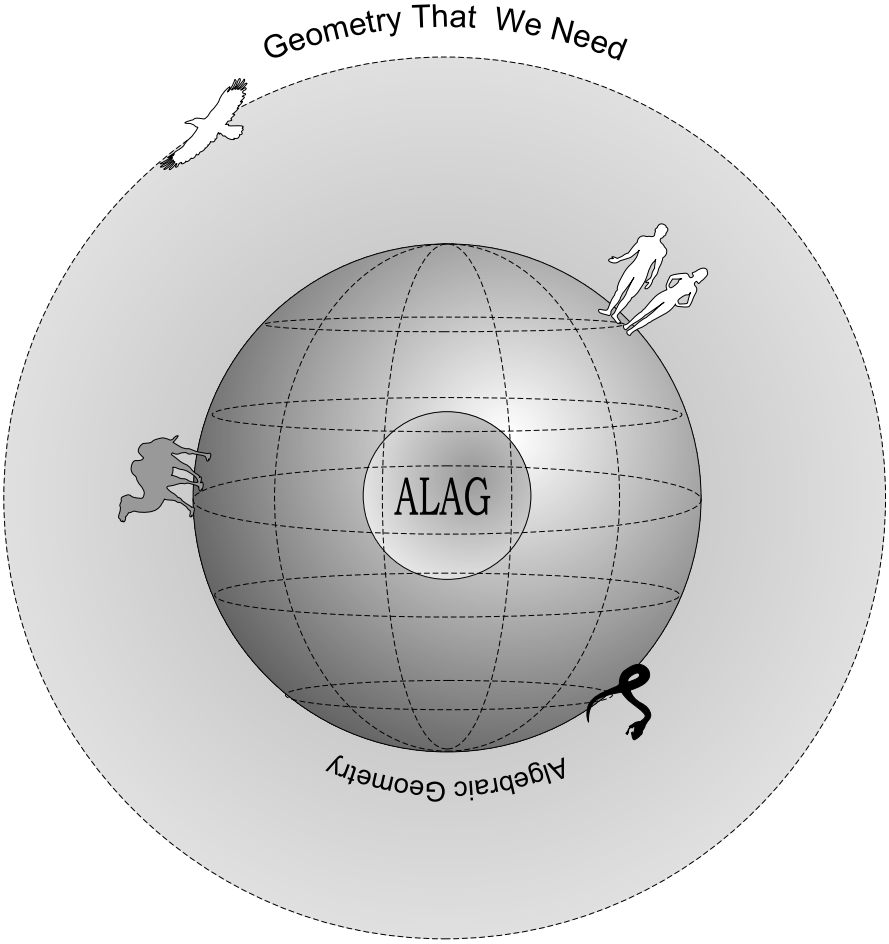

Fig. B. The Geometrical World.

[2]Note that the projective geometrical reformulation of the Dirac quantization principle sends Schrödinger equation on $\mathcal{H}$ to Hamiltonian equations on $\mathcal{B}$

§2. Lagrangian and Abelian preliminaries for ALAG.

2.1. Space of Lagrangian cycles. We fix a smooth (maybe non-compact) $2n$-dimensional symplectic C^∞-manifold M, a smooth compact oriented n-dimensional C^∞-manifold S, and some smooth homotopy class

$$Map_{\text{LA}}(S, M)$$

of maps $S \xrightarrow{\varphi} M$ such that $\varphi^*(\omega) = 0$ (such the maps are called *Lagrangian*). The orbit space

$$\mathfrak{L} \stackrel{\text{def}}{=} Map_{\text{LA}}(S, M)/Diff_0(S)$$

is called *the space of Lagrangian cycles* (of fixed topological type).

2.1.1. Crucial property of Lagrangian cycles. If φ is a smooth immersion, i. e. there is *an inclusion* of tangent bundles $TS \hookrightarrow \varphi^*(TM)$, a Lagrangian cycle $S \xrightarrow{f} M$ is called *smoothly immersed*. In this case the normal bundle $N_{M/S} \simeq \varphi^*(TM)/TS$ is naturally identified with the cotangent bundle

$$T^*S \simeq \varphi^*\left(T^*M\right)/Ann\left(TS\right) \stackrel{\omega}{\simeq} \varphi^*(TM)/TS$$

2.1.2. Main 'local' example: let $M = T^*S$ be a cotangent bundle over any smooth manifold S with the canonical projection $M \xrightarrow{p} S$. The 1-form $\eta \in C^\infty(M, T^*M)$ sending $w \in T_{(\alpha,x)}T^*S$ (with $x \in S$, $\alpha \in T_x^*S$) to $\eta(w) \stackrel{\text{def}}{=} p^*\alpha(w)$ is called *an action form*. Its differential $\omega \stackrel{\text{def}}{=} d\eta$ gives a symplectic structure on M (called *canonical*).

In local coordinates $(p_1, p_2, \ldots, p_n,\ q_1, q_2, \ldots, q_n)$, where q_i coordinate the base S and p_i are linear coordinates along dq_i in the fibers,

$$\eta(p,q) = \sum p_j dq_j\ , \quad \omega(p,q) = \sum dp_j \wedge dq_j\ .$$

A section $S \xhookrightarrow{s} M$, i. e. a graph of 1-form $\alpha_s = s^*(\eta) \in C^\infty(S, T^*S)$, is Lagrangian iff α_s is closed, because of $0 = s^*(\omega) = s^*(d\eta) = ds^*(\eta) = d\alpha_s$. So, small deformations of S as a Lagrangian cycle in T^*S presented by the zero section $S \hookrightarrow T^*S$ may be identified with a small neighborhood of zero in the space $Z^1_{\text{DR}}(S, \mathbb{R})$, of smooth real closed 1-forms on S.

2.2. The tangent space $T_{(S,\varphi)}\mathfrak{L}$ at a smoothly immersed Lagrangian cycle (S, φ) is naturally identified with $Z^1_{\text{DR}}(S, \mathbb{R})$. Indeed, $T_{(S,\varphi)}\mathfrak{L}$ consists of ω-preserving local normal vector fields near S on M modulo the fields tangent to S. We send such a vector field v to a 1-form $\alpha = \varphi^*(i_v\omega) \in C^\infty(S, T^*S)$. It is closed, because of

$$d\alpha = d\varphi^*(i_v\omega) = \varphi^*(di_v\omega) = \varphi^*(\mathcal{L}_v\omega + i_v d\omega) = \varphi^*(\mathcal{L}_v\omega) = 0\,.$$

2.3. The Darboux - Weinstein uniformization. Any smooth Lagrangian immersion $S \xhookrightarrow{\varphi} M$ can be extended to a smooth immersion $U \xhookrightarrow{\widehat{\varphi}} M$ of some tube neighborhood $U \subset T^*S$ around the zero section in such a way that $\widehat{\varphi}^*\omega = d\eta$ turns to the canonical symplectic form on T^*S. This continuation induces a smooth map from some neighborhood of zero in $Z^1_{\text{DR}}(S, \mathbb{R})$ to $\mathfrak{L}$: a small enough closed 1-form goes to the $\widehat{\varphi}$-image of its graph. The image of this map contains an open (in suitable topology) neighborhood of S in $\mathfrak{L}$.

2.4. A complex Hermitian line bundle $L \longrightarrow X$ on a C^∞-manifold X has a form $L = P \times_{U(1)} \mathbb{C}$, where P is the bundle of unit circles in L (called *a principal $U(1)$-bundle of L*). Topologically, L is uniquely defined by its *first Chern class*

$$c_1(L) \in H^1(X, \mathcal{C}^\infty(X, \mathbb{C}^*)) \simeq H^2(X, \mathbb{Z})$$

formed by its transition functions.

2.4.1. A Hermitian connection on P is a 1-form a on P such that $\mathcal{L}ie_u a = 0$ and $a(u) = 1$ for the standard $U(1)$-invariant 'vertical' vector field u dual to the 1-form u^* such that $\int_{U(1)} u^* = 1$. The kernel hyperplanes of α in TP are called *horizontal*.

2.4.2. Covariant derivation w. r. t. a is a differential operator $\mathcal{C}^\infty(X, L) \xrightarrow{\nabla_a} \mathcal{C}^\infty(X, T^*X \otimes L)$ sending a local unitary section σ over $U \subset X$ to $\nabla_a \sigma = 2\pi i\, \alpha_\sigma \otimes \sigma$, where $\alpha_\sigma = \sigma^* a$ is called *a local connection 1-form* of a. An arbitrary local section $f\sigma$ is then differentiated as

$$\nabla_a(f\sigma) = (df + 2\pi i\, f\alpha_\sigma) \otimes \sigma \ .$$

An unitary base change (*gauge transform*), which acts as $\sigma \longmapsto \sigma' = h\sigma$ with $h \in C^\infty(U, U(1))$, takes

$$\alpha_\sigma \longmapsto \alpha_{\sigma'} = \alpha_\sigma - \frac{i}{2\pi} h^{-1} dh \ .$$

Similarly, a *covariantly constant* (or *horisontal*) local sections $f\sigma$ have to satisfy the logarithmic differential equation $2\pi i\, f^{-1} df = \alpha_\sigma$. The differentials $d\alpha_\sigma$, of local connection forms, do not depend on a choice of local unitary bases σ and can be glued into a global closed 2-form $\omega_a \in C^\infty(X, \Lambda^2 T^* X)$ called *a curvature* of a. Its cohomology class $[\omega_a] \in H^2(X, \mathbb{R})$ is integer and coincides with $c_1(L) \in H^2(X, \mathbb{Z}) \subset H^2(X, \mathbb{R})$.

In terms of covariant derivative, the 'double differentiation'

$$C^\infty(X, L) \xrightarrow{\nabla_a^2} C^\infty(X, \Lambda^2 T^* X \otimes L)$$

(which is induced by ∇_a via Leibnitz rule) is *a $C^\infty(X)$-linear operator* taking $s \longmapsto 2\pi i\, \omega_a \otimes s$. In terms of the principal $U(1)$-bundle $P \xrightarrow{p} X$, we have $p^*\omega_a = da$ and this 2-form sends a pair of $U(1)$-invariant vector fields v_1, v_2 on P to

$$da(v_1, v_2) = \Big(\mathcal{L}ie_{v_1} a - d\big(a(v_1)\big)\Big)(v_2) = \mathcal{L}ie_{v_1} a(v_2) = -a([v_1, v_2]) \ .$$

2.5. Flat Hermitian connections are defined by the condition $\omega_a \equiv 0$. If it holds, L admits a global never vanishing unitary (usually, non horizontal) section $X \xhookrightarrow{\sigma} L$. Horizontal sections $f\sigma$ exist only locally over simply connected open sets and are given by $f = c\, e^{-2\pi i g}$ with an arbitrary constant $c \in \mathbb{C}$ and any smooth local function g such that $dg = \alpha_\sigma$.

Gauge equivalence classes of flat Hermitian connections are in 1–1 correspondence with unitary characters

$$\pi_1(X) \xrightarrow{\chi} U(1) \ ,$$

of the fundamental group of X. A character χ_a corresponding to a connection a presents *the holonomy* (or *the periods*) of a, i. e. it sends a loop $\gamma \in \pi_1(X)$ to a fiber shift under the horizontal transport along γ.

Considering the unitary characters as cohomology classes in

$$H^1(X, U(1)) \simeq H^1(X, \mathbb{R})/H^1(X, \mathbb{Z}) ,$$

we parameterize the gauge classes of the flat Hermitian connections on L by the points of real torus $J_X \stackrel{\text{def}}{=} H^1(X, \mathbb{R})/H^1(X, \mathbb{Z})$ called *a Jacobian* of X.

§3. Basic ALAG notions.

Let as fix some geometric prequantization data[1] (M, ω, L, a) and write $P_k \xrightarrow{p_k} M$ for the principal $U(1)$-bundles associated with $L^{\otimes k}$ and write a_k for their Hermitian connections induced by $a = a_1$). For any k the curvature $da_k = k\,\omega$ and a_k provides P_k with *a contact structure* whose volume element equals $a_k \wedge (d\alpha_k)^{\wedge n} = k^n a_k \wedge (p_k^*\omega)^{\wedge n}$.

3.1. Bohr - Sommerfeld cycles. For any Lagrangian cycle $S \xrightarrow{\varphi} M$ a pull back $\varphi^* L^{\otimes k}$ is a topologically trivial Hermitian line bundle on S equipped with the flat Hermitian connection $\varphi^* a_k$, because its curvature $\omega_{\varphi^* a_k} = k\,\varphi^*(\omega) = 0$. A Lagrangian cycle (S, φ) is called *Bohr - Sommerfeld of level k* (or *a BS_k-cycle* for shortness), if $\varphi^* L^{\otimes k}$ admits a global horizontal section over S. The Bohr - Sommerfeld cycles of level k form a subvariety $\mathcal{B}_k \subset \mathfrak{L}$. For any integer k, m there are natural inclusions $\mathcal{B}_k \xhookrightarrow{\beta_{k,m}} \mathcal{B}_{mk}$.

3.2. Planckian cycles. Let $Map_{\text{LE}}(S, P_k)$ be the space of smooth maps $S \xrightarrow{\widetilde{\varphi}} P_k$ such that $\widetilde{\varphi}^*(\alpha_k) = 0$ (such the maps are called *Legendrian*). The orbit space

$$\mathcal{P}_k \stackrel{\text{def}}{=} Map_{\text{LE}}(S, P_k)/Diff_0(S)$$

is called a space of *level k Planckian cycles*. For each Planckian cycle $S \xrightarrow{\widetilde{\varphi}} P_k$ the composition $\varphi : S \xrightarrow{p_k \circ \widetilde{\varphi}} M$ is Lagrangian, because of $\varphi^*\omega = d\widetilde{\varphi}^*\alpha_k/k = 0$. So, a Planckian cycle $(S, \widetilde{\varphi})$ is nothing but a global horizontal unitary section of $\varphi^* L^{\otimes k}$ over the Bohr - Sommerfeld cycle (S, φ).

3.2.1. Berry bundles. There are principal $U(1)$-bundle $\mathcal{P}_k \xrightarrow{\pi_k} \mathcal{B}_k$ and corresponding Hermitian line bundle $\mathcal{L}_k \longrightarrow \mathcal{B}_k$ called *Berry bundles* (of level k). Taking m-th fiberwise power of a horizontal unitary section, we get degree m covering $\mathcal{P}_k \xrightarrow{\widetilde{\mu}_{m,k}} \beta_{m,k}^* \mathcal{P}_{mk}$. In terms of the line bundles, this means that $\beta_{k,m}^* \mathcal{L}_{mk} = \mathcal{L}_k^{\otimes m}$ under the inclusions $\mathcal{B}_k \xhookrightarrow{\beta_{k,m}} \mathcal{B}_{mk}$.

3.3. Example: the Legendrian knots in S^3. Let us take the Riemannian sphere $S^2 = \mathbb{P}(\mathbb{C}^2)$ as M and the line bundle $\mathcal{O}(1)$, of homogeneous degree 1 forms, as L. The corresponding principal $U(1)$-bundle P may be identified with the unit sphere $S^3 \subset \mathbb{C}^2$ fibered over $\mathbb{P}(\mathbb{C}^2)$ via Hopf. The standard Hermitian connection on P is obtained by restricting the $U(2)$-invariant 1-form

$$2\pi i\, a \stackrel{\text{def}}{=} (\partial - \overline{\partial}) \log |z|$$

[1] recall that M is $2n$-dimensional C^∞-manifold equipped with a symplectic form ω, Hermitian line bundle $L \longrightarrow M$, and Hermitian connection a whose curvature $\omega_a = da$ coincides with $p_1^*\omega$

on $\mathbb{C}^2 \setminus \{0\}$. Its curvature $da = \frac{i}{2\pi}\partial\overline{\partial}\log|z|$ provides $\mathbb{P}_1$ with the standard symplectic structure ω such that $p^*\omega = da$. Taking $S = S^1$ as Lagrangian cycles source, we get *any* smooth immersion $S^1 \xrightarrow{\gamma} S^2$ being Lagrangian. The period of a_k along γ is

$$\oint_\gamma \alpha_k = k \iint_\gamma \omega = \frac{k}{2} A_\gamma ,$$

where A_γ is *an oriented area* bounded by $\gamma(S) \subset S^2$. The Bohr - Sommerfeld conditions mean that it is integer multiple of 2π. So, the Planckian cycles are the Legendrian knots in S^3 laying over unicursal curves cutting a *rational* part of the whole sphere area.

3.4. Infinitesimal description of $\mathcal{B}_k$ and $\mathcal{P}_k$. A tangent vector to $\mathcal{P}_k$ at $(S, \widetilde{\varphi})$ is a section

$$v \in C^\infty\big(S\,,\, \widetilde{\varphi}^*(TP_k)/TS\big)$$

such that $\mathcal{L}ie_v\alpha_k = 0$. Write its vertical component (w.r.t. α_k) as fu, where $f = \alpha_k(v) \in C^\infty(S)$ and u is the standard vertical field (as above). Let us identify the subspace of horizontal sections in $C^\infty(S, TP_k)$ with $C^\infty(S, \varphi^*TM)$ via dp_k. Then the horizontal component $v - fu$, of v, contracted with da_k and any horizontal w is

$$d\alpha_k(v - fu, w) = d\alpha_k(v, w) = \Big[\mathcal{L}ie_v(\alpha_k) - d\big(\alpha_k(v)\big)\Big](w) = -df\,(w)\ .$$

Hence, the both vertical and horizontal components of v are uniquely defined by $f \in C^\infty(S)$ and infinitesimal deformations preserving the Bohr - Sommerfeld conditions go along the subspace

$$B^1_{\mathrm{DR}}(S, \mathbb{R}) \subset Z^1_{\mathrm{DR}}(S, \mathbb{R}) = T_{(S,\varphi)}\mathfrak{L}\ .$$

Roughly speaking, each $f \in C^\infty(S)$ deforms $(S, \widetilde{\varphi})$ by moving the underlying Bohr - Sommerfeld cycle to the graph of df in T^*S and simultaneous gauging the global horizontal section $\widetilde{\varphi}$ by $e^{-2k\pi i f}$.

3.4.1. LEMMA. *Tangent space $T_{(S,\varphi)}\mathcal{B}_k$ to BS_k-cycles space at a smoothly immersed cycle $S \xrightarrow{\varphi} M$ is naturally identified with the space of exact 1-forms $B^1_{\mathrm{DR}}(S)$. Under this identification, the differential of the inclusion $\mathcal{B}_k \xrightarrow{\beta_{k,m}} \mathcal{B}_{mk}$ acts as the scalar multiplication by m.* □

3.4.2. LEMMA. *Tangent space $T_{(S,\widetilde{\varphi})}\mathcal{P}_k$ at a smoothly embedded Planckian cycle $S \xrightarrow{\widetilde{\varphi}} P_k$ is naturally identified with $C^\infty(S)$. Under this identification, the differential of the covering $\mathcal{P}_k \xrightarrow{\widetilde{\mu}_{m,k}} \beta^*_{m,k}\mathcal{P}_{mk}$ acts on $C^\infty(S)$ as the scalar multiplication by m.* □

3.4.3. COROLLARY. *The identification above takes the differential of the Berry bundle $\mathcal{P}_k \xrightarrow{\pi} \mathcal{B}_k$ to the external differentiation $C^\infty(S, \mathbb{R}) \xrightarrow{d} B^1_{\mathrm{DR}}(S, \mathbb{R})$.* □

3.5. Darboux - Weinstein uniformization. Let $S \xrightarrow{\widetilde{\varphi}} P_k$ be a Planckian cycle laying over a smoothly immersed Bohr - Sommerfeld cycle $S \xrightarrow{\varphi} M$. Then $\mathcal{P}_k$ is smooth near $(S, \widetilde{\varphi})$ and is locally modelled by some neighborhood of zero in $C^\infty(S, \mathbb{R})$. Similarly, $\mathcal{B}_k$ is modelled near (S, φ) by a neighborhood of zero in $B^1_{\mathrm{DR}}(S, \mathbb{R})$.

3.5.1. Sketch of proof. Let us continue (via Darboux - Weinstein) our Bohr - Sommerfeld cycle to a symplectic immersion $U \xrightarrow{\widehat{\varphi}} M$, where $U \subset T^*S$ is some neighborhood of the

zero section. The Hermitian line bundle $\widehat{\varphi}^* L^{\otimes k}$ admits (perhaps, over smaller U) an unitary section $U \xrightarrow{\sigma} \widehat{\varphi}^* L^{\otimes k}$ which coincides with our Planckian cycle over the zero section $S \subset U$ and such that the covariant differentiation w. r. t. the connection a_k is given in the base σ by the canonical action form η on T^*S, i. e. $\nabla_a \sigma = 2\pi i\, \eta \otimes \sigma$ over U. By the definition, the DW-coordinatization of $\mathcal{P}_k$ by some neighborhood of zero in $C^\infty(S, \mathbb{R})$ sends a small enough function f to a BS_k-cycle $\Gamma_f \subset U$, which is the graph of df, equipped with the global unitary horizontal section $e^{-if} \cdot \sigma|_{\Gamma_f}$.

3.6. Complex structure on $T\mathcal{P}_k$. The tangent bundle $T\mathcal{P}_k$ admits a natural integrable complex structure. Namely, *complex* DW-coordinatization of $T\mathcal{P}_k$ near a pair

$$S \xrightarrow{\widetilde{\varphi}} P_k\ , \quad g \in C^\infty(S, \mathbb{R}) = T_{(S,\widetilde{\varphi})}\mathcal{P}_k$$

takes a small enough $\psi = \psi_1 + i\psi_2 \in C^\infty(S, \mathbb{C})$ and treats its real part ψ_1 as a linear coordinate along the fiber of the tangent bundle and the imaginary part ψ_2 — as the DW-coordinate on $\mathcal{P}_k$. So, in terms of splitting $T_{(\widetilde{\varphi},g)}\,(T\mathcal{P}_k) = T\mathcal{P}_k \oplus T\mathcal{P}_k = C^\infty(S, \mathbb{R}) \oplus C^\infty(S, \mathbb{R})$ coming from the (real) DW-coordinatization of $\mathcal{P}_k$, the multiplication by i on sends $(\psi_1, \psi_2) \longmapsto (\psi_2, -\psi_1)$, i. e. coincides with the usual complex structure on $C^\infty(S, \mathbb{C})$. In the next section we will combine this complex structure with the canonical symplectic structure on $T^*\mathcal{P}_k$ in order to get an integrable Kähler structure on a suitable vector bundle over $\mathcal{P}_k$.

§4. Kähler structure on the spaces of half weighted cycles.

4.1. Measures. The equivalence $\lambda \sim \mu$ of two measures λ, μ on S means that $\lambda(B) = 0 \Leftrightarrow \mu(B) = 0$ for any Borel subset $B \subset S$. By the Radon - Nikodym theorem, $\lambda \sim \mu$ iff there are two real integrable positive functions

$$\varrho_{\mu\lambda} = \frac{d\mu}{d\lambda} \in L^1(S, \lambda)\ , \quad \varrho_{\lambda\mu} = \frac{d\lambda}{d\mu} \in L^1(S, \mu)$$

(called the Radon - Nikodym derivatives) such that

$$\int_B d\mu = \int_B \varrho_{\mu\lambda}\, d\lambda\ , \quad \int_B d\lambda = \int_B \varrho_{\lambda\mu}\, d\mu$$

for any Borel subset $B \subset S$. One writes usually $\lambda = \varrho_{\lambda\mu}\mu$ for two equivalent measures.

We will write $\mathfrak{M} = \mathfrak{M}(S)$ for the equivalence class of measures on S induced by its manifold structure and $\mathfrak{M}_0 \subset \mathfrak{M}$ for *smooth* measures, whose pairwise Radon - Nikodym derivatives are smooth. Certainly, $\varrho_{\mu\lambda}\varrho_{\lambda\zeta} = \varrho_{\mu\zeta}$ and $\varrho_{\mu\lambda}\varrho_{\lambda\mu} = 1$ almost everywhere w. r. t. any measure from $\mathfrak{M}$ for all $\lambda, \varrho, \zeta \in \mathfrak{M}$.

4.2. Half weighings. Consider the following equivalence of pairs (f, μ), where $\mu \in \mathfrak{M}$, $f \in L^2_{\mathbb{R}}(S, \mu)$: put $(f_1, \mu_1) \sim (f_2, \mu_2)$ iff $f_1\sqrt{\varrho_{\mu_1\lambda}} = f_2\sqrt{\varrho_{\mu_2\lambda}}$ almost everywhere w. r. t. any $\lambda \in \mathfrak{M}$. The corresponding equivalence classes usually are referred as *half weights* and denoted

as $\vartheta = f\sqrt{\mu}$. A half weight $f\sqrt{\mu}$ is called *smooth*, if $f \in C^\infty(S)$ and $\mu \in \mathfrak{M}_0$. The half weights form the real closed vector space[1] $\mathfrak{H}(S)$ equipped with the scalar product

$$\left(f_1\sqrt{\mu_1}\,,\, f_2\sqrt{\mu_2} \right) \stackrel{\text{def}}{=} \int_S f_1 f_2 \sqrt{\varrho_{\mu_1\lambda}\varrho_{\mu_2\lambda}}\, d\lambda$$

Smooth half weights form there a dense subspace $\overset{\circ}{\mathfrak{H}}(S) \subset \mathfrak{H}(S)$.

4.3. Half-weighted cycles. $\mathit{Diff}_0(S)$ acts on $\mathfrak{H}(S)$ via $(f,\mu) \overset{h}{\longmapsto} \left(f\circ h^{-1}\,,\, (h^{-1})^*\mu \right)$ and sends $\overset{\circ}{\mathfrak{H}}$ to itself. The orbit spaces of the corresponding diagonal actions:

$$\mathfrak{L}^{\text{hw}} \stackrel{\text{def}}{=} \mathit{Map}_{\text{LA}}(S,M) \times \mathfrak{H}(S)/\mathit{Diff}_0(S)$$
$$\mathcal{P}_k^{\text{hw}} \stackrel{\text{def}}{=} \mathit{Map}_{\text{LE}}(S,P_k) \times \mathfrak{H}(S)/\mathit{Diff}_0(S)\ .$$

are called spaces of *half weighted* Lagrangian and Planckian cycles of level k. Replace $\mathfrak{H}$ by $\overset{\circ}{\mathfrak{H}}$ in these definitions, we obtain the dense subspaces $\overset{\circ}{\mathfrak{L}}{}_k^{\text{hw}} \subset \mathfrak{L}_k^{\text{hw}}$ and $\overset{\circ}{\mathcal{P}}{}_k^{\text{hw}} \subset \mathcal{P}_k^{\text{hw}}$, of *smoothly* half weighted cycles. The forgetful maps $\mathfrak{L}^{\text{hw}} \xrightarrow{F} \mathfrak{L}$, $\mathcal{P}_k^{\text{hw}} \xrightarrow{\tilde{F}} \mathcal{P}_k$ (and their smooth versions) provide these spaces with the vector bundle structures. All these bundles are arranged in the commutative diagram:

$$\begin{array}{ccccc}
\mathcal{P}_k^{\text{hw}} & \longrightarrow & \mathcal{B}_k^{\text{hw}} & \hookrightarrow & \mathfrak{L}^{\text{hw}} \\
\downarrow{\scriptstyle \tilde{F}=\pi^*F|_{\mathcal{B}_k^{\text{hw}}}} & & \downarrow{\scriptstyle F|_{\mathcal{B}_k^{\text{hw}}}} & & \downarrow{\scriptstyle F} \\
\mathcal{P}_k & \xrightarrow{\pi} & \mathcal{B}_k & \hookrightarrow & \mathfrak{L}\ .
\end{array}$$

4.4. Complex structure. For any fixed half weight $f\sqrt{\mu}$ the tangent space $T_{\tilde{S}}\mathcal{P}_k = C^\infty(S)$ is included into $T_{f\sqrt{\mu}}\mathfrak{H} \simeq \mathfrak{H}$ by $f_1 \longmapsto f f_1\sqrt{\mu}$. This gives an inclusion $T\mathcal{P}_k \hookrightarrow \mathcal{P}_k^{\text{hw}}$ as a dense set. Restricting ourselves by the smooth half weights, we get the identification $T\mathcal{P}_k \xrightarrow{\sim} \overset{\circ}{\mathcal{P}}{}_k^{\text{hw}}$. To push down the canonical integrable complex structure from $T\mathcal{P}_k$ To $\overset{\circ}{\mathcal{P}}{}_k^{\text{hw}}$, consider a smooth Planckian cycle $S \xhookrightarrow{\tilde{\varphi}} P$ laying over a BS_k-cycle $S \xhookrightarrow{\varphi} M$ and half weighted by $\vartheta = f\sqrt{\mu}$. Using a local splitting $T_{(\tilde{\varphi},\vartheta)}\,\overset{\circ}{\mathcal{P}}{}_k^{\text{hw}} \simeq T_\vartheta\,\overset{\circ}{\mathfrak{H}}(S) \oplus T_{\tilde{\varphi}}\,\overset{\circ}{\mathcal{P}}{}_k^{\text{hw}} \simeq C^\infty(S) \oplus C^\infty(S)$ we coordinate a small neighborhood of $(\tilde{\varphi},\vartheta)$ in $\overset{\circ}{\mathcal{P}}{}_k^{\text{hw}}$ by smooth complex valued functions $\psi = \psi_1 + i\psi_2 \in C^\infty(S,\mathbb{C})$ as follows. The imaginary part ψ_2 produces some Planckian cycle supported by $\Gamma_{\psi_2} \subset U \subset T^*S$ and having the DW-coordinate ψ_2. The real part ψ_1 provides it with the half weight

$$pr^*\vartheta = (pr\circ f)\cdot\sqrt{pr^*\mu}\ ,$$

where $\Gamma_{\psi_2} \xrightarrow{pr} S$ is the restriction of the canonical projection $T^*S \longrightarrow S$.

4.5. Kähler structure. The product of two half weights $\vartheta_1 = f_1\sqrt{\mu_1}$ and $\vartheta_2 = f_2\sqrt{\mu_2}$ is a complete weight on S, that is

$$\vartheta_1\vartheta_2 \stackrel{\text{def}}{=} f_1 f_2 \sqrt{\varrho_{\mu_1}\varrho_{\mu_2\lambda}}\,\lambda\ ,$$

[1] linear combinations of half weights are defined as $t_1\cdot f_1\sqrt{\mu_1} + t_2\cdot f_2\sqrt{\mu_2} \stackrel{\text{def}}{=} \left(t_1 f_1\sqrt{\varrho_{\mu_1\lambda}} + t_2 f_2\sqrt{\varrho_{\mu_2\lambda}}\right)\sqrt{\lambda}$ where λ in the both formulas is an arbitrary measure from $\mathfrak{M}$

does not depend on the choice of $\lambda \in \mathfrak{M}$ and produces a well defined integration

$$f \longmapsto \int_S f\, d\vartheta_1\vartheta_2 \stackrel{\text{def}}{=} \int_S f f_1 f_2 \sqrt{\varrho_{\mu_1\lambda}\varrho_{\mu_2\lambda}}\, d\lambda$$

for $f \in C^\infty(S)$. So, each half weight ϑ produces a linear form

$$\varkappa(\vartheta) \ : \quad f \longmapsto \int_S f\, d\vartheta^2$$

on the tangent space $T_{\widetilde{S}}\mathcal{P}_k \simeq C^\infty(S)$. In other words, $\mathfrak{H}(S)$ double covers $T^*_{(S,\widetilde{\varphi})}\mathcal{P}_k$, because $\varkappa$ is quadratic in ϑ. The differential of this quadratic covering sends $\vartheta_1 \in \mathfrak{H}(S)$ to the linear form

$$d\varkappa_\vartheta(\vartheta_1) \ : \quad f \longmapsto 2\int_S f\, d\vartheta\vartheta_1 \ .$$

on $C^\infty(S) = T_{\widetilde{S}}\mathcal{P}_k$. So, $d\varkappa$ identifies $T(\mathcal{P}_k^{\text{hw}})$ with $T(T^*\mathcal{P}_k)$ an may be used to pull back the canonical symplectic data from $T^*\mathcal{P}_k$ to $\mathcal{P}_k^{\text{hw}}$.

Namely, let us provide $\mathcal{P}_k^{\text{hw}}$ with an action form $\mathrm{H} \stackrel{\text{def}}{=} \varkappa^*\eta$ and the corresponding symplectic structure $\Omega = d\mathrm{H}$, where η is the canonical action 1-form on the cotangent bundle $T^*\mathcal{P}_k$. In terms of the local splitting $T_{(S,\vartheta_0)}\mathcal{P}^{\text{hw}} \simeq \mathfrak{H}(S) \oplus C^\infty(S)$ induced by Darboux - Weinstein uniformization these two forms act on $v_1 = (\vartheta_1, f_1)$ and $v_2 = (\vartheta_2, f_2)$ as $\mathrm{H}(v_1) = 2\int_S f_1\, d\vartheta_0\vartheta_1$ and

$$\Omega\big(\,(\,\vartheta_1, f_1\,)\ ,\ (\,\vartheta_2, f_2\,)\,\big) = \int_S f_2\, d\vartheta_0\vartheta_1 - \int_S f_1\, d\vartheta_0\vartheta_2 \ .$$

In terms of the complex DW-coordinates on $\mathcal{P}_k^{\text{hw}}$, the real tangent vector, along $(\psi_1, 0)$, and an imaginary tangent vector $(0, \psi_2)$ are paired by Ω as $\Omega\big(\,(\,\psi_1, 0\,)\ ,\ (\,0, \psi_2\,)\,\big) = \int_S \psi_1\psi_2\, d\vartheta_0^2$ that coincides with L^2-product of ψ_1 and ψ_2 w. r. t. the measure ϑ_0^2. So, Ω is compatible with the complex structure on $\overset{\circ}{\mathcal{P}}{}_k^{\text{hw}}$ and produces the Kähler triple whose Riemannian metric G takes

$$G\big((\vartheta_1, f_1)\,,\,(\vartheta_2, f_2)\big) = \int_S f_1\, d\vartheta_1\vartheta_0 + \int_S f_2\, d\vartheta_2\vartheta_0 \ .$$

4.5.1. THEOREM. *The level k half weighted Planckian cycles space $\mathcal{P}_k^{hw}$ has the natural structure of an infinite dimensional Kähler variety.* □

4.6. Half weighted Bohr - Sommerfeld cycles. The natural $U(1)$-action on $\mathcal{P}_k$, which changes a covariant trivialization of L over a given $S \subset M$, has the standard lifting on $T\mathcal{P}_k$ and on $\mathcal{P}_k^{\text{hw}}$ as well. This action preserves the Kähler structure, because $z \in U(1) \subset \mathbb{C}$ multiplies the complex DW - coordinates by z . The volume function $\mathcal{P}_k^{\text{hw}} \xrightarrow{vol} \mathbb{R}$, which sends $(S, \widetilde{\varphi}, \vartheta)$ to $\int_S \vartheta^2$, is $U(1)$-invariant. Each its level hypersurface $\mathcal{P}_{k,t}^{\text{hw}}$ consists of weighted Planckian cycles whose underlying BS_k-cycle has the fixed volume $t\mathrm{S}$. The orbit space $\mathcal{B}_{k,t}^{\text{hw}} \stackrel{\text{def}}{=} \mathcal{P}_{k,t}^{\text{hw}}/U(1)$ is called a space of *half weighted* BS_k-cycles of volume t.

4.6.1. THEOREM. *The space $\mathcal{B}_{k,t}^{hw}$, of half weighted BS_k-cycles of volume t, also has a natural structure of an infinite dimensional Kähler variety induced from $\mathcal{P}_k^{hw}$.*

PROOF. In terms of Darboux - Weinstein coordinates, the tangent space $T_{(\tilde{S},\vartheta_0)}\mathcal{P}^{\mathrm{hw}}_{k,t}$ consists of $v=(f,\vartheta)\in T_{(S,\vartheta_0)}\mathcal{P}^{\mathrm{hw}}\simeq\mathfrak{H}(S)\oplus C^\infty(S)$ such that $\int_S d\vartheta\vartheta_0=0$, because the infinitesimal volume increment along v is measured exactly by this integral. The $U(1)$-factorization takes (f,ϑ) to $(df,\vartheta)\in T_{(S,\vartheta_0)}\mathcal{B}^{\mathrm{hw}}_{k,t}$. So, the both symplectic and Riemannian structures

$$\Omega\big((\vartheta_0,f_1),(\vartheta_2,f_2)\big)=\int_S f_2\,d\vartheta_0\vartheta_1-\int_S f_1\,d\vartheta_0\vartheta_2$$
$$G\big((\vartheta_1,f_1),(\vartheta_2,f_2)\big)=\int_S f_1\,d\vartheta_1\vartheta_0+\int_S f_2\,d\vartheta_2\vartheta_0$$

remain to be well defined on $\mathcal{B}^{\mathrm{hw}}_{k,t}$, since the conditions

$$\int_S d\vartheta_1\vartheta_0=\int_S d\vartheta_2\vartheta_0=0$$

annihilate an arbitrariness in lifting df_i to f_i (measured by a constant additive terms). □

§5. Dynamical correspondence and BPU-map.

5.1. Action of symplectomorphisms. All ALAG-constuctions are obviously equivariant w.r.t. the natural action of the group $Smpl(M)$, of symplectic diffeomorphisms of M. So, $Smpl(M)$ acts on the spaces $\mathcal{P}^{\mathrm{hw}}$ and $\mathcal{B}^{\mathrm{hw}}_t$ by holomorphic automorphisms preserving the Kähler structure. In particular, the Hamiltonian (w.r.t. o) flows on M produce naturally the Hamiltonian (w.r.t. Ω) flows on $\mathcal{B}^{\mathrm{hw}}_t$. This leads (for each level k and volume t) to the canonical homomorphism of Poisson algebras:

$$C^\infty(M)\longrightarrow C^\infty(\mathcal{B}^{\mathrm{hw}}_{k,t}) \tag{5-1}$$

called *the dynamical correspondence*. It was precisely described by Nik. Tyurin as follows.

5.1.1. THEOREM. *The Poisson algebra representation* (5-1) *is injective and sends a smooth real function f on M to the function F_f on $\mathcal{B}^{hw}_{k,t}$ whose value at half weighted Bohr - Sommerfeld cycle (φ,ϑ) of volume t and level k equals*

$$F_f\,(\varphi,\vartheta)=\frac{1}{2kt}\int_S\varphi^*f\,d\vartheta^2$$

□

5.1.2. Remark. The representation $f \longmapsto F_f$ preserves only the Poisson brackets but does not preserve the usual commutative product of functions, certainly. In particular, this means that when we quantize a dynamical system with hamiltonian h on M getting the dynamical system with Hamiltonian F_h on $\mathcal{B}^{\mathrm{hw}}$, then each first integral f (i. e. a function satisfying $\{h, f\} = 0$) leads to an infinite family of involutive integrals F_f^k for the quantum system: they satisfy $\{F_h, F_f^k\} = \{F_f^m, F_f^k\} = 0$ for all $m, k \in \mathbb{N}$ but are *algebraically independent* now, because of $F_{f^k} \neq F_f^k$.

5.2. Return to Kähler quantization. Let M be equipped with a Kähler structure whose Kähler form coincides with the symplectic form ω. Then the compatibility conditimns on the prequantization data provide L with the canonical structure of holomorqhic ample line bundle and we can consider the wave function spaces, i. e. the spaces of global holomorphic sections

$$\mathcal{H}_k = H^0(M, L^{\otimes k}) \ .$$

For any half weighted Planckian cycle $(S, \widetilde{\varphi}, \vartheta)$ supported by a BS_k-cycle $S \overset{\varphi}{\subset\!\longrightarrow} M$ with a horizontal unitary section $S \overset{\sigma}{\subset\!\longrightarrow} \varphi^* L^{\otimes k}$ and for any holomorphic section $s \in H^0(M_I, L^{\otimes k})$ consider a smooth complex valued function $\psi_{\sigma,\varphi} \in C^\infty(S, \mathbb{C})$ such that $\varphi^* s = \psi_{\sigma,\varphi} \cdot \sigma$ in $C^\infty(S, \varphi^* L^{\otimes k})$.

5.2.1. LEMMA. *Linear map* $H^0(M, L^{\otimes k}) \overset{s \mapsto \psi_{\sigma,\varphi}}{\subset\!\longrightarrow} C^\infty(S, \mathbb{C})$ *is injective and holomorphic.* □

5.2.2. Remark: $C^\infty(S, \mathbb{C})$ is a fiber of the *holomorphic* tangent bundle $T_{(S,\widetilde{\varphi},\vartheta)} \overset{\circ}{\mathcal{P}}{}_k^{\mathrm{hw}}$ over $\overset{\circ}{\mathcal{P}}{}_k^{\mathrm{hw}}$ considered with toe intrinsic holomorphic structure defined above.

5.3. Towards the Borthwick - Paul - Uribe map. Let us define a map

$$\overset{\circ}{\mathcal{P}}{}^{\mathrm{hw}} \xrightarrow{\mathfrak{m}_k} H^0(M, L^{\otimes k})^* \tag{5-2}$$

by sending a half weighted Planckian cycle $(\widetilde{\varphi}, \vartheta)$ to $\mathbb{C}$-linear form that takes $s \in H^0(M, L^{\otimes k})$ to

$$\int_S \psi_{\sigma,\varphi}\, d\vartheta^2 = \int_S \psi_{\sigma,\varphi}\, f^2\, d\mu \ \in \ \mathbb{C}$$

In terms of complex DW-coordinates on $\overset{\circ}{\mathcal{P}}{}_k^{\mathrm{hw}}$ near $(S, \widetilde{\varphi}, \vartheta)$ it sends $\psi_1 + i\psi_2$ to a linear form on $H^0(M, L^{\otimes k})$ that takes s to $\int_S \psi_{\sigma,\varphi} \psi_1^2 e^{i\psi_2}\, d\vartheta^2$ Its differential sends $\psi_1 + i\psi_2$ to a functional

$$s \longmapsto \int_S \psi_{\sigma,\varphi}(2\psi_1 + i\psi_2)\, d\vartheta^2 \ ,$$

Although this map is not $\mathbb{C}$-linear, the defect is measured by a constant factor. That is the map (5-2) has a *constant Kähler angle*, i. e. is almost holomorphic. In fact, using the metaplectic formalism, the definition (5-2) can be modified in order to get a holomorphic map whose differential would sesquilinearly dual to the restriction map $H^0(M, L^{\otimes k}) \overset{s \mapsto \psi_{\sigma,\varphi}}{\subset\!\longrightarrow} C^\infty(S, \mathbb{C})$. So, the Hardy spaces, which appear in the Berezin – Toeplitz quantization procedure, are just the canonical projections of the universal holomorphic tangent bundle on the space of half weighted cycles. This is the true geometrical reason for the existence of a canonical flat connection on the bundle of conformal blocks mentioned in n° 1.8.2.

Some references

5.4. References on ALAG:

- *A. L. Gorodentsev, A. N. Tyurin. ALAG (Abelian Lagrangian Algebraic Geometry).* Izvestia RAN (Math.) 65:3 (2001) p.15–50, draft version: preprint `MPI--2000--7`.
- *A. N. Tyurin. Complexification of Bohr - Sommerfeld conditions.* Preprint `arXiv: math.AG/9909094`.
- *N. A. Tyurin. Hamiltonian dynamics on the moduli space of half weighted Bohr - Sommerfeld Lagrangian subcycles of fixed volume.* Preprint `arXiv: math.DG/0010104`.

5.5. References on Lagrangian geometry:

- *V. Gullemin, S. Sternberg. Geometric asymptotics.* John Wiley & Sons Inc. (1978).
- *A. Weinstein. Symplectic geometry.* BAMS v 5, N 1 (1981)
- *A. Weinstein. Connections of Berry and Hannay type for moving Lagrangian submanifolds.* Advances in Math **82**(1990), pp. 133–159.
- *A. Weinstein. Lagrangian submanifolds and Hamiltonian systems.* Ann. of Math. **98** (1973), pp. 377–410.
- *A. Weinstein. Symplectic manifolds and their Lagrangian submanifolds.* Adv. in Math. **6** (1971), pp. 329–346.

5.6. References on gauges and connections:

- *M. F. Atiyah, R. Bott. The Yang - Mills Equations Over Riemann Surfaces.* Phil. Trans. R. Soc. Lond. **108** (1988), pp. 523–615
- *S. K. Donaldson, P. B. Kronheimer. The Geometry of Four-Manifolds.* Clarendon, Oxford (1990).
- *P. Griffits, J. Harris. Principles Of Algebraic Geometry.* AMS Math. Surv. **4** (1977).
- *N. Hitchin. Flat Connections And Geometric Quantization.* Commun. Math. Phys. **131** (1990), pp. 347–380.

The Loop Group of E_8 and K-Theory from $11d$

Allan Adams[1] and Jarah Evslin[2]

[1] Dept. of Physics and SLAC, Stanford University, Stanford CA 94305/94309

[2] Dept. of Math, UC Berkeley, and Theory Group, LBNL, Berkeley CA 94720

We examine the conjecture that an $11d$ E_8 bundle, appearing in the calculation of phases in the M-Theory partition function, plays a physical role in M-Theory, focusing on consequences for the classification of string theory solitons. This leads for example to a classification of IIA solitons in terms of that of LE_8 bundles in $10d$. Since $K(\mathbb{Z},2)$ approximates LE_8 up to π_{14}, this reproduces the K-Theoretic classification of IIA D-branes while treating NSNS and RR solitons more symmetrically and providing a natural interpretation of G_0 as the central extension of $\tilde{L}E_8$.

[1] allan@slac.stanford.edu

[2] jarah@uclink.berkeley.edu

1. Introduction and Motivation

In this note we study the classification of solitons in string theory and M-Theory. Our starting point is the intersection of two suggestive results. First, as argued by Witten [1][2] and more extensively by Diaconescu, Moore and Witten [3][4], certain subtle phases in the M-Theory partition function suggest a connection to an E_8 gauge theory over a $12d$ manifold Z bounded by Y. This follows from the fact that E_8 bundles in $12d$ are specified topologically by their Chern-Simons 3-form [5], so that the calculation of these M-Theory phases as sums over topologically distinct M-Theory 3-form configurations takes a natural form in terms of the index theory of $12d$ E_8 bundles. That this E_8 index theory result agreed precisely with a very different calculation based on IIA K-Theory led Diaconescu, Moore and Witten to suggest a deeper connection between the M-Theory 3-form and the Chern-Simons 3-form of a $12d$ E_8 bundle. Since the index calculation depends only on $\partial Z = Y$, the physical data lies in the restriction of the $12d$ bundle to an E_8 bundle in $11d$.

Secondly, it is commonly believed that the K-Theory of $\mathbb{C}P^\infty \sim K(\mathbb{Z},2)$ bundles classifies D-Brane configurations in Type IIA string theory, as argued in [6][7] and phrased in terms of $K(\mathbb{Z},2)$ in [8]. However, the physical connection of the group $K(\mathbb{Z},2)$ to M-Theory is unclear. Moreover, as fleshed out in a beautiful paper by Maldacena, Moore and Seiberg [9], the Atiyah-Hirzebruch Spectral Sequence (AHSS) construction of the K-Theoretic classification of Type II RR solitons involves anomaly cancellation conditions in an intimate and beautiful way. How this relates to the proposal of [8] is again unclear.

These lines of reasoning beg to be connected. As a first hint, note that $K(\mathbb{Z},2)$ and LE_8 are homotopically identical up to π_{14}. [3],[4] Thus the classification of LE_8 bundles over 10-manifolds agrees with that of $\mathbb{C}P^\infty$ bundles. Further, up to important questions of central extension and torsion which we address below, the classification of LE_8 bundles over 10-manifolds is precisely the classification of E_8 bundles over 11-manifolds with a compatible circle action. Thus the classification of solitons and the cancellation of anomalies in

[3] LE_8 denotes the loop group of E_8, and $\tilde{L}E_8$ its centrally extended generalization. We describe their low-dimensional topology below; for a complete discussion, see eg [10].

[4] We are deeply indebted to Petr Hořava for insightful discussions during early stages of this work suggesting looking at the loop group of E_8 as an M-Theoretic alternative to the stringy picture of $K(\mathbb{Z},2)$ arising from an infinite number of unstable D9-branes [11]. For a discussion of possible relations between these two pictures and their implications for supersymmetry and $11d$ dynamics, see [12].

M-Theory and IIA (and Heterotic, as we shall see), as well as the relationship between these as revealed by the AHSS, can all be phrased in terms of a single E_8 structure in $11d$. That an $11d$ E_8 bundle ties together so many pieces of the M-Theory puzzle strongly supports the conjecture that an $11d$ E_8 bundle plays a physical role in M-Theory, and should be reflected in its fundamental degrees of freedom.

Taking this seriously thus leads us to conjecture that the classification of RR and NSNS solitons in IIA derives from the classification of LE_8 bundles over 10-manifolds. This generalizes the accepted K-Theoretic classification of RR solitons (and adds to growing evidence that K-Theory at least approximately respects IIB S-duality, suggesting that K-Theory plays some role even beyond weak coupling) while leading to novel predictions about the complete classification of IIA solitons, including the interpretation of the cosmological "constant"[5] G_0 of (massive) IIA as the central charge of $\tilde{L}E_8$, and several constraints relating torsion in M-Theory, $\tilde{L}E_8$ and IIA.

In the remainder of this note we present further motivation for these conjectures and show how such a framework reproduces and extends the familiar classification of solitons in M-Theory and its $10d$ descendants[6]. Of course, $11d$ SUSY does not to play well with gauge bundles, and it is difficult to see how a dynamical bundle can coexist with 32 supercharges. (For further thoughts along these lines see eg [14][12].) However, objects to which the E_8 gauge connection couples in M-Theory and the string theory generically violate at least half of the supercharges, so we might expect to see gauge bundle information only in situations with reduced supersymmetry. In any case, the resolution is unclear, so we restrict ourselves in the following to studying the soliton classification, leaving questions of dynamics and SUSY to future work. We begin by reviewing the topological classification of E_8 bundles over 11-manifolds.

2. The Topological Classification of E_8 Bundles in $11d$

E_8 has exceptionally simple low-dimensional topology. In particular, its only non-trivial homotopy group below dimension 15 is $\pi_3(E_8) = \mathbb{Z}$. The basic non-trivial E_8 bundle is thus that over an S^4 whose transition functions on the S^3 equator lie in $\pi_3(E_8)$.

[5] Since the dilaton is not constant in the presence of $D8$-branes, this should properly be called a cosmological term rather than a cosmological constant.

[6] For earlier thoughts on the role of E_8 in M-Theory, see eg [13][14][15]. See also [12][16]for related current work

Due to the absence of other relevant homotopy classes, E_8 bundles over manifolds of dimension $3 < d < 16$ are topologically classified entirely by the transition functions on the S^3 equators of S^4's in the 4-skeleton of the base manifold [5]. These are measured by the restriction of the first Pontrjagin class p_1, which is the exterior derivative of the Chern-Simons 3-form C_3 on each coordinate patch [5], to the given S^4. E_8 bundles over 11-manifolds are thus topologically classified by the specification of a 3-form C_3, a remarkable fact that depends crucially on the simple low-dimensional topology of E_8.

The basic monopole in such bundles is thus a codimension 5 object supporting 4-form flux such that the integral of p_1 over an S^4 linking the defect is the monopole number,

$$\int_{S^4} \frac{G_4}{2\pi} = n \in \mathbb{Z}, \tag{2.1}$$

where $G_4 = dC_3 = dTr\ (A \wedge F + \frac{2}{3} A \wedge A \wedge A)$. There is also a codimension 4 instanton such that the integral of p_1 over a transverse 4-plane is non-zero. Such a bundle can be trivialized inside and outside any 3-sphere in this plane, with the transition functions on this linking S^3 classified by $\pi_3(E_8)$. If we restrict to configurations which are compactly supported in the transverse plane, the integral of p_1 over the transverse 4-plane is thus an integer counting instanton number. Such an instanton can be produced by considering a monopole-antimonopole pair whose fluxlines run from one to the other; the integral of p_1 over a transverse 4-plane between them is thus quantized, with the choice of orientation specifying whether this plane links the monopole or antimonopole and thus fixing the sign. If the flux takes delta-function support in the transverse plane, this is a zero-radius instanton Poincare dual to the first Pontrjagin class of the bundle.

Due to the magic of E_8,

$$p_2 = p_1 \wedge p_1 = \frac{G_4 \wedge G_4}{16\pi^2},$$

a relation that would not hold had we considered for example $U(N)$ bundles. Thus p_2 does not reveal any new topology not already contained in G_4. However, since we can always pull the codimension 5 defects to infinity, p_2 can represent a charge in compactly supported cohomology. For example, consider a bundle such that the integral of p_2 over some 8-plane is non-zero; this reveals the presence of a codimension 8 object Poincare dual to p_2. Since we can express p_2 as the exterior derivative of a 7-form G_7, we can relate this

integral over an 8-plane to an integral over its "S^7 at infinity" (again, we are looking at compactly supported cohomology) to get

$$\int_{\mathbb{R}^8} p_2 = \int_{S^7} \frac{G_7}{2\pi} = k \in \mathbb{Z},$$

so the codimension 8 objects are quantized and localized. There is again an associated codimension 7 "instanton" (properly, this is an intersection of codimension 4 instantons) such that the integral of G_7 over a transverse 7-plane is non-zero. Instanton number is quantized in a more subtle way here, since there is no homotopy class directly counting these instantons. However, since these codimension 7 instantons can be constructed as the flux stretching between a codimension 8 monopole-antimonopole pair, a quantization condition applies.

The role of these codimension 7 and 8 objects is more transparent when we consider the first non-trivial AHSS differential for such bundles,

$$d_4 = G_4 \cup + [\text{Torsion}]. \tag{2.2}$$

Ignoring torsion for the moment, this differential enforces for example the condition

$$d * G_4 = G_4 \wedge G_4.$$

This reflects the fact that the G_7 whose exterior derivative is p_2 really is the dual of G_4. Physically, this equation requires a codimension 5 object wrapping a 4-cycle supporting k units of G_4 flux to be the endpoint of k codimension 8 objects.

This classification has an immediate reading in terms of the conjecture discussed above. The codimension 5 monopole is the $M5$-brane, the codimension 8 the $M2$-brane, while the codimension 4 and 7 instantons are the M-Theory $MF6$ and $MF3$ Fluxbranes discussed by Gutperle and Strominger[17]. Moreover, the AHSS differential precisely effects the $11d$ supergravity equation of motion $d * G_4 = G_4 \wedge G_4$, which implies that an $M5$ wrapping a 4-cycle supporting k units of G_4 flux must be the endpoint of k $M2$-branes, a familiar result, and ensures the Dirac quantization of the $M2$ and $MF3$ branes.

Returning briefly to (2.2), the torsion terms can be studied by checking when the sign of the Pfaffian of the Dirac operator can be made well defined for the fermion contribution to a path integral describing an open M2-brane via the inclusion of some chiral 2-form. In particular if the M2-brane wraps a circle we recover the familiar obstruction $W_3 + H$

from [18]. We reserve further discussion of $11d$ torsion until Section 6; about $10d$ torsion we will say more shortly.

At this point it is clear that the soliton spectrum of the various perturbative string theories should be reproduced by compactifying the base manifolds of our $11d$ E_8 bundles, since it has precisely reproduced the M-Theory solitons from which they descend. Explicitly studying the dimensional reduction of the E_8 bundle will reveal several interesting details, including an intrinsically $10d$ classification of IIA solitons treating NSNS and RR solitons largely symmetrically, to which we now turn.

3. Type IIA and K-Theory from LE_8

Consider an E_8 bundle F over an 11-manifold Y with a circle action that commutes with the transition functions. Let X be the $10d$ space of orbits of the circle action. Sections of F thus define sections of an LE_8 bundle $E \to X$.

Let's pause to review the topology[7] of LE_8. By the canonical homotopy-lowering map, $\pi_p(LE_8) = \mathbb{Z}$ for $p = 2, 14, 22, ...$, and trivial otherwise. The low-dimensional cohomology is similarly simple,

$$H^{even}(LE_8) = \mathbb{Z} \qquad H^{odd} = 0.$$

Since $H_2(LE_8) = \mathbb{Z}$, LE_8 admits a central extension given by a single positive integer. This centrally extended Kac-Moody algebra has a canonically associated group manifold, both of which we shall denote by $\tilde{L}E_8$ in a heinous abuse of notation. The topology of $\tilde{L}E_8$ differs from that of LE_8 in several important ways. In particular, $\pi_2(\tilde{L}E_8)$ is trivial[8], and its low-dimensional cohomology is consequently different from that of LE_8.

We now return to our $10d$ and $11d$ bundles. For every soliton or defect in F there is a soliton or defect in E. However, the $10d$ bundle has a generalization which does not lift, measured by the integer central extension of $\tilde{L}E_8$. Since $\pi_3(E_8) = \mathbb{Z} \neq \pi^*(\pi_2(\tilde{L}E_8))$, where π^* is the pullback along the circle fibration projection map, the central extension of $\tilde{L}E_8$ obstructs a lift to $11d$. Correspondingly, Type IIA string theory has a single

[7] For a more extensive discussion of such (possibly centrally extended) loop algebras and the topology of their canonically associated group manifolds, see [10].

[8] The triviality of $\pi_2(\tilde{L}G)$ depends only on G being simple and simply connected. This is essentially the statement that LG admits a single universal central extension of which all others are cosets; see [10] for an extensive discussion of the topology of centrally extended algebras.

integer, the 0-form field strength G_0, which is the obstruction to lifting to M-Theory. Domain walls over which this integer jumps, $D8-$branes, similarly cannot be lifted. We thus conjecture that the central extension k of this $\tilde{L}E_8$ bundle over $10d$ measures the cosmological "constant" of (massive) IIA, G_0, as

$$G_0 = k. \tag{3.1}$$

That a lift is indeed possible when $G_0 = 0$ fixes a possible additive constant to zero[9].

The distinct topology of the centrally extended $\tilde{L}E_8$ implies that the spectrum of stable, consistent D-branes is altered in the presence of $D8$-branes. In particular, characteristic classes which are torsion when the central extension is non-vanishing will reveal instabilities of various brane configurations in the presence of G_0 which may be stable in the absence thereof, or vice-versa. We are thus led to study the complete topology of $\tilde{L}E_8$, including torsion, which will provide explicit, testable predictions about the (in)stability of brane configurations in massive IIA[19].

Since the homotopy and cohomology groups of LE_8 agree with those of $PU(\infty) = \mathbb{C}P^\infty = K(\mathbb{Z},2)$ up to[10] dimension 14, the classification of RR solitons via LE_8 bundles differs from that of Bouwknegt and Mathai [8] only in phenomena related to high (greater than 14) dimensional topology[11]. Remarkably, the same $\tilde{L}E_8$ structure also serves to classify the NS-NS solitons, as we now discuss.

3.1. NS-NS Solitons from LE_8

Since $\pi_2(LE_8) = \mathbb{Z}$, the primary $10d$ LE_8 defect is codimension 4, i.e. $(5+1)$ dimensional as in $11d$. An S^3 linking k such defects, or more generally any S^3 supporting k units of H-flux as in the SU(2) WZW model, has LE_8 instanton number equal to k. By

[9] Notice that this proposal is reminiscent to the situation in AdS/CFT, and particularly $AdS_3 \times S^3 \times T^4$ in which the cosomological constant on the AdS_3 is determined by the central charge of the $\hat{sl}_2$ affine Lie algebra of the boundary WZW model. We thank Liat Maoz for reminding us of this relationship.

[10] $K(\mathbb{Z},2)$ is by definition the space whose homotopy classes are all trivial except for $\pi_2(K(\mathbb{Z},2)) = \mathbb{Z}$. It is realized for example by $\mathbb{C}P^\infty$ which appears in the consideration *a la* Sen of D-brane classification via non-trivial tachyon bundles associated with the gauge bundles over D-$\bar{D}$ pairs.

[11] Bouwknegt and Mathai [8] argue that IIA D-branes are classified by the K-Theory of the algebra of sections of a vector bundle associated to a $PU(\infty) = K(\mathbb{Z},2)$ principal bundle, roughly.

this we mean that the bundle can be trivialized on the northern and southern hemispheres and the transition function is the element k of $\pi_2(LE_8)$. The defect is characterized by the fact that, at the defect itself, the LE_8 picture breaks down because the circle orbits are not closed. This $10d$ defect is the reduction of an $11d$ defect transverse to the S^1. This is precisely the IIA $NS5$-brane arising from a transverse $M5$-brane.

Similarly, a fundamental IIA string is an $11d$ codimension 8 soliton whose embedding is invariant with respect to the circle action. In particular, the $11d$ bundle is then invariant with respect to the circle action, so transition functions of the $10d$ bundle consist of zero-modes in LE_8, that is, they inhabit an E_8 subgroup. In fact the transition functions in $10d$ are just the embedding of those in $11d$ into LE_8, and so the fundamental string is, like the $M2$-brane, Poincare dual to the square of the first Pontrjagin class (the second Pontrjagin class) of this E_8 sub-bundle of the LE_8 bundle. This is however not to say that the rest of the LE_8 is unimportant - in particular, the dynamics of the $M2$-brane need not respect the circle action, so those of the fundamental string need not restrict themselves to the zero mode subgroup at finite coupling.

3.2. RR Solitons from LE_8

Let's quickly return to the classification of RR solitons via LE_8 bundles. The $D4$-brane arises as an $11d$ 5-defect whose embedding and field configuration are invariant under the circle action. Similarly to the F-string it can be realized with an $E_8 \subset LE_8$. It is characterized by the fact that each linking S^4 has E_8 instanton number one. The $D2$-brane is a $2+1$-soliton transverse to the circle, and is Poincare dual to $d * G_4$, a 7-form related to p_2 of the E_8 bundle by the canonical dimension lowering map between characteristic classes of a space and its loop space. The $D6$-brane arises from a non-trivial circle fibration, such that the π_2 of LE_8 lifts to the π_3 of E_8 via a Hopf fibration, while the $D0$-brane arises as usual as a momentum mode along the S^1 fibers. In both cases the associated flux arises from the KK gauge field, the branes representing trivial E_8 fibrations over the 11-fold.

Finally, as discussed above, $D8$-brane number is connected to the central extension of $\tilde{L}E_8$. Thus, while the $D8$-brane does not appear to have a simple geometric interpretation in terms of an $11d$ E_8 soliton, it has a deep connection to the $\tilde{L}E_8$ structure in $10d$. This connection may provide insight into the connection between $11d$ gravity and the E_8 structure[12].

3.3. Fluxbranes from LE_8

The $11d$ E_8 origin of IIA Fluxbranes is similarly automatic; its reading in terms of LE_8 follows naturally. The simplest example is the direct dimensional reduction of the codimension-4 E_8 fluxtube, which gives the NS-NS $F6$ in IIA. Similarly, a codimension-4 fluxtube which wraps the M-Theory circle remains a codimension-4 fluxtube - this is the IIA RR $F5$-brane. Analogously, the codimension-8 fluxtube reduces transversely to the RR $F3$-brane and, wrapping the M-Theory circle, to the NSNS $F2$-brane. The $F1$ and $F7$ arise as fluxtubes associated to the nontrivial bundles of the $D0$ and $D6$ branes, respectively. Thus we realize the full spectrum of RR and NSNS Fp-Branes discussed by Gutperle and Strominger [17] in terms of LE_8, as expected.

3.4. K-Theory from LE_8 and Indiscretions regarding Torsion

We have seen how the classification of both NSNS and RR solitons in Type IIA arises from the classification of LE_8 bundles in $10d$, these derived from a fundamental E_8 structure in M-Theory. Due to the remarkable topology of LE_8, this reproduces the conjectured K-Theoretic classification for RR charges and fields. We would now like to connect this construction with the AHSS approximation to the K-Theoretic classification. In the remainder of this section we will use the language of M-branes and D-branes for simplicity and clarity; in light of the above discussion, it should be clear that the entire discussion can be phrased explicitly in terms of $11d$ E_8 bundle information.

The classifying group of solitons in M-Theory is a refinement of cohomology obtained by taking the quotient with respect to a series of differentials that reflect the fact that some configurations are anomalous and so should not be included, while others are related by dynamical processes and so must carry the same conserved charges(see eg [9]). For example, an $M5$-brane wrapping a 4-cycle that supports k units of G_4 flux leads to an anomaly that, neglecting torsion, can be canceled if k $M2$-branes end on the $M5$. Thus some $M5$-brane wrappings are anomalous and some $M2$-brane configurations (such as k $M2$'s and the vacuum) are equivalent, this following from the $11d$ supergravity equation of motion

$$d * G_4 = G_4 \wedge G_4.$$

The left hand side of this equation is the intersection number of $M2$-branes with a sphere linking the $M5$, and the right is roughly the integral of the G_4 flux over the 4-cycle wrapped by the 5-brane. Both of these numbers are measured in units of the 8-form Poincare dual

to the $M2$-branes. In the absence of $M2$-branes ending on the $M5$'s, this supergravity constraint is summarized[12] by requiring that the following "differential" annihilate the G_4 flux

$$d_4 G_4 = G_4 \wedge G_4 + [\text{Torsion}].$$

We expect that the torsion terms are nontrivial because, for example, G_4 is half-integral when the $M5$ brane wraps a 4-cycle with non-vanishing w_4 [20]. Also, as we will soon see, its dimensional reduction is nontrivial.

The classification for IIA follows from dimensional reduction of this M-Theory story. There are three distinct classes of reductions of this constraint to IIA, reflecting three possible locations of the M-Theory circle x^{11} in the above scenario. First consider an $M5$-brane wrapping x^{11} which is not in the 4-cycle, so that the anomaly-canceling $M2$-branes do wrap x^{11}. This leads to an anomaly condition requiring F-string insertions on a $D4$ as follows. The $M5$-brane wraps x^{11} and so the G_4 flux that it generates has no 11 component; it is thus not Kaluza-Klein reduced. Similarly, the 4-cycle does not wrap and so the G_4 supported on the 4-cycle is not reduced. Thus the $10d$ anomaly condition arising from this situation is identical to the $11d$ condition:

$$d_4 G_4 = G_4 \wedge G_4 + [\text{Torsion}],$$

now a $10d$ constraint with G_4 identified with the 4-form RR fieldstrength.

Next consider the case in which both the $M5$-brane and the 4-cycle wrap x^{11}, yielding a $D4$ with $D2$ insertions as follows. The G_4 flux sourced by the $M5$-brane is still not reduced, but now the 4-cycle is reduced to a 3-cycle, the G_4 flux it supports dimensionally reduced to the 3-form H. The resulting anomaly constraint is thus

$$d_3 G_4 = H \wedge G_4 + [\text{Torsion}].$$

This is a well-known differential from the AHSS for twisted K-Theory [21], which was seen to be the relevant constraint in [9]. In particular the torsion correction was seen to be $Sq^3 G_4$.

The final case involves an $M5$-brane not wrapping x^{11}, reducing to an $NS5$-brane with $D2$-brane insertions. In this case the 4-form flux is dimensionally reduced to H while the flux in the 4-cycle is not reduced, yielding the constraint

$$d_4 H = G_4 \wedge H + [\text{Torsion}].$$

[12] This was seen in type II in [9].

The torsion in this case is as yet poorly understood.

Combining these three constraints, as well as the AHSS conditions on other RR fluxes, we hope to arrive at a K-Theoretic classification of both NSNS and RR charged objects in IIA. We expect this classification to be T-dual to the S-duality covariant classification in [22]. Independently of our proposal, it would be interesting to better understand the $11d$ lifts of the other constraints on RR fluxes.

For example, anomaly cancellation on a $D2$-brane in IIA wrapping a 3-cycle C with k units of H flux requires k $D0$-brane insertions. Lifting this to M-Theory we learn that, while we know of no restrictions on what cycle an $M2$-brane may wrap, if it wraps a 3-cycle C such that

$$\int_{C\times S^1} \frac{G_4}{2\pi} = k \neq 0$$

then k units of momentum around x^{11} must be absorbed by the brane. To get an intuitive understanding of the physics at work[13], let us pretend that C is a 2-cycle times the time direction, with a constant H flux density, and then KK reduce on the 2-cycle. Before reducing, this corresponds to a constant flux of $D0$-branes incident on the $D2$-brane in IIA, while in M-Theory this corresponds to a steady injection of p^{11} into the $M2$. KK reducing, the G_4-flux reduces to an electric field along the circle, while the $M2$-brane reduces to a particle charged under this field. This flux drives the charged particle to accelerate around the circle with a constant acceleration, that is, to absorb p^{11} at a constant rate. The anomaly condition lifted to M-Theory is thus simply $F = ma$! Although we do not understand the deep connection of the M-Theory E_8 bundle to gravity, this relation between G_4 and p^{11} is perhaps a significant clue.

4. The Heterotic String and the Small Instanton Transition

Consider now an E_8 bundle over an 11-fold $X = M \times S^1/\mathbb{Z}_2$. The bulk bundle naturally restricts to two $10d$ E_8 bundles, one over each of the two boundary components. At this point the realization of the various objects in Heterotic string theory in terms of instantons of the E_8 bundle follows naturally from the beautiful arguments of [24]. For example, an $M2$-brane stretching between the two boundary components is precisely the strongly-coupled fundamental Heterotic string. Moreover, anomaly considerations descend

[13] See also the beautiful discussion in [23], which addresses an analogous effect for dielectric branes in a non-compact geometry.

naturally. In 11-d, there is a mod 2 relation between the Pontrjagin classes of the E_8 bundle, $w(F \to Y)$, and that of the base manifold's tangent bundle, $w(TY)$ - thus for example $G_4 = w_4(TY)/2$. This condition reduces on the induced bundle over the orbifold fixed point to the $10d$ condition, which arises from a gravitational anomaly [24][25].

It is easy to see the Heterotic 5-brane arising from the bulk E_8 bundle. Recall that the $11d$ E_8 5-defect is defined such that a 4-sphere linking the 5-defect has instanton number one. Consider a parallel $11d$ 5-$\bar{5}$ pair separated a finite distance in a transverse direction, y, of $\mathbb{R}^{(10,1)}$. For every point y_p there is a $10d$ bundle given by the restriction of the $11d$ bundle to the $10d$ slice $y = y_p$. Since any 4-plane in the slice $y = y_p$, with y_p between the two defects, links one or the other of the defects, the $10d$ bundles over points between the two 5-defects have instanton number ± 1, the sign fixed by choice of orientation, while the $10d$ bundles over points not between the two defects have instanton number zero. Since the $10d$ bundles over points between the $11d$ defects are non-singular, their instantons are "large". The singular $10d$ bundles which contain the $11d$ 5-defects, by contrast, contain "small" instantons. These are the Heterotic 5-branes.

Next consider a similar configuration with the two defects pulled away to infinity, leaving a single codimension-4 instanton stretched along the coordinate y and taking compact support in the transverse 4-plane. If we pinch the instanton over a point $y = y_*$, we can nucleate a $5 - \bar{5}$ pair at y_* and move them away to infinity, leaving behind no flux in the interval between them. From the point of view of the $11d$ bundle, this is a completely continuous process respecting all conserved charges and symmetries. From the point of view of the induced $10d$ bundle over any point $y = y_o \neq y_*$, however, things look rather odd; the originally large and fluffy instanton shrinks to a singular "small" instanton and then disappears altogether!

Now consider an E_8 bundle over the 11-manifold $Y = \mathbb{R}^{(9,1)} \times (\mathbb{R}/\mathbb{Z}_2)$, where the y coordinate along which the $11d$ instanton is extended has been orbifolded by a Z_2 reflection. If we repeat the pinching-transition over the point $y = 0$, which from the point of view of the covering space is completely continuous and respects all conservation laws, as well as the orbifold symmetry, we find a transition in the orbifold theory in which a "large" instanton in the boundary bundle shrinks to a singular "small" instanton before disappearing from the boundary and moving into the bulk as an $11d$ 5-defect, i.e. an M5-brane. This is precisely the Heterotic small instanton transition studied near one boundary component, as read by the $11d$ E_8 bundle. Note that, while the number of boundary instantons $n_{\partial Y}$ is not conserved, $n_{\partial Y} + n_Y$ is.

5. Speculations about E_8 Bundles and $11d$ SUSY

Since objects to which the E_8 gauge connection couples in M-Theory and string theory violate at least half of the 32 $11d$ supercharges, we should perhaps expect to see gauge bundle information only in situations with reduced supersymmetry. It is thus reasonable to wonder if the gauge connections inhabit representations of only a sub-algebra of the $11d$ superalgebra, representations that in particular contain neither gravitons nor gravitinos. The Chern-Simons 3-form of this connection can then be set equal to the 3-form in the $11d$ supermultiplet, for example via a Lagrange multiplier[14],

$$\delta S \sim \int_{M^{11}} \alpha(C_3^M - C_3^{E_8}).$$

It is worth keeping in mind that both the M-Theory 3-form and the E_8 Chern-Simons form respect an abelian gauge symmetry, since for example under a local E_8 gauge transformation with gauge parameter Λ the CS-3-form transforms as $C \to C + d\mathrm{Tr}(\Lambda F)$, so this action is in fact gauge invariant and respects all the requisite symmetries.

Of course, not all bundles in the same topological equivalence class correspond to BPS solitons. Rather, the bundles in each equivalence class are related by a change in boundary conditions which does not change the topology; in the associated SUGRA class, this corresponds (roughly, as the equations of motion are non-linear) to a shift by a solution to the vacuum equations of motion. However, since the topological classification of bundles is precisely the classification by charge (at least up to torsion terms), there is some choice of background fields which does not affect the topological class and yields precisely the BPS soliton. In particular we attribute an array of classical moduli, such as the size of Heterotic instantons, to precisely such a freedom of choice of boundary conditions.

6. Conclusions and Open Questions

We have argued that the topological classification of E_8 bundles in $11d$, which naturally reproduces the soliton spectrum of M-Theory, reproduces when reduced on $S^1/\mathbb{Z}_2$ the spectrum of Heterotic $E_8 \times E_8$, while reduced on S^1 reproduces the spectrum and

[14] We particularly thank Eva Silverstein for discussions on this topic.

K-classification of RR and NSNS solitons in Type IIA[15]. Remarkably, while there appears to be no simple dynamical role for E_8 in Type IIA, there does appear to be a deep role for its loop group LE_8 in the K-Theoretic classification of IIA solitons, including in an important way its central extension. The relevance of E_8 bundles even for perturbative string theories with no dynamical gauge bosons suggests an important role for E_8 in the construction of the fundamental degrees of freedom of M-Theory.

The most obvious open question is how, precisely, an $11d$ gauge theory fits with $11d$ supersymmetry. This is extremely confusing. Perhaps a natural place to look for hints to this puzzle is in Heterotic $E_8 \times E_8$, where the gauge boson couples in an intricate but natural and beautiful way. Extending this story to $11d$ would be an exciting advance.

Another obvious omission in our presentation is the absence of torsion terms in (2.2). That this is an important omission is clear from any geometry where, for example, an $M5$-brane lies inside not an S^4 but some orbifold thereof. Following [3], one thus expects the torsion terms to include some $\mathbb{Z}$ lift of sq^4; however, as there is no canonical lift of the $\mathbb{Z}_2$ Steenrod squares of even rank, identifying the correct "derivation" is somewhat delicate. In the language of Witten, and in the orientable case, one might expect the fourth AHSS differential to take the form $d_4 = \lambda + G_4 \cup$. However, the sign in front of λ is not obvious. It could of course be fixed by comparison with the 5-brane anomaly, but would still leave ambiguous the correct torsion terms in non-orientable cases, where some lift of the $\mathbb{Z}_2$ Steenrod square sq^4 must obtain.

One avenue of approach might be to identify a canonical lift for the special case of 11-folds with compatible circle actions. As a first guess, define

$$\tilde{Sq}^4 = \pi^*(Sq_3),$$

where π^* is the pullback of the projection of the S^1 fibration. From various Adem relations one can argue that this restricts correctly to sq^4 if $\pi^*(\beta) = sq^2$. A case where one might test this possibility would be an $M5$-brane wrapping $SU(3)/SO(3) \equiv M_5$, whose anomaly requires an $M2$-brane to end upon the $M5$-brane. Reducing on an S^1 to a $D4$-$D2$, the anomaly arises from Sq^3 in the $D4$-brane worldvolume, which is canceled by the incident

[15] While we of course do not have a candidate for what the complete K-Theory of $\tilde{L}E_8$ bundles is, it should be identical to that of the universal classifying group $K(\mathbb{Z}, 2)$ up to corrections involving topology well above $11d$, as discussed above. One might for example attempt to generalize Rosenberg's K-Theory, [21].

$D2$. Pulling back along the S^1 fibration, Sq^3 should lift to a $\mathbb{Z}$-graded rank-four differential which measures the correct $10d$ anomaly under bundle projection. It would be interesting to explicitly check when, if ever, such a non-trivial pullback exists, and when it does whether it restricts to the $\mathbb{Z}_2$-graded sq^4. We leave such questions to future work.

Finally, it would be particularly interesting to revisit the beautiful and delicate calculations of Diaconescu, Moore and Witten in [3], who showed that the cancellation of anomalies in IIA and M-Theory agree, though the structures underlying the calculations in the two cases were apparently unrelated. DMW read this unlikely agreement as strong evidence for the conjecture that RR fields and charges in IIA are indeed classified by K-Theory. We expect that the IIA computation will take a natural form in terms of $\hat{E}_8$ bundles, and that in this language the relation to anomaly cancellation in M-Theory will be immediate. This would be interesting to check directly.

Acknowledgments

We would like to thank Michal Fabinger, Petr Hořava, Albion Lawrence, John McGreevy, Hisham Sati, Mike Schulz, Eric Sharpe, Eva Silverstein and Uday Varadarajan for discussions. We are particularly indebted to Petr Hořava for essential insights and motivation early on. J. E. particularly thanks Uday Varadarajan for many conversations. A. A. especially thanks Eva Silverstein and John McGreevy for many stimulating conversations regarding early drafts, and Petr Horava for very enjoyable conversations on this and related topics. We thank Don Marolf and Andreas Gomberoff for hospitality at PASI 2002, where much of this work was conducted. The work of A. A. was supported in part by DOE contract DE-AC03-76SF00515 and by an NSF Graduate Fellowship.

References

[1] E. Witten, "On flux quantization in M-Theory and the effective action," J. Geom. Phys. **22**, 1 (1997) arXiv:hep-th/9609122.

[2] E. Witten, "Duality relations among topological effects in string theory," JHEP **0005**, 031 (2000) arXiv:hep-th/9912086.

[3] D. E. Diaconescu, G. W. Moore and E. Witten, "E(8) gauge theory, and a derivation of K-Theory from M-Theory," arXiv:hep-th/0005090

[4] D. E. Diaconescu, G. W. Moore and E. Witten, "A derivation of K-Theory from M-Theory," arXiv:hep-th/0005091.

[5] E. Witten, "Topological Tools In Ten-Dimensional Physics," Int. J. Mod. Phys. A **1**, 39 (1986).

[6] E. Witten, "D-branes and K-Theory," JHEP **9812**, 019 (1998) arXiv:hep-th/9810188.

[7] G. W. Moore and E. Witten, "Self-duality, Ramond-Ramond fields, and K-Theory," JHEP **0005**, 032 (2000) arXiv:hep-th/9912279.

[8] P. Bouwknegt and V. Mathai, "D-branes, B-fields and twisted K-Theory," JHEP **0003**, 007 (2000) arXiv:hep-th/0002023.

[9] J. Maldacena, G. W. Moore and N. Seiberg, "Geometrical interpretation of D-branes in gauged WZW models," JHEP **0107**, 046 (2001) arXiv:hep-th/0105038.

[10] A. Pressley and G. Segal, "Loop Groups," *Oxford, UK: Clarendon (1988) 318 p. (Oxford Mathematical Monographs).*

[11] P. Horava, "Type IIA D-branes, K-Theory, and matrix theory," Adv. Theor. Math. Phys. **2**, 1373 (1999) arXiv:hep-th/9812135.

[12] P. Hořava and U. Varadarajan, *Work in Progress*

[13] C. Gomez and J. J. Manjarin, "Dyons, K-Theory and M-Theory" arXiv:hep-th/0111169

[14] P. Hořava, "M-Theory as a holographic field theory," Phys. Rev. D **59**, 046004 (1999) arXiv:hep-th/9712130.

[15] M. Fabinger and P. Hořava, "Casimir effect between world-branes in Heterotic M-theory," Nucl. Phys. B **580**, 243 (2000) arXiv:hep-th/0002073.

[16] A. Adams, M. Fabinger, P. Horava and U. Varadarajan, *Work in Progress*

[17] M. Gutperle and A. Strominger, "Fluxbranes in string theory," JHEP **0106**, 035 (2001) arXiv:hep-th/0104136.

[18] D. S. Freed and E. Witten, "Anomalies in string theory with D-branes," arXiv:hep-th/9907189.

[19] A. Adams, *Work In Progress*

[20] E. Witten, "Five-brane effective action in M-Theory," J. Geom. Phys. **22**, 103 (1997) arXiv:hep-th/9610234.

[21] J. Rosenberg, *Continuous trace algebras from the bundles theoretic point of view*, Jour. Austr. Math. Soc., **47** (1989), 368-381

[22] J. Evslin and U. Varadarajan, "K-Theory and S-duality: Starting over from square 3," arXiv:hep-th/0112084.

[23] W. Taylor, "D2-branes in B fields," JHEP **0007**, 039 (2000) arXiv:hep-th/0004141.

[24] P. Hořava and E. Witten, "Eleven-Dimensional Supergravity on a Manifold with Boundary," Nucl. Phys. B **475**, 94 (1996) arXiv:hep-th/9603142.

[25] P. Hořava and E. Witten, "Heterotic and type I string dynamics from eleven dimensions," Nucl. Phys. B **460**, 506 (1996) arXiv:hep-th/9510209.

More on Noncommutative Superstring Worldsheet

Davoud Kamani

Institute for Studies in Theoretical Physics and Mathematics (IPM)

P.O.Box: 19395-5531, Tehran, Iran

e-mail: kamani@theory.ipm.ac.ir

Abstract

In this paper some properties of the superstring with noncommutative worldsheet are studied. We study the noncommutativity of the spacetime, generalization of the Poincaré symmetry of the superstring, the changes of the metric, antisymmetric tensor and dilaton.

1 Introduction

The noncommutative geometry [1] has been considered for some time in connection with various physics subjects. Recent motivation to study the noncommutative geometry mainly comes from the string theory. String theories have been pointing towards a noncommuting scenario already in the 80's [2]. Recently Yang-Mills theories on noncommutative spaces have emerged in the context of M-theory compactified on a torus in the presence of constant background three-form field [3], or as low-energy limit of open strings in a background B-field, describing the fluctuations of the D-brane worldvolume [4, 5, 6]. The worldvolume of a D-brane with constant background B-field, is an example of a noncommutative spacetime, in which gauge and matter fields live [3, 4, 5, 7]. In other side, fundamental strings in the R$\otimes$R background B-field become noncommutative. This was shown in the context of matrix theory [8].

Field theory on a noncommutative space has been proved to be useful in understanding various physical phenomena. Noncommutative field theory means that fields are thought of as functions over noncommutative space. At the algebraic level, the fields become operators acting on a Hilbert space as a representation space of the noncommutative space [9].

Previously we considered the superstring action as a two dimensional noncommutative field theory [10]. Up to the first order of the noncommutativity parameter, and some additional terms to the noncommutative superstring action, some physical quantities are obtained. For example, we obtained new supersymmetric action for string, extended boundary state of closed superstring, new boundary conditions for open string which lead to the generalization of the noncommutativity parameter of the spacetime.

In this paper, we do not consider the additional terms to the superstring action. According to this, now we study some other properties of the superstring with noncommutative worldsheet, to all orders of the noncommutativity parameter. Noncommutative worldsheet of string gives a noncommutative spacetime. If some directions of the spacetime are compacted on tori, the vacuum expectation value of the spacetime noncommutativity parameter can be non-zero. Noncommutative worldsheet also enables us to generalize the Poincaré symmetry. That is, some additional terms can be added to the ordinary Poincaré transformations. Therefore, we obtain a generalized conserved current. Furthermore, the NS$\otimes$NS fields of superstring modify by a common phase. Making use of the Refs.[10, 11], one can find descriptions of the noncommutativity parameter of the worldsheet. For $\theta = 0$, all these results reduce to the known cases of the superstring theory with ordinary worldsheet, as expected.

This paper is organized as follows. In section 2, we study the action of the superstring with noncommutative worldsheet. In section 3, the noncommutativity of the spacetime, extracted from the noncommutativity of the string worldsheet, is studied. In section 4, a general form of the Poincaré symmetry is given. In section 5, the effects of the noncommutativity of the worldsheet on the metric, Kalb-Ramond field and dilaton are extracted.

2 Noncommutative worldsheet

We look at the superstring action as a two dimensional noncommutative field theory. In other words, assume that the superstring worldsheet is a two dimensional noncommutative space. In this space superstring with worldsheet supersymmetry has the action

$$S_* = -\frac{1}{4\pi\alpha'}\int d^2\sigma\Big(\partial_a X^\mu * \partial^a X_\mu - i\bar{\psi}^\mu * \rho^a\partial_a\psi_\mu\Big) \ , \tag{1}$$

where the spacetime and the worldsheet metrics are $\eta_{\mu\nu} = \mathrm{diag}(-1,1,...,1)$ and $\eta_{ab} = \mathrm{diag}(-1,1)$. We later discuss about the supersymmetry of this action. The star product in this action is defined between any two functions of the worldsheet coordinates $\sigma^a = (\sigma,\tau)$

$$f(\sigma,\tau) * g(\sigma,\tau) = \exp\Big(\frac{i}{2}\theta^{ab}\frac{\partial}{\partial\zeta^a}\frac{\partial}{\partial\eta^b}\Big) f(\zeta^0,\zeta^1)g(\eta^0,\eta^1)\Big|_{\zeta^a=\eta^a=\sigma^a} . \tag{2}$$

The antisymmetric tensor θ^{ab} has only one independent component i.e., $\theta^{ab} = \theta\epsilon^{ab}$, where $\epsilon^{01} = -\epsilon^{10} = 1$. Definition (2) gives the noncommutativity between the worldsheet coordinates as

$$\sigma^a * \sigma^b - \sigma^b * \sigma^a = i\theta^{ab} \ . \tag{3}$$

The equations of motion of the worldsheet fields are

$$(\partial_\tau^2 - \partial_\sigma^2)X^\mu = \partial_+\psi_-^\mu = \partial_-\psi_+^\mu = 0 \ , \tag{4}$$

where $\partial_\pm = \frac{1}{2}(\partial_\tau \pm \partial_\sigma)$. Therefore, ψ_-^μ and ψ_+^μ are the right moving and the left moving components of ψ^μ. These equations are the same that appear for the superstring with ordinary worldsheet. For the next purposes we need the solutions of these equations. For closed string there is

$$X^\mu(\sigma,\tau) = x^\mu + 2\alpha' p^\mu\tau + 2L^\mu\sigma + \frac{i}{2}\sqrt{2\alpha'}\sum_{n\neq 0}\frac{1}{n}\Big(\alpha_n^\mu e^{-2in(\tau-\sigma)} + \tilde{\alpha}_n^\mu e^{-2in(\tau+\sigma)}\Big) \ , \tag{5}$$

where L^μ is zero if the direction X^μ is non-compact, and is $N^\mu R^\mu$ if this direction is compact on a circle with radius R^μ. In this case the momentum of the closed string is quantized i.e.,

$p^\mu = \frac{M^\mu}{R^\mu}$. The integers N^μ and M^μ are the winding and the momentum numbers of the closed string respectively.

For open string we have the solution

$$X^\mu(\sigma,\tau) = x^\mu + 2\alpha' p^\mu \tau + i\sqrt{2\alpha'}\sum_{n\neq 0}\frac{1}{n}\alpha_n^\mu e^{-in\tau}\cos n\sigma \ . \tag{6}$$

Note that this solution satisfies the boundary conditions of the variation of the action (1). In this variation there are infinite number of boundary terms. These terms contain derivatives that originate from the noncommutativity of the string worldsheet. The boundary condition

$$(\partial_\sigma X^\mu)_{\sigma_0} = 0 \ , \tag{7}$$

is sufficient to drop all the boundary terms of the above variation. $\sigma_0 = 0, \pi$ shows the boundaries of the open string worldsheet.

Consider global worldsheet supersymmetry transformations

$$\begin{aligned} \delta X^\mu &= \bar{\epsilon}\psi^\mu \ , \\ \delta\psi^\mu &= -i\rho^a\partial_a X^\mu \epsilon \ . \end{aligned} \tag{8}$$

Invariance of the action (1) under these transformations leads to the worldsheet super-current

$$J_a = \frac{1}{2}\rho^b\rho_a\psi^\mu * \partial_b X_\mu \ . \tag{9}$$

According to the equations of motion, this is a conserved current i.e., $\partial^a J_a = 0$.

3 Spacetime noncommutativity

Noncommutativity of the string worldsheet directly leads to the noncommutativity of the spacetime. Making use of the formula

$$e^{ip(\tau+k\sigma)} * e^{iq(\tau+l\sigma)} = e^{\frac{i}{2}\theta pq(k-l)}e^{ip(\tau+k\sigma)}e^{iq(\tau+l\sigma)} \ , \tag{10}$$

we obtain the following noncommutativities for the spacetime

$$\begin{aligned} [X^\mu(\sigma,\tau) \ , \ X^\nu(\sigma,\tau)]_* &= \theta(2\alpha')^{3/2}\sum_{n\neq 0}(p^\mu\alpha_n^\nu - p^\nu\alpha_n^\mu)e^{-in\tau}\sin n\sigma \\ -2\alpha'\sum_{m\neq 0}\sum_{n\neq 0}&\left(\frac{1}{mn}(\alpha_n^\mu\alpha_m^\nu - \alpha_n^\nu\alpha_m^\mu)e^{-i(m+n)\tau}\cos m(\sigma+\frac{1}{2}n\theta)\cos n(\sigma-\frac{1}{2}m\theta)\right) \ , \end{aligned} \tag{11}$$

from the open string point of view, and

$$
\begin{aligned}
&[X^\mu(\sigma,\tau)\ ,\ X^\nu(\sigma,\tau)]_* = 4i\theta\alpha'(p^\mu L^\nu - p^\nu L^\mu) \\
&+i\theta(2\alpha')^{3/2}\sum_{n\neq 0}\Big((\alpha_n^\mu p^\nu - \alpha_n^\nu p^\mu)e^{-2in(\tau-\sigma)} - (\tilde\alpha_n^\mu p^\nu - \tilde\alpha_n^\nu p^\mu)e^{-2in(\tau+\sigma)}\Big) \\
&+2i\theta\sqrt{2\alpha'}\sum_{n\neq 0}\Big((\alpha_n^\mu L^\nu - \alpha_n^\nu L^\mu)e^{-2in(\tau-\sigma)} + (\tilde\alpha_n^\mu L^\nu - \tilde\alpha_n^\nu L^\mu)e^{-2in(\tau+\sigma)}\Big) \\
&-i\alpha'\sum_{n\neq 0}\sum_{m\neq 0}\Big(\frac{1}{mn}(\tilde\alpha_n^\mu\alpha_m^\nu - \tilde\alpha_n^\nu\alpha_m^\mu)\sin(4mn\theta)e^{-2i(m+n)\tau}e^{2i(m-n)\sigma}\Big)\ ,
\end{aligned}
\tag{12}
$$

from the closed string point of view. The right hand sides of the relations (11) and (12) are non-zero. This is because of the non-zero value of the parameter θ. Therefore, the noncommutativity of the spacetime, resulted from the noncommutativity of the string worldsheet, depends on the fact that the propagating string in the spacetime is open or is closed.

Now consider the following expectation values of the commutators (11) and (12)

$$
\begin{aligned}
&\langle 0|[X^\mu(\sigma,\tau)\ ,\ X^\nu(\sigma,\tau)]_*|0\rangle = 0\ , \qquad \text{for open string,} \\
&\langle v|[X^\mu(\sigma,\tau)\ ,\ X^\nu(\sigma,\tau)]_*|v\rangle = i\Theta^{\mu\nu}, \quad \text{for closed string}\ ,
\end{aligned}
\tag{13}
$$

where $|v\rangle = |0,\tilde 0\ ;\{M^\mu\},\{N^\nu\}\rangle$ is a closed string state with the momentum numbers $\{M^\mu\}$ and the winding numbers $\{N^\mu\}$, and

$$
\begin{aligned}
\Theta^{\mu\nu} &\equiv 4\alpha'\theta(p^\mu L^\nu - p^\nu L^\mu) \\
&= 4\alpha'\theta\Big(M^\mu N^\nu\frac{R^\nu}{R^\mu} - M^\nu N^\mu\frac{R^\mu}{R^\nu}\Big)\ ,
\end{aligned}
\tag{14}
$$

therefore, if some of the directions of the spacetime are compactified on tori with radii $\{R^\mu\}$, a closed string with noncommutative worldsheet, momentum numbers $\{M^\mu\}$ and winding numbers $\{N^\mu\}$, probes the expectation value of the noncommutativity of the spacetime like the relation (14). Open strings with noncommutative worldsheet do not probe the vacuum expectation value of the spacetime noncommutativity.

4 Poincaré symmetry

Poincaré transformations $\delta X^\mu = a^\mu{}_\nu X^\nu + b^\mu$ and $\delta\psi^\mu = a^\mu{}_\nu\psi^\nu$, are global symmetries of the superstring theory with ordinary worldsheet, where $a_{\mu\nu}$ is a constant antisymmetric tensor and b^μ is a constant vector. Two conserved currents are associated to them. For the superstring theory with noncommutative worldsheet, these transformations can be generalized.

Therefore, the effects of this generalization also appear in the currents. The generalized transformations are

$$\begin{aligned}\delta X^\mu &= a^\mu{}_\nu X^\nu + b^\mu \ , \\ \delta\psi^\mu &= a^\mu{}_\nu(\psi^\nu + \psi^\nu * \phi - \psi^\nu\phi) \ ,\end{aligned} \tag{15}$$

where $\phi(\sigma,\tau)$ is a scalar of the worldsheet. It will be determined in terms of the coordinates σ and τ.

Making use of the equations of motion, the variation of the action (1) under the transformations (15), is

$$\delta S_* = \frac{i}{4\pi\alpha'} a_{\mu\nu} \int d^2\sigma \Big(\bar\psi^\mu * \rho^a(\psi^\nu * \partial_a\phi - \psi^\nu\partial_a\phi)\Big) \ . \tag{16}$$

For vanishing of this variation, one possibility is that $\partial_a\phi$ be constant i.e., independent of the coordinates σ and τ,

$$\partial_a\phi(\sigma,\tau) = c_a \ . \tag{17}$$

This equation has the solution

$$\phi(\sigma,\tau) = c_a\sigma^a + \phi_0 \ , \tag{18}$$

where c_0, c_1 and ϕ_0 are constants.

The currents associated to the transformations (15) are

$$P^\mu_a = \frac{1}{2\pi\alpha'}\ \partial_a X^\mu \ , \tag{19}$$

$$\begin{aligned} J^{\mu\nu}_a \ &= \ \frac{1}{4\pi\alpha'}\Big((X^\mu * \partial_a X^\nu - X^\nu * \partial_a X^\mu + \partial_a X^\nu * X^\mu - \partial_a X^\mu * X^\nu) \\ &\quad + i\bar\psi^\mu * \rho_a(\psi^\nu * \phi - \psi^\nu\phi) - i\bar\psi^\nu * \rho_a(\psi^\mu * \phi - \psi^\mu\phi)\Big) \\ &\quad + i(\bar\psi^\mu * \rho_a\psi^\nu - \bar\psi^\nu * \rho_a\psi^\mu) \ . \end{aligned} \tag{20}$$

The constant ϕ_0 has no effects on the transformations (15) and on the current (20). According to the equations of motion, these currents are conserved i.e., $\partial^a P^\mu_a = 0$ and $\partial^a J^{\mu\nu}_a = 0$. If the noncommutative worldsheet changes to the ordinary worldsheet, the transformations (15) and the current (20) reduce to the ordinary case, as expected.

more generalization

Transformations (15) can be generalized as

$$\begin{aligned}
&\delta X^\mu = a^\mu{}_\nu X^\nu + b^\mu \ , \\
&\delta\psi^\mu = a^\mu{}_\nu(\psi^\nu + b_1\psi_1^\nu + b_2\psi_2^\nu + ... + b_N\psi_N^\nu) \ ,
\end{aligned} \tag{21}$$

where N is an integer and $\{b_1, b_2, ..., b_N\}$ are arbitrary coefficients, and

$$\begin{aligned}
&\psi_n^\mu = \psi_{n-1}^\mu * \phi - \psi_{n-1}^\mu\phi \quad , \quad 1 \leq n \leq N \ , \\
&\psi_0^\mu = \psi^\mu \ .
\end{aligned} \tag{22}$$

Again with the choice (18) for ϕ, the variation of the action (1) under the transformations (21) vanishes. Define differential operator D as

$$D = -\frac{1}{2}i\theta^{ab}c_a\partial_b = \frac{1}{2}i\theta(c_1\partial_\tau - c_0\partial_\sigma) \ , \tag{23}$$

therefore, ψ_n^μ can be written as

$$\psi_n^\mu = D^n\psi^\mu \ . \tag{24}$$

This simplifies the second transformation in (21) as the following

$$\delta\psi^\mu = a^\mu{}_\nu \sum_{n=0}^{N} b_n D^n\psi^\nu \quad , \quad b_0 = 1 \ . \tag{25}$$

For the special choices $b_n = \frac{1}{n!}$ and $N \to \infty$ this transformation becomes

$$\begin{aligned}
\delta\psi^\mu &= a^\mu{}_\nu \exp\left(\frac{1}{2}i\theta(c_1\partial_\tau - c_0\partial_\sigma)\right)\psi^\nu(\sigma,\tau) \\
&= a^\mu{}_\nu\psi^\nu\left(\sigma - \frac{i\theta}{2}c_0 \ , \ \tau + \frac{i\theta}{2}c_1\right) \ ,
\end{aligned} \tag{26}$$

which follows by combination of the shifts on the worldsheet coordinates and a rotation in the spacetime.

The currents associated to the transformations (21), are the current (19) and

$$\begin{aligned}
J_a^{\mu\nu} &= \frac{1}{4\pi\alpha'}\Big((X^\mu * \partial_a X^\nu - X^\nu * \partial_a X^\mu + \partial_a X^\nu * X^\mu - \partial_a X^\mu * X^\nu) \\
&\quad + i\sum_{n=0}^{N} b_n(\bar\psi^\mu * \rho_a D^n\psi^\nu - \bar\psi^\nu * \rho_a D^n\psi^\mu)\Big) \ ,
\end{aligned} \tag{27}$$

which is conserved i.e., $\partial^a J_a^{\mu\nu} = 0$. This is more general than the current (20).

Note that the parameters $\{b_n\}$, c_0 and c_1 in the transformation (25) and in the current (27), remain arbitrary. For $c_0 = \pm c_1$, the operator D is proportional to $\partial_\mp$. In this case,

according to the equation (10), the effects of the noncommutativity of the worldsheet on the fermionic part of the current (27), for $n \geq 1$, are collected only in the derivative D. That is, the star product appears as usual product. Also the transformation (25) for $n \geq 1$ only has derivatives of the left moving or the right moving components of the worldsheet fermions $\{\psi^\mu\}$.

5 The fields $g_{\mu\nu}$, $B_{\mu\nu}$ and Φ

We are interested in to know the effects of the noncommutativity of the string worldsheet on the metric, antisymmetric tensor and dilaton. We discuss on these fields both in the bosonic string and in the superstring theories. The states of these fields can be extracted from their vertex operators.

For the bosonic string consider the operator

$$\Omega^{\mu\nu}(p) = -\frac{2i}{\pi\alpha'}\int d^2\sigma : \partial_- X^\mu * \partial_+ X^\nu * e^{ip.X} : \quad . \tag{28}$$

Making use of the solution (5), therefore from the state

$$\Omega^{\mu\nu}(0)|0\ ,\tilde{0}\ ; p=0\rangle\ , \tag{29}$$

we read the state

$$e^{-4i\theta}\alpha^\mu_{-1}\tilde{\alpha}^\nu_{-1}|0\ ,\tilde{0}\ ; p=0\rangle\ . \tag{30}$$

According to this state we have

$$\begin{aligned} g^{\mu\nu}_\theta &= e^{-4i\theta}g^{\mu\nu}\ , \\ B^{\mu\nu}_\theta &= e^{-4i\theta}B^{\mu\nu}\ , \\ \Phi_\theta &= e^{-4i\theta}\Phi\ . \end{aligned} \tag{31}$$

Therefore, these fields take only a phase. Modification of the dilaton changes the string coupling constant.

For the superstring, $g_{\mu\nu}$, $B_{\mu\nu}$ and Φ are the NS$\otimes$NS sector fields. The states of these fields can be extracted from the following state

$$-\frac{2i}{\pi}\int d^2\sigma : \psi^\mu_- * \psi^\nu_+ : |0\ ,\tilde{0}\ ; p=0\rangle\ . \tag{32}$$

From this state we read the state

$$e^{-i\theta}b^\mu_{-1/2}\,\tilde{b}^\nu_{-1/2}|0\ ,\tilde{0}\ ; p=0\rangle\ . \tag{33}$$

According to this state, we obtain

$$
\begin{aligned}
g_\theta^{\mu\nu} &= e^{-i\theta} g^{\mu\nu} \ , \\
B_\theta^{\mu\nu} &= e^{-i\theta} B^{\mu\nu} \ , \\
\Phi_\theta &= e^{-i\theta} \Phi \ .
\end{aligned} \tag{34}
$$

Therefore, the corrections of the metric, antisymmetric tensor and dilaton in the superstring theory are different from their corrections in the bosonic string theory. Since θ-parameter is real, the real parts of these fields can be interpreted as physical fields.

6 Conclusions

The noncommutativity of the string worldsheet leads to the noncommutativity of the spacetime. The latter depends on probing by open or closed string. If some of the spacetime directions are compactified on tori, the noncommutativity of the spacetime depends on the momentum numbers and the winding numbers of the probing closed string.

By adding some additional terms to the Poincaré transformations of the worldsheet fermions, the Poincaré symmetry of the superstring was generalized. The noncommutativity of the superstring worldsheet permits this generalization and consequently the generalized form of the associated conserved current.

The NS$\otimes$NS fields of the type II superstring (i.e., the metric, antisymmetric tensor and dilaton) changed only by a phase. The changes of these fields in the bosonic string theory, are different from their changes in the superstring theory.

References

[1] A. Connes, "*Noncommutative Geometry*, Academic Press"(1994).

[2] E. Witten, Nucl. Phys. **B268**(1986)253.

[3] A. Connes, M.R. Douglas and A. Schwarz, JHEP **9802**(1998)003, hep-th/9711162.

[4] Y.E. Cheung and M. Krogh, Nucl. Phys. **B528**(1998)185, hep-th/9803031; C.S. Chu and P.M. Ho, Nucl. Phys. **B550**(1999)151, hep-th/9812219; Nucl. Phys. **B568**(2000)447, hep-th/9906192; V. Schomerus, JHEP**9906**(1999)030, hep-th/9903205; F. Ardalan, H. Arfaei and M.M Sheikh-Jabbari, JHEP**9902**(1999)016, hep-th/9810072; Nucl. Phys. **B576**(2000)578, hep-th/9906161; M.R. Douglas and N.A. Nekrasov, Rev. Mod. Phys.

73 (2002)977, hep-th/0106048; P.M. Ho and Y.T. Yeh, Phys. Rev. Lett. **85** (2000)5523, hep-th/0005159; D. Bigatti and L. Susskind, Phys. Rev. **D62** (2000)066004, hep-th/9908056.

[5] N. Seiberg and E. Witten, JHEP **9909**(1999)032, hep-th/9908142.

[6] M.R. Douglas and C. Hull, JHEP **9802**(1998)008, hep-th/9711165; G. Landi, F. Lizzi and R.J. Szabo, Commun. Math. Phys. **206**(1999)603, hep-th/9806099.

[7] E. Fradkin and A. Tseytlin, Phys. Lett. **B158**(1985)316; A. Schwarz, Nucl. Phys. **B534**(1998)720, hep-th/9805034; C. Hofman and E. Verlinde, JHEP **9812**(1998)010, hep-th/9810116.

[8] R. Schiappa, Nucl. Phys. **B608**(2001)3, hep-th/0005145.

[9] S. Minwalla, M. van Raamsdonk and N. Seiberg, JHEP **0002**(2000)020, hep-th/9912072; M. van Raamsdonk and N. Seiberg, JHEP **0003**(2000)035; N. Seiberg, L. Susskind and N. Toumbas, JHEP **0006**(2000)044, hep-th/0005015; O.J. Ganor, G. Rajesh and S. Sethi, Phys. Rev **D62**(2000)125008, hep-th/0005046; R. Gopakumar, J. Maldacena, S. Minwalla and A. Strominger, JHEP **0006**(2000)036, hep-th/0005048.

[10] D. Kamani, "*Noncommutative Superstring Worldsheet*", to appear in Euro. Phys. Jour. C, hep-th/0008020.

[11] D. Friedan, "*A tentative theory of large distance physics*", hep-th/0204131.

THE POLARISATION OF THE SCATTERING PARTICLES ON HIGH ENERGY APPROXIMATION

S.G. ABDULVAHABOVA, E.A. RASULOV
Baku State University

The differential cross-section of diffraction p^9Be scattering at high energies and polarization effects are calculated in the framework of the multiple scattering theory. By taking explicitly into account the composite structure of nucleons exchange effects we eliminate some discrepancies between the theory and the data that were recently pointed out.

1. Introduction

The available experimental data point to the absence of the energy interval of scattering. This makes a basis for the hypothesis about the existence of a non-zero polarization research on the future accelerators will provide information about the structure of the nucleon interaction at large distances.

Using different hypotheses about the property of the nucleon interaction at large distances a number of model approaches leads to the nondisappearing polarization in high -energy processes at small transfer moment.

In this paper we regard the model results for the polarization effects of nucleon-nuclei scattering. Early, it was shown [1] that in the framework of the hypothesis concerning the existence of quark bag in nuclei we managed to describe the behaviour of the formfactors of nuclei at large q and structure functions of nuclei. The parameters of quark distribution in the bag at $k>>k_0$ (the parameter k_0 may in principle be different for different bags) extracted from the data on formfactors and on deep inelastic scattering of nucleons on nuclei proved to be very close.

The purpose of this paper is to show that disagreement between the high energy Glauber theory and the data disappears if the composite structure of nucleons is explicitly taken into account in the calculation of the differential cross section and polarization effects p^9Be reaction according to the multiple scattering theory.

2. The model formalism

In agreement with the Glauber theory [2], which is a rather accurate one at high energy< the amplitude of the direct reaction of proton on a nucleus may be written as

$$f(q) = \frac{ik}{2p}\int exp(iqb)\langle \Psi|\Gamma(b)|\Psi\rangle db, \tag{1}$$

$$\Gamma(b) = 1 - \prod_{j=1}^{A}\left[1 - \varepsilon_j(b - s_j)\right]. \tag{2}$$

Here q is the momentum transfer, k is the value of the wave vector of the scattering proton, b is the impact-parameter vector, $\Psi(r_1, r_2, ..., r_A)$ is the ground state wave function of the nuclei, $\Gamma(b)$ is the total proton – nuclei interaction profile function, $\varepsilon_j(b)$ is the profile function for the elementary proton-nucleon interaction, brackets $\langle|\rangle$ mean interactions over the nucleon coordinates.

A nucleus in the quark model is described as a system of many clusters, and each cluster consists of three quarks. Then a nuclear non-antisymmetrized wave function in the oscillator-cluster model can be written as [3]

$$\Psi_{^9Be} = \phi_{N_1}(r_1, r_2, r_3)\cdots\phi_{N_9}(r_{25}, r_{26}, r_{27})\chi(R_1, R_2, ..., R_9), \tag{3}$$

where the nucleus is pictured as a bag with radius R_A, located at R_9 enclosing A nucleons with radius located at R_i. Using the relations

$$R = \frac{r_{3i-2} + r_{3i-1} + r_{3i}}{3}, \quad i=1,2,...9 \tag{4}$$

and

$$\phi(r) = (\sqrt{\pi} R_h^2) exp(-r^2 / R_h^2), \tag{5}$$

we can write (3) in a factorised form

$$\Psi_{^9Be} = \prod_{j=1}^{9} exp[\frac{r_{3j-2}^2 + r_{3j-1}^2 + r_{3j}^2}{R_h} - 2i\left(\frac{1}{R_A^2} - \frac{1}{R_h^2}\right)(\boldsymbol{s}_{3j-2} + \boldsymbol{s}_{3j-1} + \boldsymbol{s}_{3j}) - \tag{6}$$

$$-3\left(\frac{1}{R_A^2} - \frac{1}{R_h^2}\right)] P_n(r_j) Y_{lm}(\vartheta, \varphi).$$

Then scattering amplitude (1) may be written in the form

$$f(q) = (ik/2\pi)\int d\boldsymbol{b}\, exp(i\boldsymbol{qb})(\delta_{mn}\delta_{MN}) - Det\left|\delta_{mn}\delta_{MN} - \left\langle M \left| \prod_{i=1}^{3}\prod_{j=1}^{3}(1-\gamma(\boldsymbol{b} - \boldsymbol{s}_i + \boldsymbol{r}_j)) \right| N \right\rangle\right|. \tag{7}$$

The matrix element of the profile function between the single particle states described by the quantum numbers *M* and *N*.

We consider the case where spin-flip is neglected. It is important to emphasise that the case of the nucleon-nuclei scattering the leading asymptotic terms of the spiral amplitudes is also determined by the contribution of the quark cluster with the evident replacement of $f(q)$ by the pion-nucleon scattering amplitudes.

Use of the spin-non-flip amplitude of the p^9Be reaction, obtained from the formulae (7) permits us to calculate the correct picture of polarisation at p_L=40 GeV . Note that in work [3] it was supposed for simplicity that the form of the cross-even amplitudes of nucleon-nuclei scattering is equal to the cross-odd part.

3. Comparison with the experimental data.

Figure 1 compares the results of the calculation based on formulae (7), with the experimental data for p^9Be scattering [4]. The solid line corresponds to the cross section calculated eq.(7). The dashed line corresponds to the experimental data. Figure 1 shows that the composite nucleon model yields better agreement, and the Glauber approach extended to the nucleus-nucleus scattering leads to satisfactory

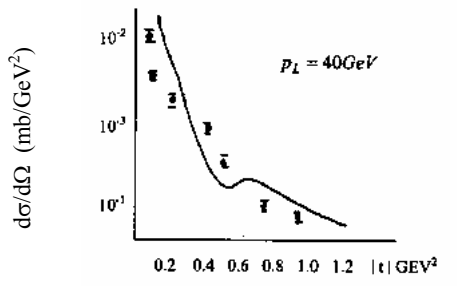

Fig.1 The differential cross sections of the p^9Be reaction

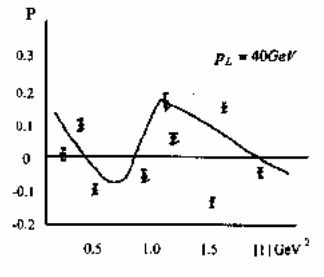

Fig.2 The polarisation of the of the p^9Be reaction

consistency of the calculated cross section and their *t*-dependence with those obtained experimentally. However, taking into account the exchange terms improved the agreement between theory and experiment.

The model prediction for the polarisation of elastic p^9Be scattering, corresponding to the experimental data at p_L=40 GeV is shown in fig.2. Note that the model predicts a large polarisation at high energies in the range of the diffraction peak. The analysis shows that when the preasymptotic corrections are absent, we have the zero polarisation.

The authors express their gratitude to prof. S.Hajiyev for discussion of the trend of this work.

[1] *E.A. Rasulov.* II Eurasian Conference on Nuclear Science and its Application, Almaty, 2002, p.176.
[2] *А.Г. Ситенко.* ЭЧАЯ, 1973, Том 4, Вып.2, стр.546.
[3] *S.G. Abdulvagabova*. Conference Proceeding: First International Conference on Technical and Physical Problems in Power Engineering , Baku, 2002, p.452.
[4] *V.G. Ableev, et.al*. Acta Phys Pol., B16, 1985, p.1895.

С.Г. Ябдцлващабова, Е.А. Рясулов

СЯПИЛЯН ЗЯРРЯЪИКЛЯРИН ЙЦКСЯК ЕНЕРЖИ ЙАХЫНЛАШМАСЫНДА ПОЛЙАРИЗАСИЙАСЫ

Йцксяк енержилярдя p^9Be дифраксийа сяпилмясинин дифференсиал кясийи вя полйаризасийа еффектляри чохдяфяли сяпилмя нязяриййясинин чярчивясиндя щесабланмышдыр. Нуклонларын мцряккяб структуруну вя нуклон мцбадиляси иля баьлы еффектляри нязяря алараг, нязяриййя вя тяърцбя арасында олан уйьунсузлуглар арадан эютцрцлмцшдцр.

С.К. Абдулвагабова, Э.А. Расулов

ПОЛЯРИЗАЦИЯ РАССЕЯННЫХ ЧАСТИЦ В ВЫСОКОЭНЕРГЕТИЧЕСКОМ ПРИБЛИЖЕНИИ

Дифференциальное сечения дифракционного p^9Be рассеяния и поляризационные эффекты при высоких энергиях вычислены в рамках теории многократного рассеяния. При учете составной структуры нуклонов и эффектов с обменами нуклонов устранены расхождения между теорией и экспериментом.

Received:

FIIZIIKA 2002 CIIILD VIIIII
№ 3

CONTENTS